

T
4-89
GUP

**STUDIES ON
SEISMIC SURFACE WAVE DISPERSION,
CRUSTAL STRUCTURE OF HIMALAYA REGION
AND GLOBAL SEISMICITY.**

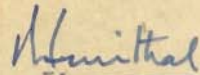
THESIS SUBMITTED BY
HARSH KUMAR GUPTA
FOR THE DEGREE OF DOCTOR OF PHILOSOPHY



DEPARTMENT OF GEOLOGY & GEOPHYSICS
UNIVERSITY OF ROORKEE
ROORKEE (INDIA)

February 1969

The thesis presented by Shri Harsh Kumar Gupta embodies the results of investigation carried out by him from January 1966 onwards. The work was done under my supervision and guidance. I certify that this work has not been presented for any degree or prize elsewhere, and that the candidate has completed the specified period (equivalent to 24 months full time research) in this University.



(Dr. R.S.Mithal)

Professor and Head of the Department
Department of Geology & Geophysics,
University of Roorkee, Roorkee.

ABSTRACT

In the present thesis the importance of the observational surface wave group velocity dispersion studies of the fundamental mode of Rayleigh and Love waves has been emphasised. Specifically:

- a) group velocity dispersion of Love waves has been investigated for Eurasia, which has been divided into thirteen regions according to their dispersion characteristics.
- b) crustal structure of the Himalaya and Tibet Plateau region; where very low Rayleigh and Love wave group velocities have been observed; is delineated.
- c) based upon the Rayleigh wave division pattern, the lateral surface wave group velocity gradients have been studied and a new significant relationship has been sought between these velocity gradients and global seismicity and
- d) the recent seismic activity of the Koyna region has been comprehended in view of the much steeper velocity gradients near Bombay and some outstanding features investigated for the seismic activity of Koyna region have been discussed.

In the beginning, the historical development of the surface wave dispersion studies is presented briefly. The observational difficulties of Love wave dispersion have been pointed out. Dispersion of the fundamental mode of Love waves along various paths in Eurasia has been studied and using the 'crossing path technique', Eurasia has been divided into 13 regions of similar group velocity dispersion character. This division pattern has been compared with Rayleigh wave division pattern. Rayleigh wave to Love wave group velocity ratios for the same period and region are calculated.

Himalaya and the Tibet Plateau region is found to be of special interest in view of the very low Rayleigh and Love wave group velocities delineated for this region and the observed dispersion has been compared with theoretical dispersion curves computed for a three layer earth model. The results are supported by profile seismological observations and deep seismic soundings carried out in some of the common portions by Russian scientists.

Similarity in Rayleigh and Love wave division patterns for Eurasia suggests that the Rayleigh wave division pattern; which is based on 30 sec period waves; in general depicts the seismic wave velocity distribution in the upper 40-50 km section of the earth. This divisioning of Eurasia, Africa,

Pacific Ocean, Atlantic Ocean and the Indian Ocean has been mainly used for calculating the lateral velocity gradients. Seismicity; for the first time; has been correlated with the lateral elastic wave velocity gradients. The investigation reveals that the regions of high seismicity most unambiguously correspond to regions of steep gradients.

The puzzling seismic activity in the Western side of the stable Indian Shield also seems understandable in view of the much steeper gradients near Bombay. The Koyna earthquake of December 10, 1967 has been studied in detail.

ACKNOWLEDGMENTS

It is a great pleasure for me to acknowledge the invaluable guidance provided through out the progress of work by Dr. R.S. Mithal, Prof. and Head - Department of Geology and Geophysics. I am extremely grateful to Dr. Hari Narain, Director - National Geophysical Research Institute, who has been an unfailing source of inspiration and offered many helpful suggestions. Discussion with Prof. Yasuo Satô of Earthquake Research Institute - Tokyo University, Dr. T. Santô of International Institute of Seismology and Earthquake Engineering - Tokyo and Dr. J.G. Negi - Head, Theoretical Geophysics Division of National Geophysical Research Institute had been very useful and I am grateful to them for the same. Dr. A. Roy and Dr. M.N. Qureshy very kindly provided me the prepublished copies of their papers.

I am also thankful to Messers Indra Mohan, B.K.Rastogi and M.V.D. Sitaram for their help in the preparation of the manuscript and to Mr. A. Narendra Nath for typing.

Harsh Kumar Gupta

CONTENTS

Abstract	
Acknowledgments	
List of figures	
List of tables	

Page No.

Chapter I : INTRODUCTION

1.1	General considerations	1
1.2	Importance of Surface wave studies	4
1.3	Surface wave dispersion studies - A survey	5

Chapter II : LOVE WAVE DISPERSION STUDIES IN EURASIA

2.1	Introduction	11
2.2	Crossing path technique	14
2.3	Statement of the problem	17
2.4	Love wave observations	18
2.5	Plotting of dispersion curves	22
2.6	Standard Love wave dispersion curves & division of Eurasia	26
2.7	Discussion	30
2.7 .1	Himalaya - Tibet Plateau region	32
2.7 .2	Other regions	37
2.7 .3	Rayleigh versus Love wave group velocities	38
2.8	Conclusions	41

Chapter III : CRUSTAL STRUCTURE IN HIMALAYA AND
TIBET PLATEAU

3.1	Introduction	42
3.1 .1	The concept of isostasy and roots of mountains	42
3.1 .2	Investigations of roots of mountains	47
3.2	Statement of the problem	51
3.3	Part I	
3.3 .1	Observational data	53
3.3 .2	Theoretical model	61
3.3 .3	Interpretation and discussion	63
3.4	Part II	
3.4 .1	Observational data	72
3.4 .2	Computation of group velocities for region '12'	78
3.4 .3	Comparison with theoretical dispersion curves and discussion	81
3.5	Conclusions	84

Chapter IV : LATERAL VELOCITY GRADIENTS AND GLOBAL
SEISMICITY

4.1	Introduction	86
4.2	Velocity division pattern and shallow focus earthquakes	87
4.3	Lateral velocity gradients in active areas	91
4.4	Correlation with distribution of earthquakes of magnitude 8.6 and above	99
4.5	Velocity gradients in active areas	100

	Page No.
4.6 Importance of correlation	100
4.7 Conclusions	105
 Chapter V : A STUDY OF KOYNA EARTHQUAKE	
5.1 Introduction	107
5.2 Origin time and epicenter	109
5.3 Field evidence	116
5.4 Fault plane solution	118
5.5 Correlation between water levels in the reservoir and seismic activity	120
5.6 Other examples of the associa- tion of seismic activity with water reservoirs	124
5.7 Foreshocks - aftershocks of Koyna earthquake	125
5.8 Conclusions	133
 Chapter VI : SUMMARY AND CONCLUDING REMARKS	
6.1 Summary	134
6.2 Concluding remarks	138
 APPENDIX I	 140
APPENDIX II	142
REFERENCES	143

LIST OF TABLES

Table	Page No.
1. Regions corresponding to different standard dispersion characteristics	11
2. Data of earthquakes used	20
3. List of stations	21
4. Calculation of group velocities	24
5. Group velocities (km/sec) of Love waves for various standard dispersion curves at different periods in sec.	31
6. Frequency distribution of $(T_o - T_c) / T_o$	31
7. Details of computation of T_c for a few paths	36
8. Rayleigh to Love wave group velocity ratios for 30 and 40sec period	40
9. Particulars of WSSS stations (Chapter III Part I)	57
10. Group velocities of Rayleigh waves	59
11. Group velocities of Love waves	60
12. Group velocities of Rayleigh waves and corresponding crustal thicknesses	71
13. Details of the paths (Figure 26) studied	73
14. Calculation of Rayleigh wave group velocities for region '12'	79
15. Rayleigh wave group velocities for region '12' along sections 'a' to 'f' (Figure 26) for different periods.	82
16. List of earthquakes; magnitude 8.6 and above (Richter - 1956) from 1898 to 1956	93
17. Velocity gradients along sections 'a' to 'f' of figure 34	102
18. P wave residual time (observed - calculated) for Indian observatories with respect to I.M.D origin time	111
19. List of the places where rotational movements have been measured with magnitudes and directions	116
20. Earthquake data used in Figure 44	125

LIST OF FIGURES

Figure	Page No.
1. Standard Rayleigh ^{wave} dispersion curves	12
2. Division of Eurasia into regions of similar Rayleigh wave dispersion characteristic	12
3. Schematic representation of the crossing path path technique	15
4. Seismic stations, earthquake epicenters, and wave paths used for Love wave dispersion studies	19
5. Long period N-S component seismogram at Shillong	23
6. Love wave group velocity dispersion curve from the above seismogram	23
7. Earthquakes around Himalaya and Tibet Plateau region and their wave paths to Japan	27
8. Standard Love wave dispersion curves	28
9. Love wave dispersion regions	29
10. Seismograms recorded at Shiraz	33
11. Orbital motion of Shiraz seismogram	34
12. Love wave dispersion as observed at Helsinki	39
13. Schematic representation of the deviation of plumb line due to attraction of Himalaya at Kaliana, Assuming plumb line to be normal at Kalianpur	44
14. Airy's (1855) explanation of isostasy	46
15. Pratt's (1859) explanation of isostasy	46
16. Crustal section across continental boarder of western South America	48
17. Relief map of Asia (based on 'Chart of the World' H.O. 1262 A published by U.S. Naval Oceanographic Office) showing the epicenter, recording stations and the great circle paths.	54
18. Section of three seismograms showing typical Love and Rayleigh wave dispersion	55
19.a. Rayleigh wave - particle motion	56
19 b. Love wave - particle motion	56

Figure	Page No.
20. Rayleigh wave dispersion-25th August, 1964	64
21. Love wave dispersion - Dorman case 201	64
22. Rayleigh wave dispersion-Dorman case 8007	65
23. Love wave dispersion -Dorman case 208	65
24. Topography between epicenter and recording stations, vertical exaggeration 125 times	68
25. Rayleigh wave dispersion	68
26. Rayleigh wave paths studied for the region '12'	74
27, 28, 29. Rayleigh wave dispersion curves for region '12'	75,76,77
30. Rayleigh wave group velocities for region '12' for paths 'a' to 'j'	80
31. Rayleigh wave dispersion curves for paths not including region '12'	83
32. Apparent Pn velocities in the United States	89
33. Rayleigh wave divisioning of United States and surroundings	90
34. Map showing shallow global seismicity, Rayleigh wave division map, earthquakes of magnitude 8.6 and above and sections 'a' to 'f'	92
35. Standard Rayleigh wave group velocity dispersion curves used for divisioning and legend to Figure 34.	94
36. Paths used for Rayleigh wave divisioning	96
37. Velocity variations along sections 'a' to 'f' of figure 34	97
38. Shallow seismic activity and Rayleigh wave division of a part of Africa	101
39. Map of the Koyna region showing the locations of the various observatories, two epicenters, isoseismals and the rotational displacements	110
40. Sections of seismograms of New Delhi and Meerut supporting the multiplicity of the shock	113

Figure

Page No.

41.	Rotational movement registered on a pillar Helwak Chiplun road - near Dondchiwadi	117
42.	Fault plane solution based on sense of P wave motion plotted on Byerly's extended distance projection	119
43.	Inflow Hydrograph, reservoir water level in the Shivajisagar Lake and the seismic activity in the Koyna region	123
44.	Frequency-magnitude relation for the aftershock sequence of December 10, earthquake	126
45.	Foreshock - aftershock sequence for the Koyna earthquake of September 13, 1967	127
46.	Foreshock - aftershock sequence for the Koyna earthquake of December 10, 1967	128
47.	Mogi's (1963) three types of earthquake sequences and their relations to the structures of the materials and the applied stresses	129

CHAPTER - I
INTRODUCTION

CHAPTER - I

INTRODUCTION

1.1 GENERAL CONSIDERATIONS:

Among the various disciplines of Geophysics, seismic methods have contributed most towards the understanding of the structure of the earth and its other physical properties.

In investigating earth's interior, one of the major handicap is the lack of the experimental data. As remarked by Jacobs (1956) this lack is not due to any short comings on the part of the experimental geophysicist, but due to the inescapable fact that it is not possible to sample a piece of material from deep within the earth's interior. We are still struggling to put a hole through the crust of the earth. The great advances made in the high temperature and pressure techniques may produce pressures and temperatures corresponding to great depths within the earth but one cannot allow for the time factor and there is no counterpart in the laboratory for the geological times involved in various processes going in the earth's interior.

Howsoever little, the main experimental data comes from the study of earthquakes. Mohorovičić as early as (1909) plotted the arrival times of various waves observed at many observatories against the epicentral distances for the Kulpa valley earthquake and delineated the existence of a

discontinuity, which later has been traced all over the world and named as Mohorovicic discontinuity in the honour of the investigator. Similarly Conrad (1925) suggested a discontinuity above Mohorovicic discontinuity from the study of two central European earthquakes.

Bullen (1940, 1942) made a number of subdivisions of earth's interior based upon the character of P and S velocity distributions, as determined by Jeffreys (1939-A, 1939-B). Distribution of seismic velocities in the mantle and core was later worked out by Gutenberg (1948, 1951). The velocities given by these two workers agreed within 0.3 km/sec at practically all depths, the differences being more pronounced in respect to the variation of the velocity gradient. The velocity-depth variations are obtained by integrating the travel time curves and depend to some extent on the mathematical method employed. Bullen (1940, 1942) has also used these velocities for the determination of densities within the earth.

Industry has gained a lot from seismology by applying the knowledge acquired from earthquakes in seismic methods of prospecting for oil and minerals. To-day, among the geophysical methods of prospecting the seismic methods are most useful and are credited to have discovered 90% of the total oil fields during the last few decades all over the world.

Seismology, on one hand has given us information about the earth's interior, while on the other hand it has taught us how to combat the earthquake disasters. Engineering seismology is a very fast developing branch. It is not out of place to give an example of the achievements made by engineering seismology. The Long Beach, California earthquake of March 10, 1933 did not have a very high magnitude, but because of poor construction, 85 schools in Long Beach valued at \$ 50,000,000 were more or less completely destroyed. Consequently the legislature of California passed a bill known as the 'Field Act' making it compulsory that school buildings in California be designed and built to resist earthquakes. The wisdom of 'Field Act' was immediately realized while during the higher magnitude Kern County earthquake of South California on July 21, 1952; all buildings designed to resist earthquakes came through almost undamaged.

In seismology, the main research effort is now directed for predicting the earthquakes. Currently, there is a national programme underway in Japan for earthquake prediction. The use of seismographs in the detection of nuclear explosion has brought the seismologists from the relative obscurity of their pure science into the very center of world affairs. Dr. Frank Press (1967) observes:

"If a successful technique is found for predicting the earthquakes, large scale arrays of sensors will be deployed in seismic belts as part of an earthquake warning system. If we add to this the large scale arrays needed to monitor nuclear test ban treaty, we might find a seismograph explosion competing with the population explosion ! Seriously, these two contributions of seismology - earthquake warning and arms control - represent oppertunities for geophysicists to help prevent man-made disaster and mitigate the effects of natural disaster".

One of the latest development is the extra-terrestrial seismology. It is interesting to note that the operation of lunar seismograph has been given a high initial priority in the United States programme of experiments to be conducted on the moon's surface.

1.2 IMPORTANCE OF SURFACE WAVE STUDIES:

Surface waves have been intensively used for the determination of the crustal structure. Instrumental improvements and extensive calculations of dispersion in two and three layer systems have made it possible to determine average crustal thicknesses in many parts of the world. Mantle Rayleigh waves, first described by Ewing and Press (1954-a, 1954-b), have been found to be a very potential new tool for studying the structure of the mantle.

Surface waves are complementary to body waves and provide an alternate method for studying the velocity distribution in the earth. Besides, they are particularly sensitive to the shear wave velocity, which is the least accurately determined body wave velocity. Moreover, they are also functions of the density distribution. If we know seismic velocities completely and accurately from body wave studies, then the density distribution could directly be obtained from the study of surface wave dispersion. Surface wave calculations so far have used densities calculated from seismic velocities by indirect methods but even so, an investigation of the effect of density on dispersion allows us to rule out certain proposed density structures. Another distinct advantage is that the surface waves can be used to determine average structure over regions inaccessible to body wave studies. Also, there are no shadow zones to frustrate this type of study. Since the fundamental surface wave data is velocity-period rather than amplitude-distance or time-distance, a single seismogram of a single earthquake, in principle, contains all the information needed for structural interpretation.

1.3 SURFACE WAVE DISPERSION STUDIES - A SURVEY:

Ever since the recording of earthquakes by seismometers, the presence of large transverse waves on the seismograms was detected. However, they were not understood till 1911 when Love

(1911) gave a theoretical explanation showing that a free surface could support surface wave, provided the speed of S waves increased with depth. Rayleigh (1885) had earlier shown that a free surface could support a wave having longitudinal and vertical components, whose amplitude decreased with depth. Because of the predominance of horizontal movement at right angles to the direction of propagation then observed by the seismologists, Rayleigh's (1885) work did not get much attention. Similar to the finding of shear and longitudinal type of body waves by Poisson and Stokes, Love's work (1911) following Rayleigh's (1885) and Lamb's (1903) researches showed the existence of two types of surface waves. Much of the later theoretical work was then carried out by Jeffreys and Stoneley. In 1925, Stoneley pointed out that group velocity, and not the wave velocity is obtained by dividing the epicentral distance by the travel time of a wave of a given period.

Tams (1921) was first to use the observational data for the investigation of earth's crust, followed by Gutenberg (1923, 1924, 1925). In 1924, Gutenberg found that the group velocity of both Rayleigh and Love waves in 30 sec period range is higher for Atlantic and Pacific paths than for Eurasia indicating a different structure. Jeffreys (1925) assuming a granitic crust overlying ultrabasic rocks, computed Love wave group velocity dispersion curves and compared Gutenberg's (1925) observational data.

During the next two decades i.e. 1930's and 1940's, many workers used the surface wave dispersion data for studying crust in various parts of the world. Noteworthy among them are Byerly (1930), Stoneley (1931), Röhrbach (1932), Labrouste (1933), Carder (1934), Jeffreys (1934), Sezawa (1935), Bullen (1939), Wilson (1940), Stoneley (1948), Wilson and Baykal (1948). Theoretical work carried out by Pekeris (1948) and experimental work carried out by Worzel and Ewing (1948) gave much insight to the understanding of surface waves.

For the better recording of surface waves, the Galitzen type seismograph was extensively modified by Press and Ewing at Columbia in 1951. Instrumental improvements with the advancement of computational techniques gave a big boost to surface wave dispersion studies. Extensive surface wave dispersion studies were carried out during 1950's in U.S.A., Japan and Europe. Besides group velocity studies, elegant technique for phase velocity studies were developed. Press (1956) developed the tripartite method, Satô (1960) - the Fourier phase method and Brune et al (1960) - the phase correlation method. Ewing, Jardetzky and Press (1957) have given an excellent review of the work carried out prior to 1957 in various disciplines of surface wave studies. In another review article Arkhangel'skaya (1960) has summarized most of the observed surface wave dispersion data by European investigators prior to 1960. Nuttli (1963) and Anderson (1965) have described the application of surface wave studies and the

inferences drawn about the structure of the earth's mantle. In another analogous study entitled 'Seismic surface waves some observations and recent developments', Kovach (1965) has given a very good review including the instrumental developments for recording long-period seismic waves, observations of fundamental mode continental and oceanic Rayleigh and Love waves, long-period Love and Rayleigh wave data, higher mode surface waves - their observation and numerical calculations.

In most of the earlier surface wave dispersion studies, dispersion was studied along one or two paths and conclusions were drawn by comparing it with certain theoretical dispersion curves. Examples are Brilliant and Ewing's (1954) study for U.S. continent; crustal structure from surface wave dispersion studies for Africa by Press, Ewing and Oliver (1956); Båth and Vogel's (1957) study for paths between Turkey and Uppsala; Kovach's (1959) study of an Afroasian and Eurasian path, and many more.

Shechkov (1961) was one of the first to study the dispersion of both Rayleigh and Love waves along a number of paths in Eurasia for crustal investigations. He compared the observational data with theoretical dispersion curves computed for Rayleigh waves by Stoneley (1955) and for Love waves by Dorman (1959) for a two layer earth crust. The observed dispersion data could be divided into three groups i.e. for

paths between 1: Central Asia and Kuril Islands,
 2: European part of USSR and Japanese Islands and
 3: European part of USSR and East China sea. In another
 analogous study Savarensky and Shechkov (1961) studied
 the crustal structure in Siberia and Far East from Rayleigh
 and Love wave dispersion studies using a number of earth-
 quakes recorded at Sverdlovsk, Irkutsk Kyakhta and Semipala-
 tinsk. They also made use of Stoneley's and Dorman's theo-
 retical dispersion curves for comparison and concluded that
 in general the thickness of earth's crust in middle latitudes
 of Siberia and in the Far East is probably somewhat less than
 in the northern and southern parts of Siberia.

Later, Shechkov (1964) used data from 376 earthquakes
 recorded at 32 USSR stations and making use of both group
 and phase velocities of Rayleigh and Love waves determined
 crustal thicknesses in various parts of the USSR. The large
 number of intersections in the same region and many parallel
 close paths studied increased the reliability of the results
 considerably. He found that for almost all sectors and along
 almost all individual paths the group velocity values obtain-
 ed were in good agreement with each other and the deviation
 from the mean value did not exceed 0.07 km/sec. The results
 were in agreement with deep seismic sounding findings.

Remarkable work has been carried out on Rayleigh wave
 dispersion studies by Santô (1960, ^{61 A+B, 62 A+B,} ~~61, 62 A, B and C,~~ 63, 65
 A and B, 66, 67 and 68). Starting from the investigations of
 the dispersion of Rayleigh waves by Columbia-type seismograph.

installed at Tsukuba station in Japan in 1960, Santô (1960) divided the south-western Pacific area into several regions in each of which Rayleigh waves have the same dispersion character. Later, Santô studied the dispersion along various continental and oceanic (Arctic and Atlantic Oceans) paths to Uppsala. During 1963, Santô and Båth (1963) investigated crustal structure in the Pacific Ocean from dispersion of Rayleigh waves and later Santô (1963) divided the Pacific area into seven regions in each of which Rayleigh waves have the same group velocity. From the exhaustive observational data collected from these studies, Santô (1965 A and B) studied the lateral variation of Rayleigh wave dispersion character in Eurasia and using the Crossing Path Technique divided it into 12 regions of similar group velocity ^{dispersion} characteristic. The same work was extended for Africa, Atlantic Ocean and Indian Ocean by Santô and Satô (1966) and for Gulf of Mexico, Caribbean Sea and North American continent by Santô (1967, 1968).

CHAPTER-II

LOVE WAVE DISPERSION STUDIES IN EURASIA

CHAPTER - II

LOVE WAVE DISPERSION STUDIES IN EURASIA*

2.1 INTRODUCTION:

Using 'crossing path technique' Santô (1965 A, 1965 B) divided Eurasia into regions of similar group velocity dispersion character of Rayleigh waves and standardized the dispersion curves for these regions. Later this work was extended for Africa, Atlantic Ocean and Indian Ocean by Santô and Satô (1966) and for the Gulf of Mexico, Caribbean Sea, North America and Arctic Ocean by Santô (1967, 68).

Figure 1 shows the standard dispersion curves used by Santô (1965-B) for the divisioning of Eurasia shown in Figure 2. Table 1 gives the characteristic numbers and the corresponding types.

Table 1

Characteristic number	Type
1.5 and below	Deep oceanic
1.6 - 3.5	Oceanic
3.6 - 5.5	Oceanic transitional
5.6 - 6.5	Continental transitional
6.6 - 7.5	Continental
7.6 - 9.5	Mountainous
9.6 and above	High mountainous

* The contents of this chapter have been published in the Bulletin of the Earthquake Research Institute, University of Tokyo. Vol. 46 (1968). pp. 41-52.

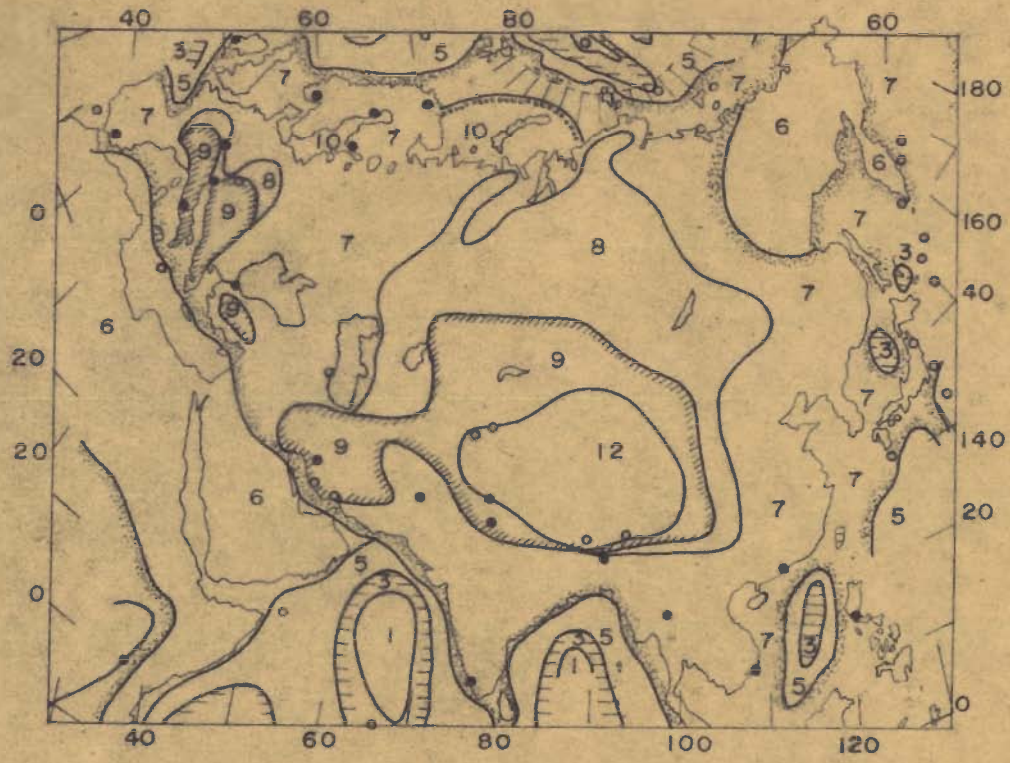


Fig. 2. DIVISION OF EURASIA INTO REGIONS OF SIMILAR RAYLEIGH WAVE DISPERSION CHARACTERISTIC (SANTÔ, 1965)

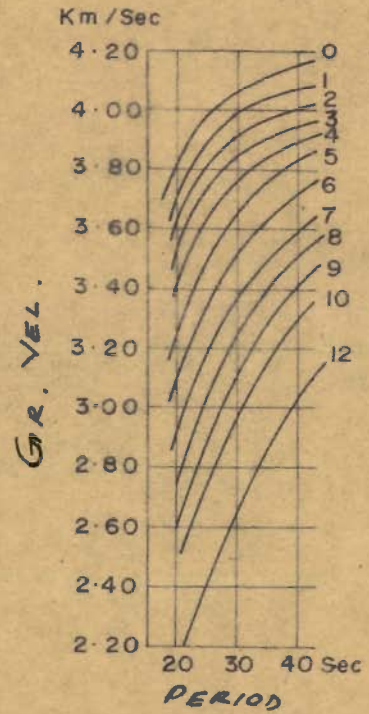


Fig. 1. STANDARD RAYLEIGH WAVE DISPERSION CURVES (SANTÔ, 1965)

The divisioning was possible because:

- a. most of the observed dispersion curves were found to be parallel and
- b. any of the observed dispersion curves can be assumed to have resulted from the mixed path composed of different dispersion regions.

Santô (1965-B) has cited a number of examples of Rayleigh waves travelling through a mixed path composed of different regions and the resulting dispersion curve for the mixed path is found to coincide with the dispersion curve for another region. Rayleigh waves travelling two different regions 1 and 5 with path length ratios 1:4 result in the standard curve 2. With a path ratio of 2:3, resulting curve is approximately 3; and 4 when this ratio is 3:2.

Some more established relations are:

$$\frac{1}{2} (1/V_8 + 1/V_1) = 1/V_6$$

$$\frac{1}{2} (1/V_{10} + 1/V_3) = 1/V_7$$

$$\frac{1}{2} (1/V_8 + 1/V_{10}) = 1/V_9$$

The first relation shows that when the Rayleigh waves have travelled two different regions 8 and 1 with equal path lengths, the resulting dispersion character for the total path becomes 6 and so on. Santô argues that such relations make it possible to divide any path, Δ , into several segments Δ_i with dispersion number i , using the observed dispersion j along the total path.

2.2 CROSSING PATH TECHNIQUE:

This technique, which is essentially based upon the method of trial and error, was developed and used by Santo (1961) for the divisioning of the Pacific Ocean into several regions and was named by Dr. Markus Bâth. The purpose of the technique is to divide a given area into several regions of similar group velocity dispersion character using observed group velocities along various paths crossing the area in various directions. The schematic Figure 3 explains the procedure adopted by Santô (1963). From the previous experience it is suggested that the continental low lands have a dispersion characteristic 7. It is further assumed that generally crust becomes more continental with increasing elevations and correspondingly the dispersion character of the Rayleigh waves. Hence the contour lines of 200 meter, 1,000 meter and 3,000 meter may be taken as the preliminary dispersion boundaries (7,8), (8,9) and (9,10) respectively. For such a division the travel time of Rayleigh waves of a particular period, say 30 sec, crossing the area may be calculated as:

$$t_c = \sum \frac{\Delta i}{V_i}$$

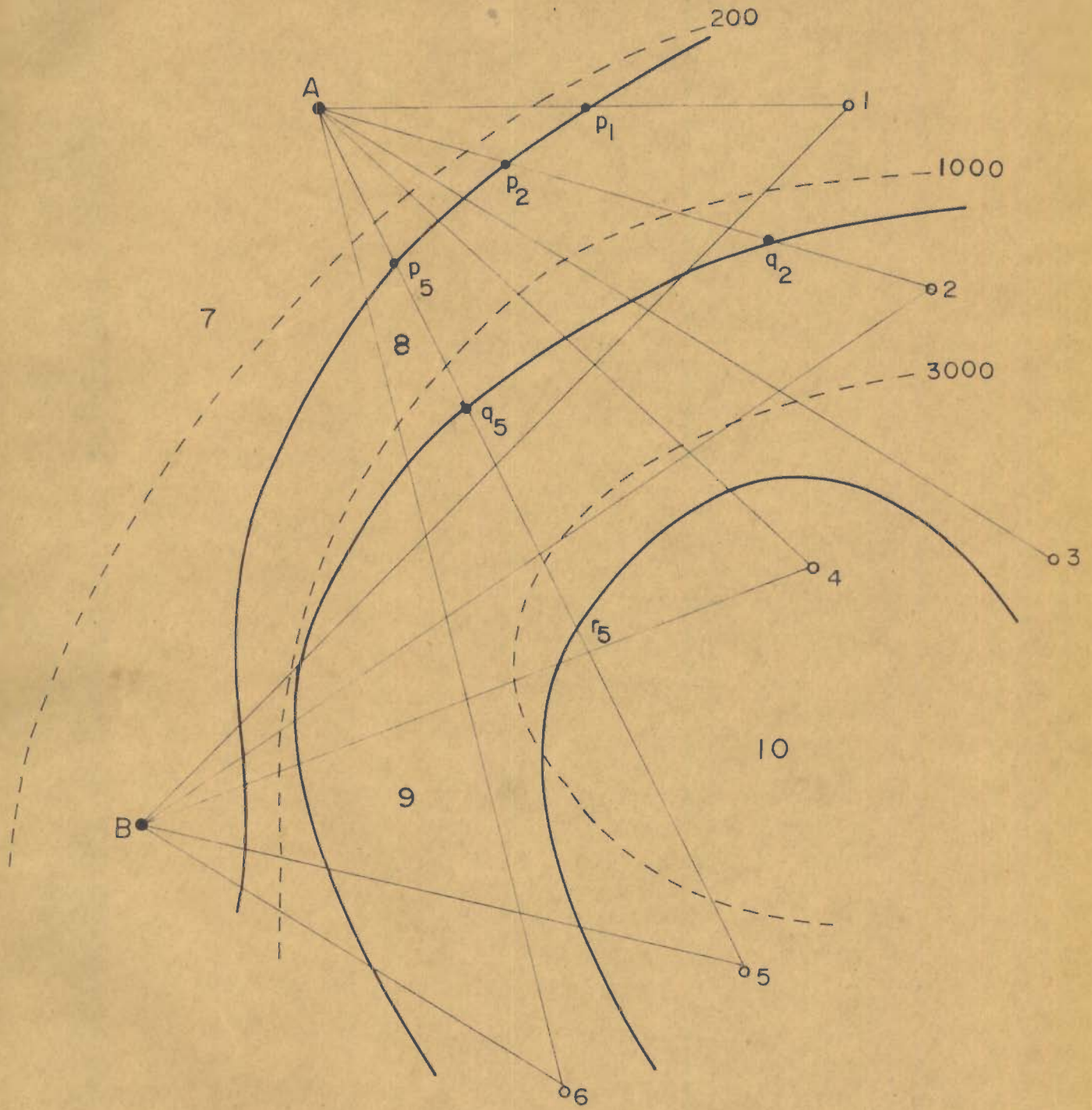
Where,

$$i = 7, 8, 9, 10$$

$$\Delta i = \text{path length in the } i \text{ region}$$

$$V_i = \text{group velocity for } i \text{ regions for 30 sec period.}$$

The value of t_c thus calculated generally differs from the observed travel time value of t_o and the preliminarily assumed boundaries are shifted to minimize $|(t_o - t_c)|$.



- A,B Observation stations
- 1 to 6, Epicenters

- Contour lines of elevation
- Boundaries of regions

Fig.3. SCHEMATIC REPRESENTATION OF THE CROSSING

It is most convenient to start with a path which lies on a flat topography such as 1 to A in Figure 3 which crosses only the 200 meter contour. It is now quite easy to find uniquely the most suitable division point p_1 , to make $|(t_o - t_c)| = 0$, separating region 7 from 8. Now, a curve approximately parallel to the contour is drawn and p_2 lies close to p_1 on the path A - 2. We will not expect any serious error in the location of p_2 which divides A - 2 into 7 and 8 regions. A - 2 also crosses the 1,000 meter contour line. The shift of the boundary is mainly performed for this new crossing point q_2 marking the division of 8 and 9 regions for making $|(t_o - t_c)| = 0$.

This procedure is successively repeated for each path and by joining these division points, one by one, the division pattern is drawn. This division pattern is based upon the data for the paths radiating from a single station and hence is not unique. The division pattern could be improved by repeating the same procedure for another station B and epicenters 1, 2, 4, 5 and 6. With the increase of the analysis of these crossing paths, the division pattern improves.

As mentioned earlier, the divisioning is done for the group velocity of a particular period only. However, since the dispersion data lies on more or less parallel dispersion curves, a similar division pattern would be obtained if the technique is repeated for other periods close to the one used for initial divisioning.

2.3 STATEMENT OF THE PROBLEM:

All the studies carried out by Santô and others, as mentioned in the introduction, are confined to the division based upon the Rayleigh wave dispersion character. Because of their very complimentary nature, it is important to study the dispersion of Love waves in a similar manner and find whether the Rayleigh wave division pattern holds good for Love waves also.

Among the continents, Eurasia is largest. Geologically also it is important since it comprises the whole Alpidic belt including Alps, Caucasus, Karakoram, Tibet Plateau, Hindukush, Himalaya and many other mountain ranges. Moreover, the earthquakes of its Pacific Coasts (Circum - Pacific belt) and recorded at European stations and earthquakes of Middle East, recorded at Southeast Asian stations provide purely continental paths for these investigations.

In the present work, dispersion of the fundamental mode of Love waves is studied along various paths in Eurasia. The observed group velocity dispersion curves are found to be parallel for most of the paths. This makes it possible to utilise the 'crossing path technique' and divide Eurasia into different regions having similar Love wave dispersion characteristics and to examine whether it agrees with the Rayleigh wave division of Eurasia.

2.4 LOVE WAVE OBSERVATIONS:

Unlike Rayleigh waves, which being vertically polarized can easily be picked up from the long-period vertical component seismograms, observation of Love waves is difficult. This difficulty is mainly because of two reasons. Firstly, for oceanic paths, Love waves are not very dispersive and appear like a pulse on the seismogram. Secondly, when these waves arrive at a station around 45° with the axis of orientation of the horizontal component seismometers, they are strongly affected by Rayleigh waves and we can not measure the group velocities of Love waves for the time range in which Rayleigh waves also arrive. Because of the horizontally polarized transverse locus of Love waves, horizontal component seismograms for the stations where waves arrive along one of the co-ordinate axis are most suitable. With this consideration in mind, seismograms of the Eurasian W.W.S.S.N. stations for 1964 and 1965 were examined and finally 18 earthquakes recorded at 16 stations were found suitable for this study. Tables 2 and 3 give the information about these stations and earthquakes and Figure 4 shows the corresponding great circle paths studied. Epicentral distances and the azimuthal angles are measured using standard trigonometrical relations with the help of an electronic computer. The shortest and the longest distances are 2,142 km and 14,096 km respectively. In most of the cases the azimuthal angle is within $\pm 10^{\circ}$ of either of the co-ordinate axes. The identity of the Love waves was checked by comparing the horizontal component seismogram with the vertical component seismogram. In doubtful cases, particle motion diagrams were plotted to confirm the identity.

Table 2

Data of Earthquakes used

Date				Origin Time (G.M.T)			Epicenter	
				h	m	s		
1	Jan	15	64	21	36	05.0	39.1 N	140.8 E
2	Jan	22	64	15	58	46.5	22.4 N	93.6 E
3	May	02	64	16	11	00.2	45.5 N	150.3 E
4	May	31	64	00	40	36.4	43.5 N	146.8 E
5	Aug	19	64	15	20	13.9	28.2 N	52.7 E
6	Aug	25	64	13	47	20.6	78.2 N	126.6 E
7	Oct	21	64	23	09	18.8	28.1 N	93.8 E
8	May	04	65	08	34	39.8	41.7 N	79.4 E
9	May	16	65	11	35	46.0	5.3 N	125.7 E
10	May	17	65	17	19	25.9	22.5 N	121.3 E
11	May	20	65	00	40	10.9	14.7 S	167.4 E
12	May	23	65	23	46	12.0	52.2 N	175.0 E
13	June	21	65	00	21	14.5	28.1 N	56.0 E
14	Sept	04	65	14	32	47.9	58.2 N	152.6 W
15	Sept	11	65	06	53	01.5	5.3 S	153.0 E
16	Sept	12	65	22	02	34.3	6.4 S	70.8 E
17	Nov	12	65	17	52	24.1	30.5 N	140.2 E
18	Nov	18	65	21	58	12.4	53.9 N	160.7 E

Fig. 4. SEISMIC STATIONS (●), EARTHQUAKE EPICENTERS (○), AND WAVE PATHS USED FOR LOVE WAVE DISPERSION STUDIES

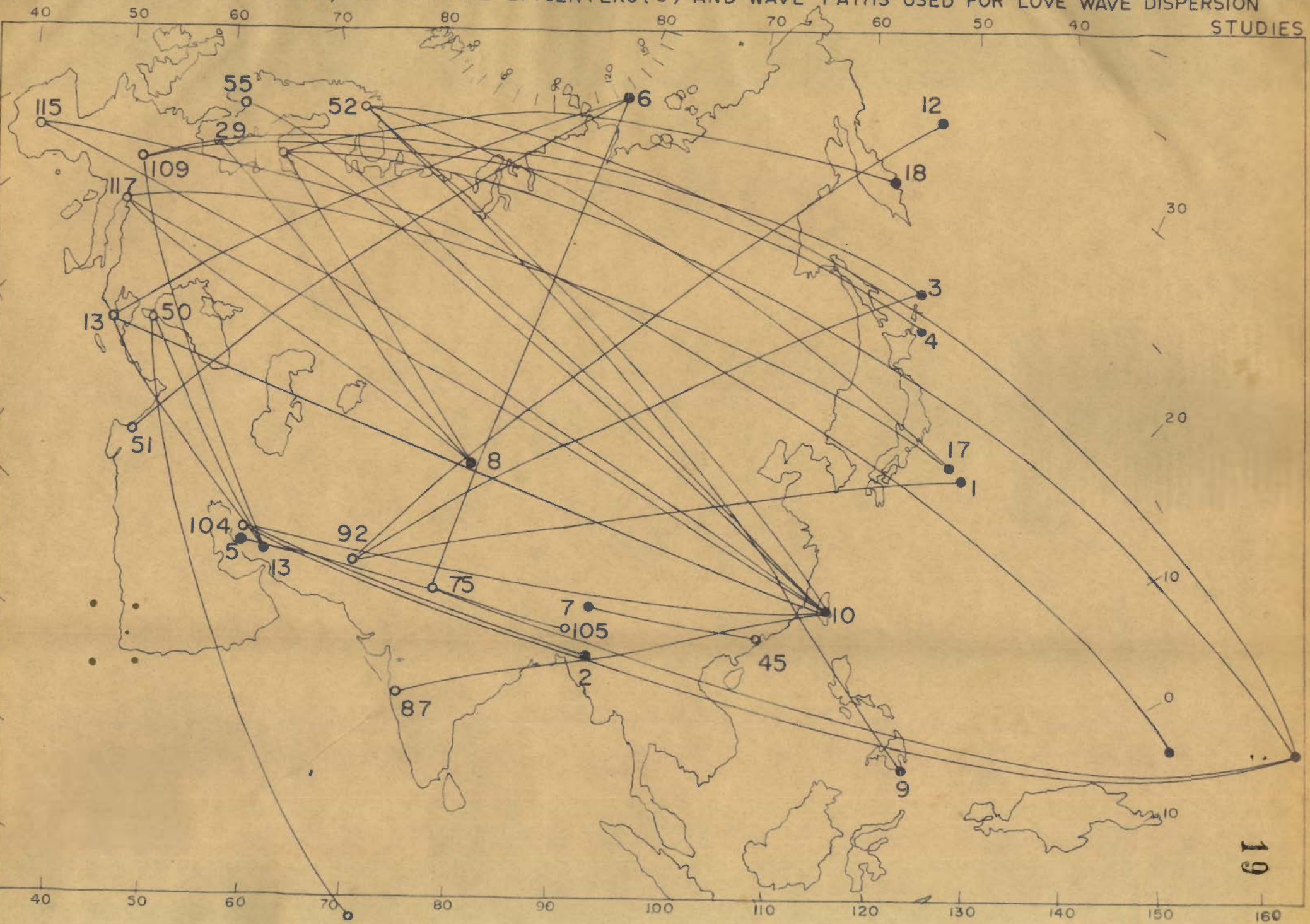


Table 3

List of Stations

Station		Country	Latitude	Longitude
ATHENS	(ATU 13)	Greece	37 58 22 N	23 43 00 E
COPENHAGEN	(COP 29)	Denmark	55 41 00 N	12 26 00 E
HONG KONG	(HKG 45)	Hong Kong	22 18 13 N	114 10 19 E
ISTANBUL	(IST 50)	Turkey	41 02 36 N	28 59 06 E
JERUSALEM	(JER 51)	Israel	31 46 19 N	35 11 50 E
KEVO	(KEV 52)	Finland	69 45 21 N	27 00 45 E
KONGSBERG	(KON 55)	Norway	59 38 57 N	09 37 55 E
NEW DELHI	(NDI 75)	India	28 41 00 N	77 13 00 E
NURMIJARVI	(NUR 81)	Finland	60 30 32 N	24 39 05 E
POONA	(POO 87)	India	18 32 00 N	73 51 00 E
QUETTA	(QUE 92)	Pakistan	30 11 18 N	66 57 00 E
SHIRAZ	(SHI 104)	Iran	29 30 40 N	52 31 34 E
SHILLONG	(SHL 105)	India	25 34 00 N	91 53 00 E
STUTTGART	(STU 109)	Germany	48 46 15 N	09 16 36 E
TOLEDO	(TOL 115)	Spain	39 52 53 N	04 02 55 W
TRIESTE	(TRI 117)	Italy	45 42 32 N	13 45 51 E

2.5 PLOTTING OF DISPERSION CURVES:

The technique described by R. Satô (1958) has been used for the plotting of the dispersion curves. Table 4 explains the procedure for a seismogram (Figure 5) written at the Shillong seismological observatory. The arrival times of the successive peaks and troughs of the well dispersed Love wave train are determined and from this origin time is subtracted giving the travel time. For example in the seismogram the arrival time of a particular peak (n) is 15-38-04.6 and that of following trough (n+1) is 15-38-26.0 (All times are given in G.M.T.). The origin time of the earthquake is 15-20-13.9. So we obtain the travel time of (n) as 1070.7 sec and for (n+1) as 1092.1 sec. Dividing the epicentral distance of 3,877 km by these travel times, group velocity for (n) is found to be 3.621 km/sec and 3.550 km/sec for (n+1). Doubling the difference of travel times (1092.1 sec - 1070.7 sec) i.e. 21.4 sec we get the period of the cycle as 42.8 sec and the arithmetic mean of the two group velocities $(3.621 + 3.550)/2$ gives us the corresponding group velocity of 3.585 km/sec. Same operation is repeated for (n+1), and (n+2) and (n+3) and so on. Plotting of the group velocities, thus obtained, against the period and drawing a smooth mean curve through these points gives us the required dispersion curve. Figure 6 shows the group velocity dispersion curve obtained for this Shillong record.

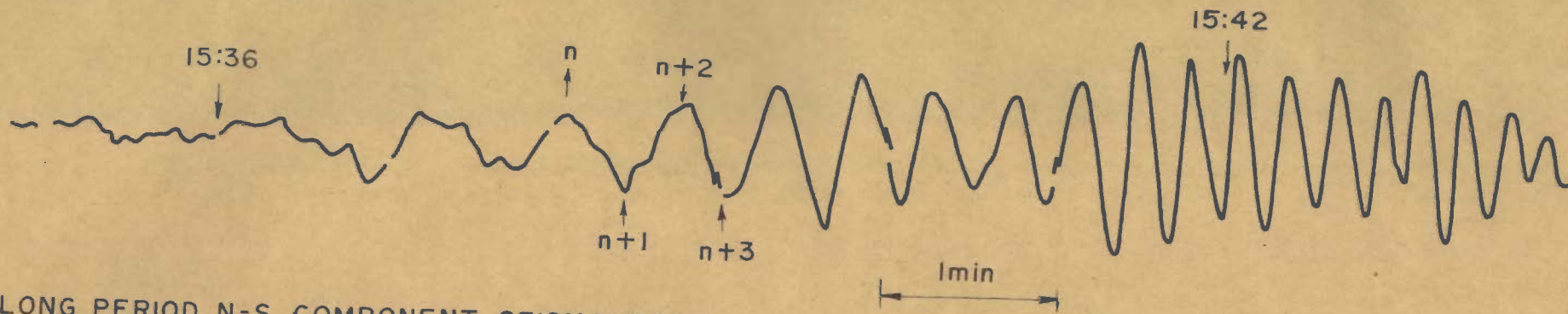


Fig.5. LONG PERIOD N-S COMPONENT SEISMOGRAM AT SHILLONG.

Dt. 19-8-1964

Epc. 28.2N 52.7E

O.T. 15:20:13.9

Dist. 3877 Km

Fig.6. LOVE WAVE GROUP VELOCITY DISPERSION CURVE FROM THE ABOVE SEISMOGRAM.

SHILLONG - Epc (28.2N, 52.7E)

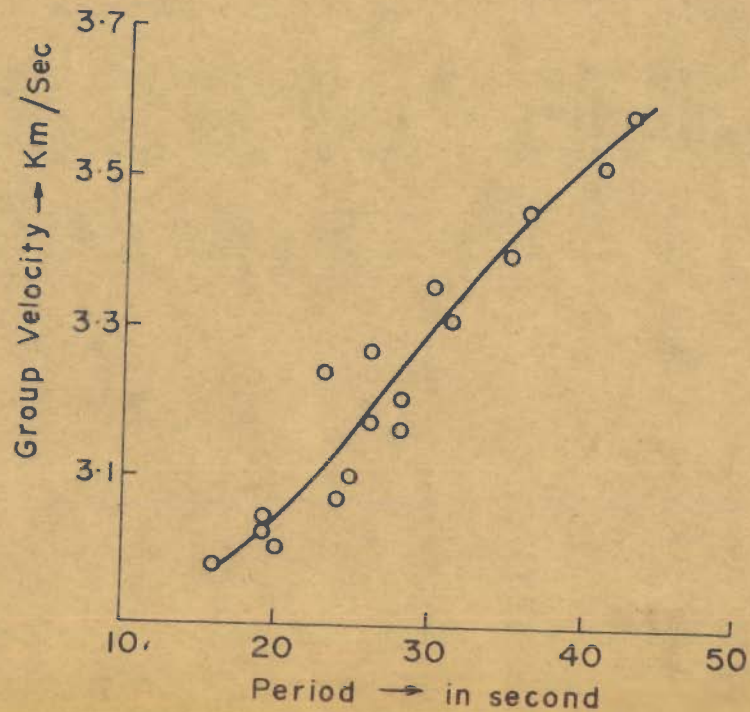


Table-4

CALCULATION OF GROUP VELOCITIES

Recording station: Shillong

Origin time : 15 hrs 20 min 13.9 sec

Component : N-S

Epicenter : 28.2° N 52.7° E

Epicentral distance: $\Delta = 3,877$ km

Phase	Arrival time			Travel time			$(n+x)-(n+x-1)$	Period $2[(n+x)-(n+x-1)]$	Group vel. $\frac{\Delta}{(3)}$	Average group velocity for (5)
	(1)	(2)	(3)	(4)	(5)	(6)				
	h	m	s	m	s	sec	Sec	Sec	Km/Sec	Km/Sec
n	15	38	04.6	17	50.7	1070.7			3.621	
n+1		38	26.0	18	12.1	1092.1	21.4	42.8	3.550	3.585
n+2		38	46.4	18	32.5	1112.5	20.4	40.8	3.485	3.518
n+3		39	04.5	18	50.6	1130.6	18.1	36.2	3.430	3.457
n+4		39	22.0	19	08.1	1148.1	17.5	35.0	3.378	3.401
n+5		39	37.0	19	23.1	1163.1	15.0	30.0		3.356

contd ...

Table-4 Continued

	(1)	(2)	(3)	(4)	(5)	(6)	(7)
	h m s	m s	Sec	Sec	Sec	Km/sec	Km/sec.
n+5	15 39 37.0	19 23.1	1163.1			3.334	
				15.6	31.2		3.312
n+6	39 52.6	19 38.7	1178.7			3.290	
				12.9	25.8		3.272
n+7	40 05.5	19 51.6	1191.6			3.254	
				11.5	23.0		3.239
n+8	40 17.0	20 03.1	1203.1			3.224	
				14.0	28.0		3.205
n+9	40 31.0	20 17.1	1217.1			3.186	
				13.0	26.0		3.169
n+10	40 44.0	20 30.1	1230.1			3.152	
				14.0	28.0		3.135
n+11	40 58.0	20 44.1	1244.1			3.117	
				12.1	24.2		3.102
n+12	41 10.0	20 56.1	1256.1			3.087	
				12.0	24.0		3.072
n+13	41 22.0	21 08.1	1268.1			3.057	
				9.4	18.8		3.046
n+14	41 31.4	21 17.5	1277.5			3.035	
				9.6	19.2		3.042
n+15	41 41.0	21 27.1	1287.1			3.012	
				10.0	20.0		3.000
n+16	41 51.0	21 37.1	1297.1			2.988	
				8.0	16.0		2.980
n+17	41 59.0	21 45.1	1305.1			2.972	

2.6 STANDARD LOVE WAVE DISPERSION CURVES & DIVISION OF EURASIA:

Santô (1961), in his study of Love waves along various paths to Japan, summarized the Love wave dispersion into eleven categories. He has also shown the various paths around Japan which are responsible for these eleven different dispersion curves. Earthquakes with their epicenters in Northeastern India, Western China, Sinkiang province and Northern Burma and recorded in Japan belong to dispersion curve 6. Figure 7 shows these paths plotted on the Rayleigh wave group velocity division map.

Calculations reveal that the Rayleigh waves travelling along these paths correspond to the number 8 standard Rayleigh wave dispersion curve of Santo (1965-B). Hence Santô's (1961) previous Love wave dispersion curve number 9 has been adopted as number 8 in the present study. Similar correspondence holds as follows:

	Region				
Santô's (1961) Love wave study for various paths to Japan	7	8	9	10	11
Present Love wave study for Eurasia	6	7	8	9	10

Validity of this adoption is further supported by some simple cases. For example, the earthquake of 17th May, 1965, recorded at Poona, traversed only region 7 of the Rayleigh wave division. The Love wave dispersion curve for this path is in good agreement with the adopted number 7 Love wave dispersion curve.

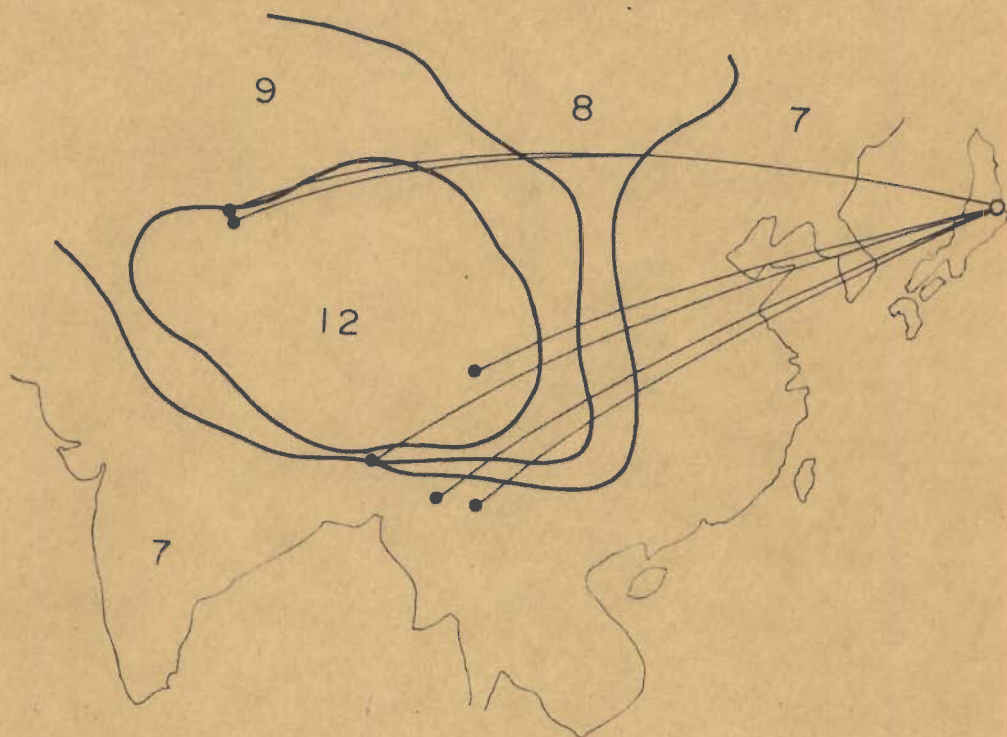


Fig. 7. EARTHQUAKES AROUND HIMALAYA AND TIBET PLATEAU REGION AND THEIR WAVE PATHS TO JAPAN

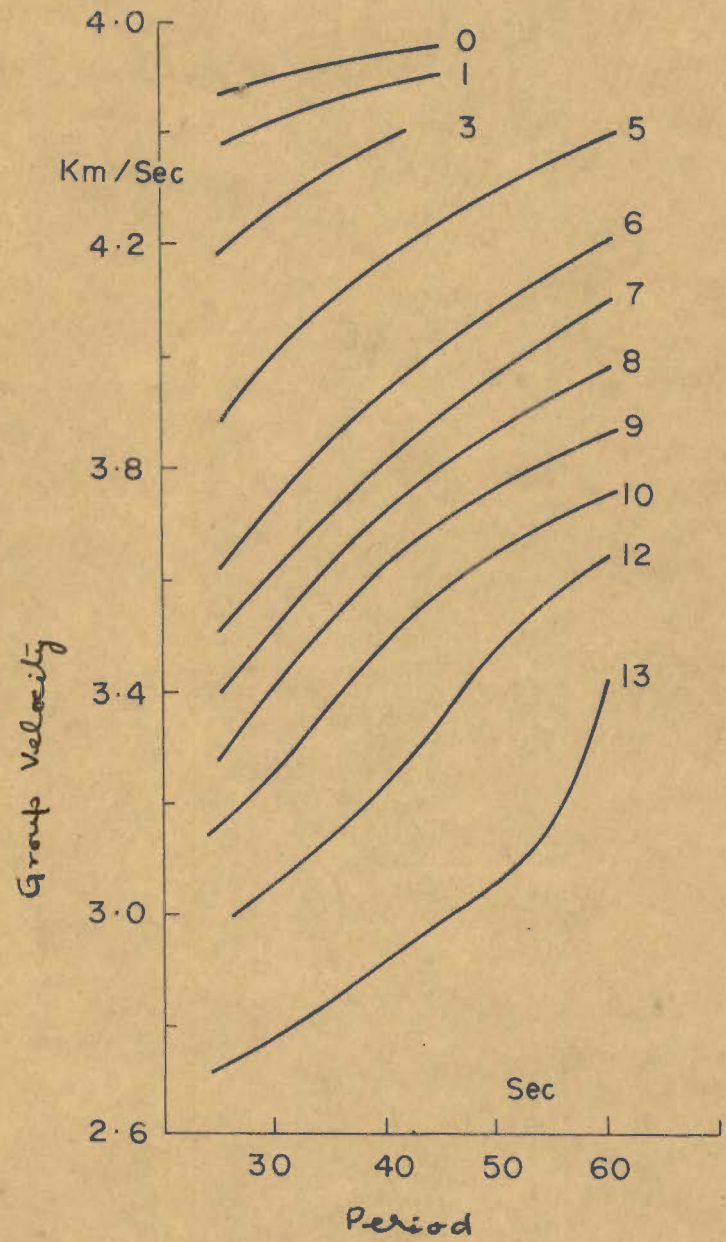


Fig. 8. STANDARD LOVE WAVE DISPERSION CURVES



Fig. 9
LOVE WAVE DISPERSION REGIONS
● Epicenters
○ Recording stations

For obtaining Love wave dispersion curves-numbers 0, 1, 3 and 5 such paths are chosen which traverse one of these unknown regions and the other known regions i.e. 6, 7, 8, 9 or 10 on the Rayleigh wave division. Then, after subtracting the time corresponding to these known regions from the total travel time, group velocities for the unknown regions are calculated. However, curve numbers 12 and 13 were taken to explain exceptionally low group velocities across the Himalaya and Tibetan Plateau (details given under discussion). By successive approximation the dispersion curves and the division pattern are adjusted, so that using the 'crossing path technique', the calculated travel time $\sum \Delta i/U_i$ (where Δi is the length of segment in region i and U_i is the corresponding group velocity), is within $\pm 1\%$ of the observed travel time for a particular period.

In all cases, these calculations are made for 30, 35, 40 and 45 sec periods. However, in some cases, these are extended up to 60 sec. Figure 8 and Table 5 show the standard Love wave group velocity dispersion curves and Figure 9 shows the division pattern of Eurasia. Table 6 gives the frequency distribution of $(T_o - T_c)/T_o$ for all cases.

2.7 DISCUSSION

The basic element in this study is the areal division of Eurasia based upon the Rayleigh wave dispersion study by Santô (1965-B). When necessary, this division has been

Group velocities (km/sec) of Love waves for various standard dispersion curves at different periods in sec.

Region	25	30	35	40	45
0	4.46	4.49	4.52	4.54	4.55
1	4.37	4.42	4.46	4.48	4.50
3	4.18	4.27	4.33	4.39	4.42
5	3.88	4.00	4.10	4.18	4.24
6	3.62	3.74	3.86	3.94	4.02
7	3.51	3.62	3.72	3.82	3.90
8	3.39	3.52	3.63	3.73	3.81
9	3.27	3.41	3.53	3.63	3.71
10	3.16	3.26	3.38	3.50	3.58
12	2.98	3.05	3.14	3.23	3.36
13	2.72	2.77	2.85	2.91	2.98

TABLE 6

Frequency Distribution of $(T_o - T_c)/T_o$

$(T_o - T_c)/T_o \cdot 100$	Number
+ 1.00	2
+ 0.75	2
+ 0.50	3
0.00	10
- 0.25	4
- 0.50	4
- 0.75	2
- 1.00	2
Sum	35

altered so as to conform with the observed Love wave dispersion. Principally, however, the two divisions are similar, i.e. the regions with low (or high) Rayleigh wave velocities correspond to regions with low (or high) Love wave velocities.

2.7 .1 HIMALAYA - TIBET PLATEAU REGION:

Exceptionally low group velocities are observed in the Himalaya and the Tibetan Plateau region. For the earthquake of 17th May, 1965 the calculated travel time of Love waves at Kevo and Nurmijarvi was equal to the observed time and at Kongsberg 0.8% greater than the observed time. These paths traverse region Numbers 7, 8, 9 and 10. But the observed time of Love waves recorded at Shiraz, was 9.0% larger than the calculation, which traverse the 12th region of the Rayleigh wave division (assuming a 3.2 km/sec group velocity for 40 sec period). The identification of Love waves was indisputable. Figure 10 shows the N-S and vertical component of the seismograms and Figure 11 the particle motion. Similarly, very low group velocities were obtained for other paths including the Himalaya and the Tibetan Plateau region. Hence, taking into consideration the geomorphological setting of the Tarim basin and elevations above 15,000 ft as the guiding factors, a new region No. 13 was formed for this very high mountainous region. Standard dispersion curves number 12 and 13 were obtained by calculating the travel time corresponding to these regions from the

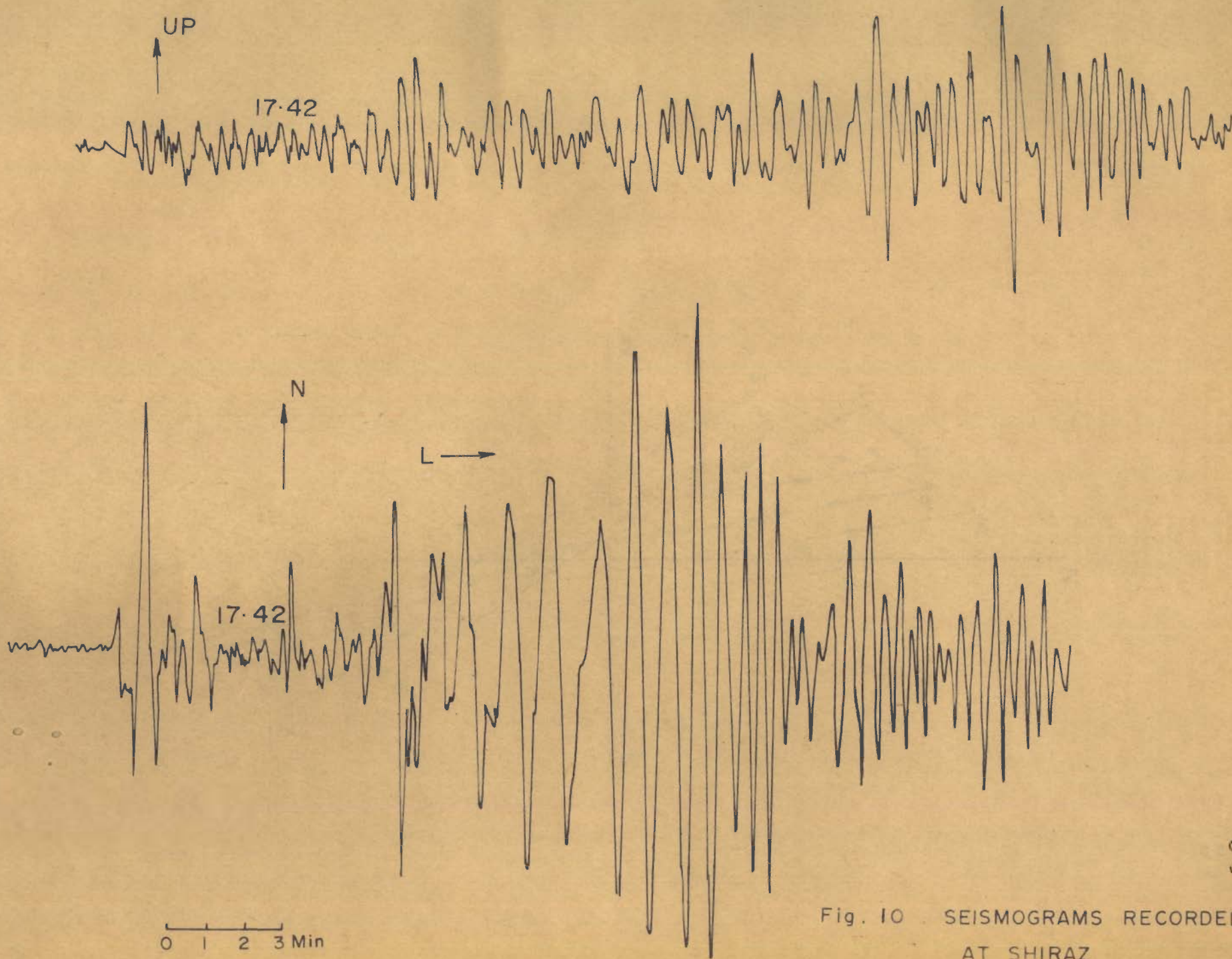


Fig. 10 SEISMOGRAMS RECORDED
AT SHIRAZ

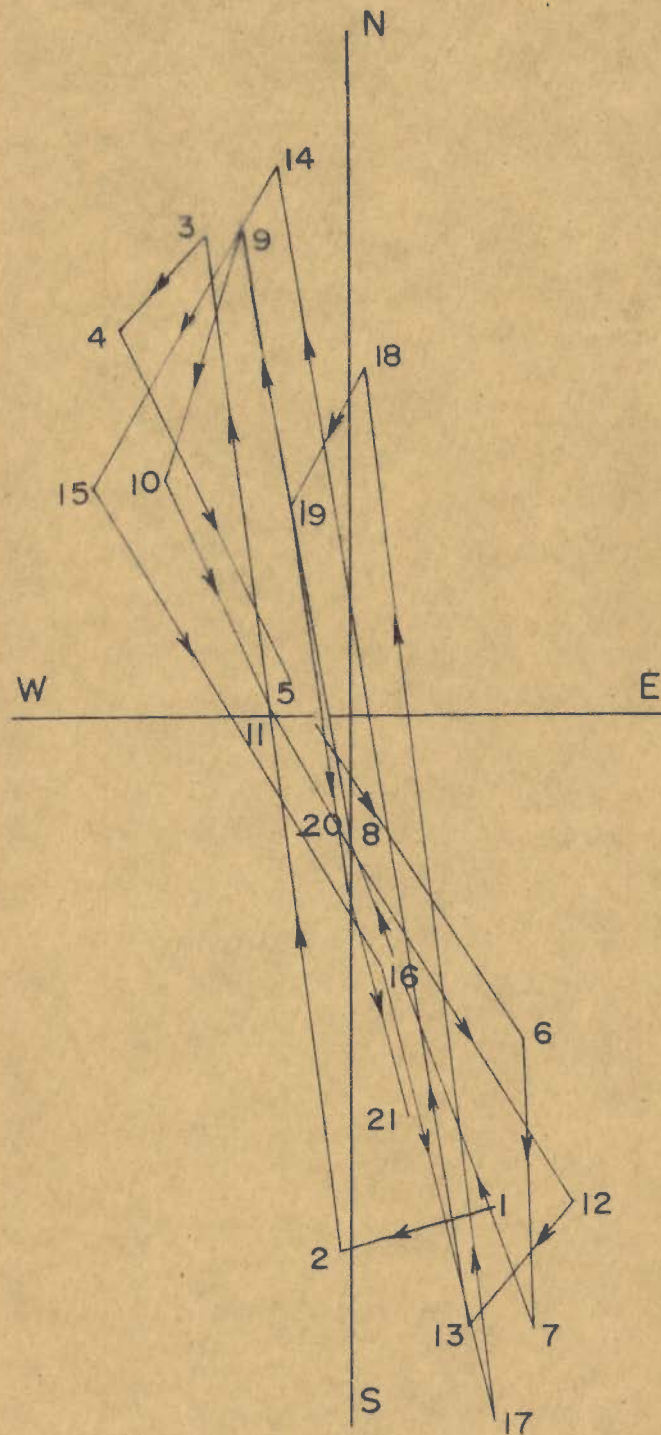


Fig II. ORBITAL MOTION OF SHIRAZ SEISMOGRAM
(From Fig. 10)

total path for different periods. Table 7 shows some examples. Very low group velocities in this region were earlier obtained by Gupta and Narain (1967). Other workers such as Porkka (1961), Stoneley (1955), Tandon and Chaudhury (1963), have also contributed the lower average group velocities for paths crossing the Himalaya and the Tibetan Plateau region to the thick crust beneath them.

In Figure 9, the concentration of the regional contours towards the Indian Subcontinent and their relative sparseness to the north of the Himalaya and the Tibet Plateau is also remarkable. This probably reflects the underground crustal structure. In the south, from the low level Indogangetic planes, the elevation increases within a very short distance to the high peaks of Himalaya, whereas towards the north, from the plateau of Pamir and Tarim basin the elevation decreases gradually. Hence it is likely that the crust thickens rapidly from beneath the Indogangetic planes to the high mountainous regions and thins out gradually towards the north. Another important fact is the rapid increase of the group velocities with period on curve numbers 12 and 13 (see Figure 8). It seems that the mountain roots in this region will affect the shorter period Love waves more than those with longer periods.

In the foot hills of the Himalaya, region 10 has been introduced and region 9 is extended to the Indogangetic planes where thick sediment is known to exist. This explains the observed dispersion of Love waves at Shillong from the earthquake of 19th August, 1964, and at Shiraz for the earthquake of 22nd January, 1964. Both mainly traversed the foot hills of the Himalaya. Earlier work by Chaudhury (1966) also supports this extension.

2.7 .2 OTHER REGIONS:

The region 6 in East Siberia in the Rayleigh wave division is not delineated by Love waves. Considering it to be region 7, the calculated time agreed with the observed time.

The existence of region 10, corresponding to the high mountainous type, in the water-covered area around Novaya Zemlya and Baltic Sea - an unexpected result according to Santô (1965) is found to hold good for Love waves also. This region around Novaya Zemlya required further eastward extension up to the southern end of Severnaya Zemlya. These low group velocities are probably due to a thick soft sedimentary layer in the sea, similar to those reported by Shurbet (1960) for the Gulf of Mexico.

Another worth mentioning change has occurred in Turkey, the Caucasian Mountains and the Persian regions. These regions (mostly numbers 7 and 9 according to the

Rayleigh wave division) are replaced by number 10 to explain the Love waves recorded at Istanbul and Athens from the earthquake of 21st June, 1965. In western Europe around the Alps, Yugoslavia and Rumania, regions 8 and 9 have been extended, based upon Love wave paths crossing these regions.

Figure 12 shows Porkka's (1961) Love wave group velocity data for paths between (a) Japan and Helsinki and (b) Tibet and Helsinki, and the standard Love wave dispersion curve for numbers 7, 8, 9 and 10. It is interesting to note that the Love waves recorded from the earthquake around Japan show distinctly higher group velocities than those from the Tibet region; the former falls around the curve number 8 and the latter between curve numbers 9 and 10.

The above mentioned are the major differences between the Love wave and the Rayleigh wave division pattern of Eurasia.

2.7 .3 RAYLEIGH VERSUS LOVE WAVE GROUP VELOCITIES:

Since the regionalisation of Eurasia by Love wave dispersion agrees reasonably well with the Rayleigh wave division, a comparison of the Rayleigh wave and Love wave group velocities for the same numbers is made. Table 8 shows the group velocity ratio of Rayleigh to Love waves for 30 and 40 sec period. The minimum value of this ratio

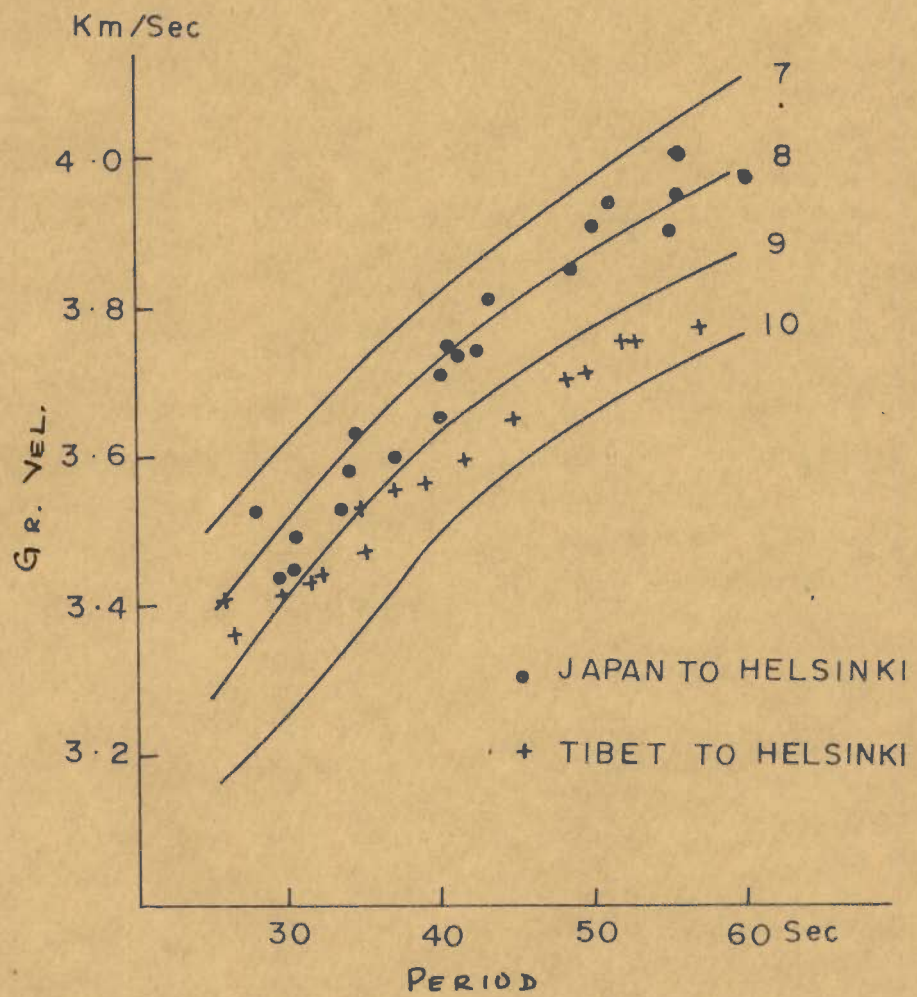


Fig.12. LOVE WAVE DISPERSION AS OBSERVED AT HELSINKI (PORKKA, 1961)

Table 8
Rayleigh to Love wave group velocity ratios for
30 and 40 sec period

Region	T = 30 sec			T = 40 sec		
	Rayleigh wave Velocity	Love wave velocity	Ratio	Rayleigh wave velocity	Love wave velocity	Ratio
	km/sec	Km/sec		Km/sec	Km/sec	
0	4.08 /	4.49 =	0.91	4.16 /	4.53 =	0.92
1	3.99 /	4.42 =	0.90	4.06 /	4.47 =	0.91
3	3.86 /	4.27 =	0.90	3.94 /	4.38 =	0.90
5	3.66 /	4.00 =	0.92	3.83 /	4.18 =	0.92
6	3.52 /	3.74 =	0.94	3.71 /	3.94 =	0.94
7	3.36 /	3.62 =	0.93	3.59 /	3.82 =	0.94
8	3.24 /	3.52 =	0.92	3.51 /	3.73 =	0.94
9	3.06 /	3.41 =	0.90	3.40 /	3.63 =	0.94
10	2.98 /	3.26 =	0.91	3.30 /	3.50 =	0.94
12	2.68 /	3.05 =	0.88	3.06 /	3.24 =	0.94

is 0.88 (region 12, period 30 sec) and the maximum value is 0.94 (region 6 and 12 period 30 and 40 sec). It is remarkable that this ratio for most of the cases is around 0.91. No such correlation could be made for Love wave dispersion curve number 13 since this region was not delineated by Rayleigh wave study.

2.8 CONCLUSIONS:

Love wave group velocity along various sections in Eurasia has been investigated, and it reveals that:

1. It is possible to divide Eurasia into different regions having similar group velocity dispersion characteristics.
2. This division supports Santô's (1965-A) division of Eurasia based on Rayleigh wave group velocity observations.
3. Extremely low group velocities, probably the lowest in the world, are observed in the Himalaya and the Tibet Plateau regions.
4. In general, a good agreement is observed between the division pattern and the regional elevation.

CHAPTER-III

CRUSTAL STRUCTURE IN HIMALAYA AND TIBET PLATEAU

CRUSTAL STRUCTURE IN HIMALAYA AND TIBET PLATEAU *

3.1 INTRODUCTION:

In the second chapter, Love wave dispersion along various paths crossing Eurasia was studied and Eurasia was divided into different regions of similar group velocity dispersion character of Love waves. This divisioning pattern was compared with Rayleigh wave division pattern and both were found to be similar. It is interesting to note that Rayleigh as well as Love wave group velocities are found to be lowest for the Himalaya and the neighbouring Tibet Plateau.

3.1 .1 THE CONCEPT OF ISOSTASY AND ROOTS OF MOUNTAINS:

It has been observed in the computation of Bouguer anomalies that over the deep oceans, where the Bouguer correction is made by replacing the sea water with earth material of average crustal density, the anomalies are generally positive. Whereas for elevated surfaces, well above the sea level, Bouguer anomalies are mostly found to be negative. For land areas near sea level, the average Bouguer anomaly is close to zero. These observations suggest that beneath the oceanbottoms the density of the rocks is greater than normal; while beneath the elevated land masses, below the geoid, it is less than normal.

* A part of this chapter has been published in the Bulletin of Seismological Society of America. Vol.47 (1967) pp.235-248.

The concept of isostasy proposes that the excess of mass above sea level, as in the mountain system, is compensated by a deficit below sea level, so that at a certain depth the total weight per unit area is equal all around the world. This particular depth is known as the depth of compensation. The concept owes its origin to a precise triangulation survey carried out in the foot-hills of Himalaya in India during the middle of the nineteenth century. A discrepancy of 5" (500 ft) between the distance of two stations (about 375 miles away on a north - south line) was found, as measured geodetically and their separation as computed from astronomic observations. Though 500 ft. appears to be negligible enough over a distance of 375 miles, but the precision of the triangulation was too good even to account for this discrepancy. Figure 13 shows the position of the two stations Kaliana and Kalianpur w.r.t. Himalaya. Kaliana is in the foot-hills of Himalaya while Kalianpur is far away in plains. To explain the discrepancy in distance, J.H.Pratt conceived that the mass of the Himalaya would tend to deflect the plumb line north ward at both stations, but more at Kaliana than Kalianpur. Since such deflection would tend to deviate the plumb line from actually pointing to the centre of the earth, the astronomic computations would be erroneous. Pratt considered the horizontal attraction of Himalaya and was surprised to find that the calculated discrepancy worked out to be 15" in latitude instead of 5". He presented a paper (1855) on his calculations and two months later Airy (1855) offered a solution explaining that:

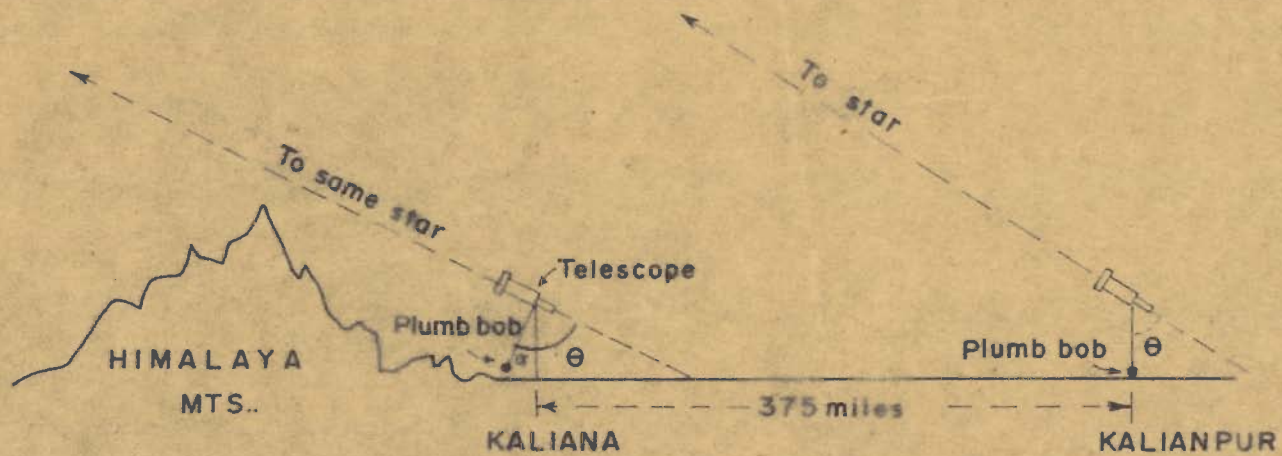


Fig.13. SCHEMATIC REPRESENTATION OF THE DEVIATION α OF PLUMB LINE DUE TO ATTRACTION OF HIMALAYA AT KALIANA, ASSUMING PLUMB LINE TO BE NORMAL AT KALIANPUR

"The state of earth's crust lying upon the lava may be compared with perfect correctness to the state of a raft of timber floating upon the water; in which, if we remark one log whose upper surface floats much higher than the upper surfaces of the others, we are certain that its lower surface lies deeper in the water than the lower surfaces of the others".

Accordingly, crustal material beneath Himalaya penetrating into a heavier sub-stratum would account for a deficiency of mass below it and the crust under deep oceans would be thinner than under land surfaces at or near sea level. The roots of Himalaya being lighter than the surrounding material would reduce the effect of the mass of Himalaya on the plumb line. If the compensation were complete, the two effects would nullify each other. In case of Himalaya, according to Airy's hypothesis this compensation has reduced the residual effect to one-third of what it would have been other wise (Figure 14).

Four years later, Pratt (1859) proposed an equally plausible different explanation for his observations. He agreed that the excess mass beneath the mountains had to be compensated by a deficit below the sea level, but he supposed the crust to have a uniform thickness below the sea level everywhere and its base supporting the same uniform weight over unit area. Accordingly the crust beneath mountains would be composed of less denser material than the crust beneath the oceans. Figure 15 explains Pratt's hypothesis.

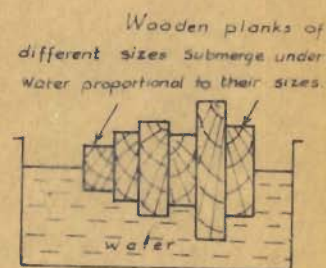
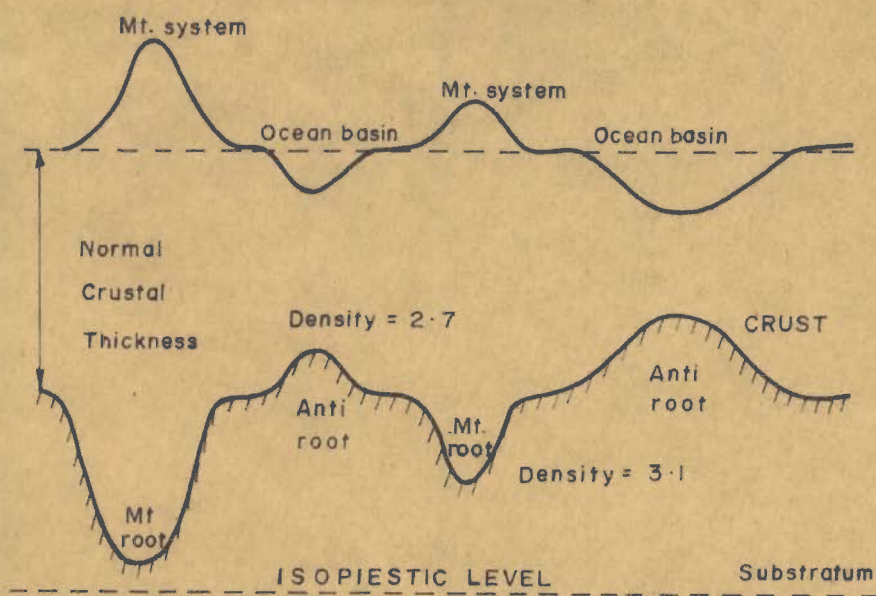


Fig. 14. AIRY'S (1855) EXPLANATION OF ISOSTASY

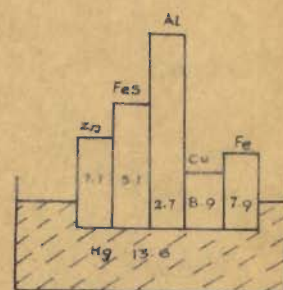
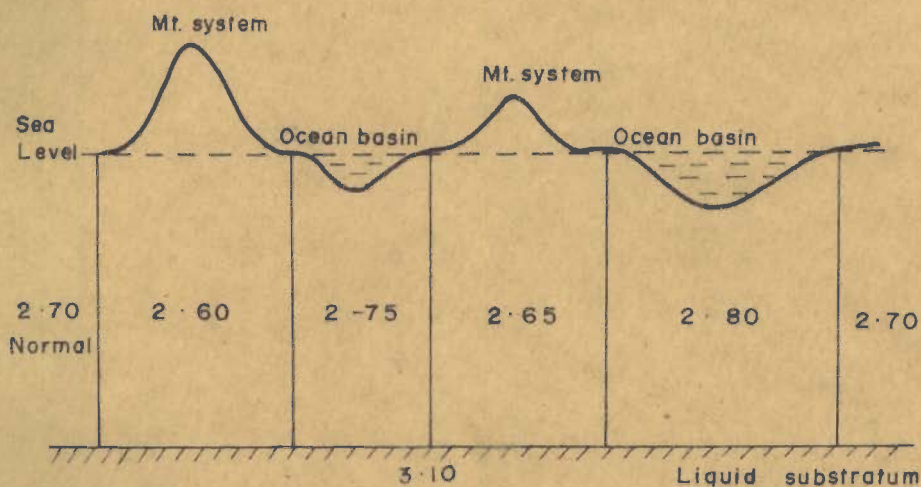


Fig. 15. PRATT'S (1859) EXPLANATION OF ISOSTASY

3.1 .2 INVESTIGATIONS OF ROOTS OF MOUNTAINS:

For over a century now, Pratt's and Airy's hypothesis have been subjected to controversies. Some investigations support the existence of roots beneath high land masses while others do not.

The pioneering work in this field was carried out by Gutenberg (1933) when he confirmed the existence of roots for the Alps in Europe by studying the travel time of longitudinal waves across it. Byerly (1938) reported a delay of few seconds across Sierra Nevada for longitudinal waves. The existence of roots was endorsed by Caloi (1958) for the Alps and by Gutenberg (1943) and Byerly (1956) for the Sierra Nevada. Studies have been carried out by Savarensky and Ragimov (1958), Ewing and Ewing (1959), Press (1960), Cisternas (1961), Thompson and Talwani (1964) for different other regions. An extremely interesting profile across the Pacific coast of Southern America, near Chile, has been discussed by Woolard (1965). The probable crustal section along this profile across the continental boundary, based upon explosion seismology data, is shown in Figure 16. This profile also explains the regional Bouguer gravity anomalies very well and shows a considerable thickening of the crust beneath the altiplano near Antofagasta.

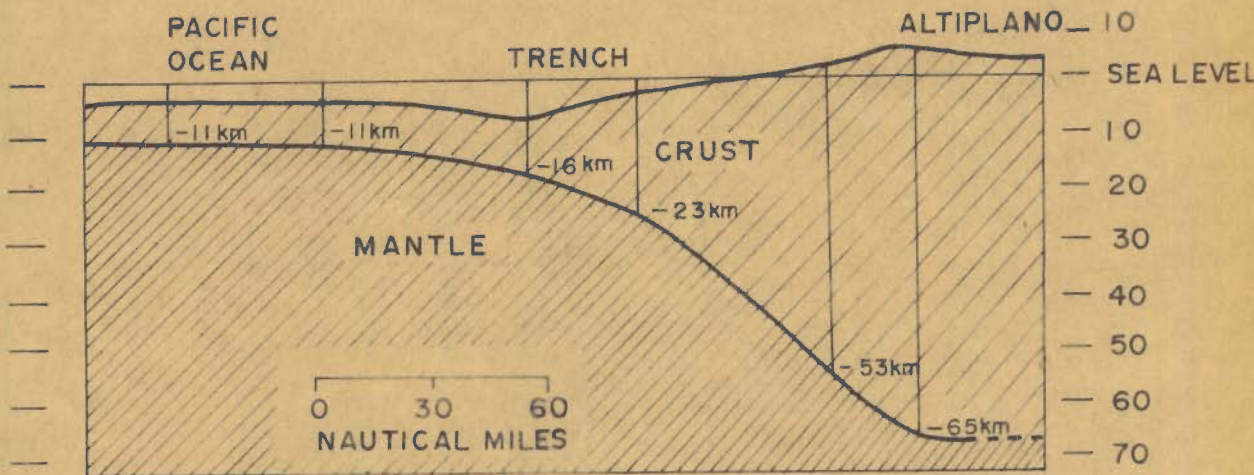


Fig. 16. CRUSTAL SECTION ACROSS CONTINENTAL BORDER OF WESTERN SOUTH AMERICA (WOOLARD - 1965)

Detailed crustal investigations have been carried out in U.S.S.R. A number of the results have been discussed by Kosminskaya and Riznichenko (1964) and Kosminskaya (1965). From these results they conclude that in Eurasia, in general, considerable thickening of the consolidated crust is observed in mountain regions.

The International Geophysical Year gave a big impetus to the crustal investigations and a lot more unknown areas were studied. Veitsman and Kosminskaya (1965) have summarized these studies.

By and large, seismological work seems to substantiate the Airy's hypothesis of isostasy of roots under mountains. However, in certain areas seismological data suggest that the crustal thickness is the same or even less under certain mountain systems compared to the coastal planes. Pakiser and Steinhart (1964) in their report on "Explosion Seismology in the Western Hemisphere" conclude that high mountains have roots at many places while at others they do not. The crust in the Sierra Nevada thickens to more than 50 km compared with about 30 km in the Basin and Range Province to the east, whereas the crust beneath the northern Rocky mountains is thinner than the crust in the Great Plains farther east.

Our knowledge of the thickness of the crust beneath Himalaya - the highest mountains in the world and the neighbouring Tibet Plateau is very limited. Stonely (1955),

Tandon and Chaudhury (1963) and Saha (1965) have observed higher average crustal thickness from surface wave dispersion studies for paths crossing the Himalaya and Tibet Plateau. From this they have inferred greater crustal thickness beneath Himalaya and Tibet Plateau region.

Datta (1961) has obtained a delay of 4 sec in Pn travel times for ray paths which have penetrated the roots to those which have not. This he explains by an extra crustal thickening of 20-25 km beneath Himalaya. However, his model has been discarded by Roy and Jain (1968) and assuming a more realistic model and considering gravity anomalies they have concluded a crustal thickening of 20-24 km below Himalaya.

Qureshy (1968) has recently reviewed the available Free Air, Bouguer and Isostatic anomaly data along with seismological, aeromagnetic and deep drilling data for the Peninsular Shield, Indogangetic Planes and Himalaya and concluded the general validity of Isostasy in India. Based upon a gravity profile running from Gaya to as close as 25 km areal distance from the Mount Everest, Qureshy (1968) has calculated a crustal thickness of 81 km for the middle Himalaya (Results based upon Airy-Heiskanen anomalies).

Among the seismic methods, deep seismic sounding gives the most reliable results for crustal investigations.

In principle the deep seismic sounding method is same as seismic prospecting method for mineral exploration in geophysical prospecting. Usually a number of seismographs are set up in a straight line and these seismographs receive signals from several shot points placed along that line. (The techniques & interpretational details have been discussed by Steinhart and Meyer - 1961).

Another method, named as the profile seismological observation method (PSO) by the U.S.S.R. seismologists, makes use of the signal generated by irregularly functioning sources; i.e. natural earthquakes, mining and industrial explosions etc. One of the distinguishing feature of the PSO is that the stations are set up approximately along straight lines and analysis is carried for signals coming from epicenters lying near this line.

3.2 STATEMENT OF THE PROBLEM:

Keeping in view the scanty information available about the crustal structure beneath the Himalaya, as mentioned before, it is important to delineate the same and find out whether Airy's hypothesis or Pratt's hypothesis of isostatic compensation holds good for this region.

In the absence of facilities for explosion seismology and the lack of a sufficiently large number of seismological observatories suitably situated for profile seismological observations, the study of dispersion of surface waves and travel time studies of body waves recorded at sparsely distributed seismological observatories remain the only

seismological methods to study the crust in this region.

The problem has been tackled in the following two ways:-

1st case:

Dispersion of the fundamental mode of the Rayleigh and Love surface waves recorded at conveniently situated stations; where the entire path is continental and where for comparison purposes great circle paths to some recording stations go under the Himalaya and Tibet Plateau region, has been studied. The difference in characteristics of the dispersion curves for the paths passing below the Himalaya and those not passing below it has been investigated. The observed dispersion curves are then compared with suitable theoretical dispersion curves for the estimation of crustal thickness below Himalayas. This is discussed in Part I.

2nd case:

Rayleigh wave dispersion along a number of great circle paths crossing the region '12' of Santô's (1965) division of Eurasia (region '12' approximately encompasses the high Himalaya ranges) has been studied. Using Santô's (1965) standard Rayleigh wave dispersion curves, the travel time of these paths corresponding to the segments in region '12' has been calculated and from this the group velocities for region '12' have been determined. Later, group

velocities thus obtained for different sections of region '12' are compared with suitable theoretical dispersion curves and the crustal thickness has been estimated. This is discussed in Part II.

Only vertical component seismograms have been used for Rayleigh wave dispersion studies. To make sure that the first longperiod waves recorded are Rayleigh waves and are not mixed with long-period S wave reflections, the phase difference between the vertical and the longitudinal components are measured and found to be of the order of 90° . In doubtful cases, particle motion has been also plotted from the vertical and the longitudinal components for confirming the identity of Rayleigh waves by retrograde elliptical movement.

3.3

PART I

3.3 .1 OBSERVATIONAL DATA:

For the above mentioned study, the earthquake of 25th August 1964, (Epicenter 78.17° N, 126.65° E ; origin time 13 hrs 47 min 20.6 sec; magnitude 6.1; depth of focus 50 km - U.S.C.G.S.), east of Severnaya Zemlaya was found suitable. Rayleigh waves from this earthquake are very well developed at Seoul, Hong Kong, Shillong, New Delhi and Quetta. ~~seismograms~~. Love waves are very clearly recorded on the Hong Kong and New Delhi records. Table 9 gives the particulars of these stations.

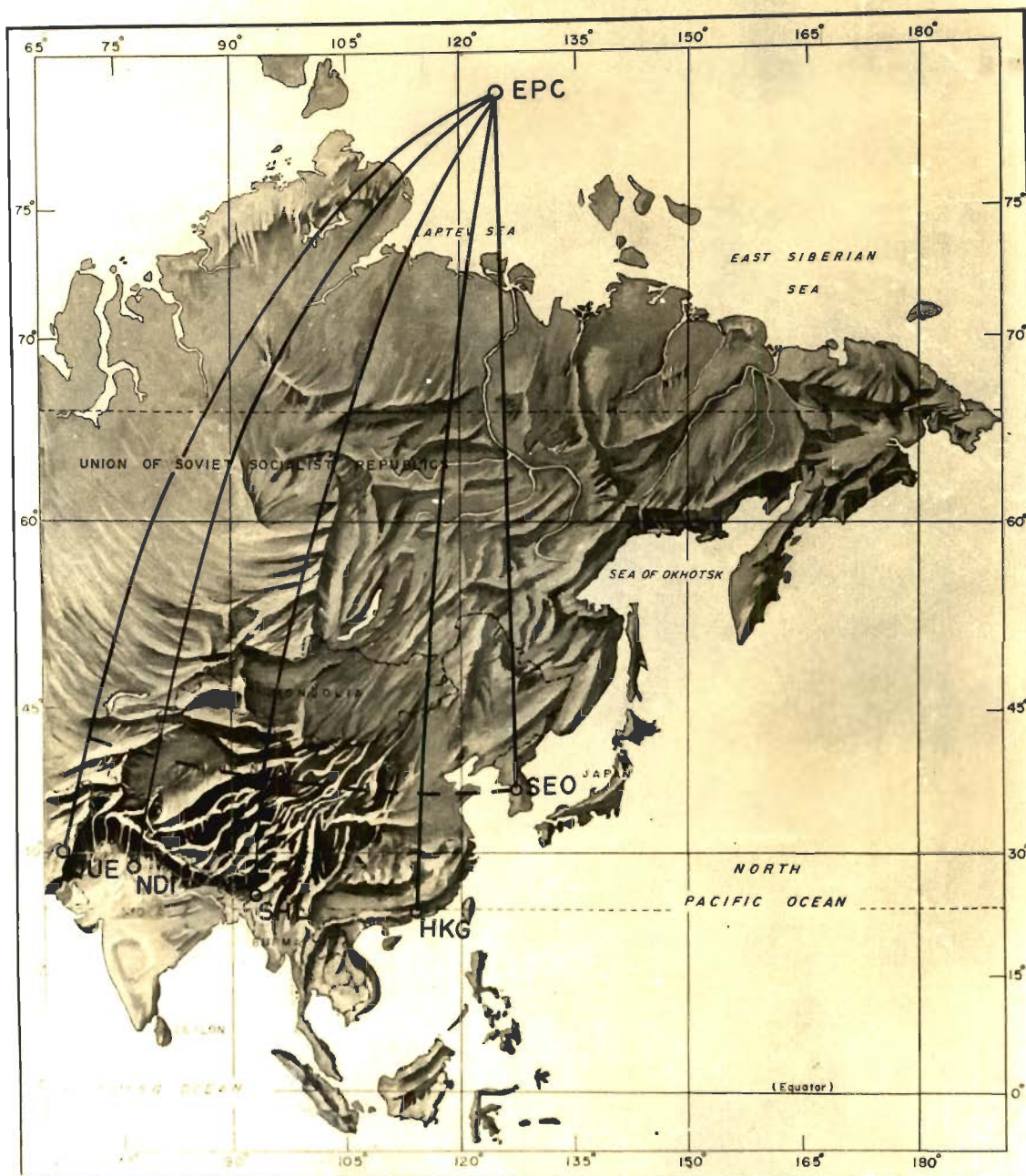
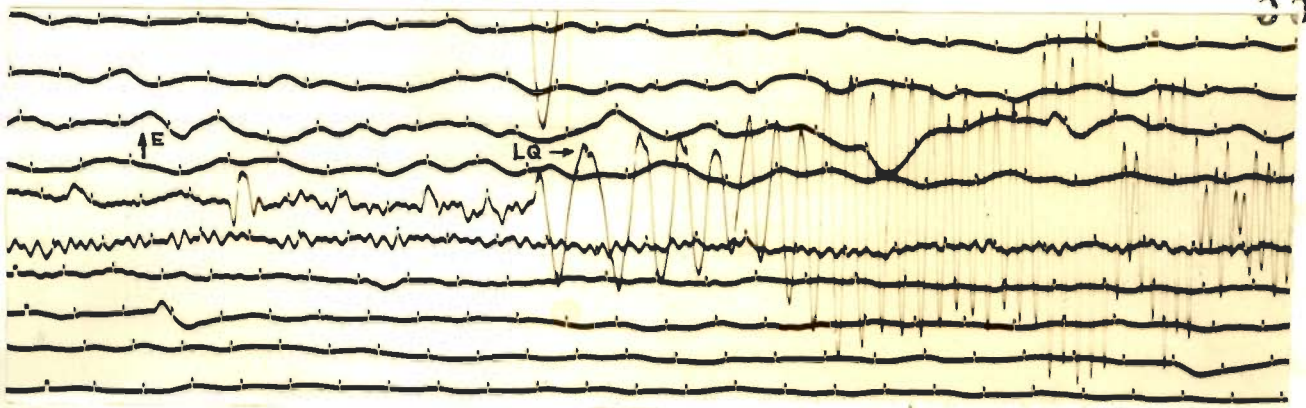
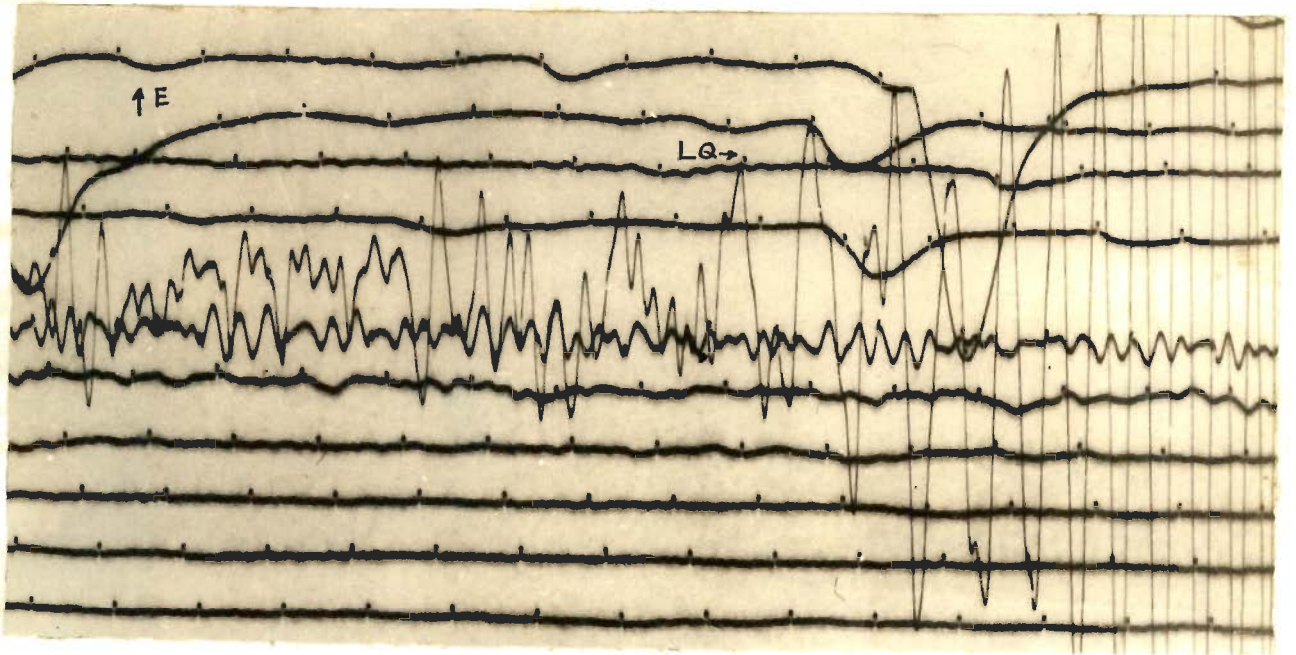


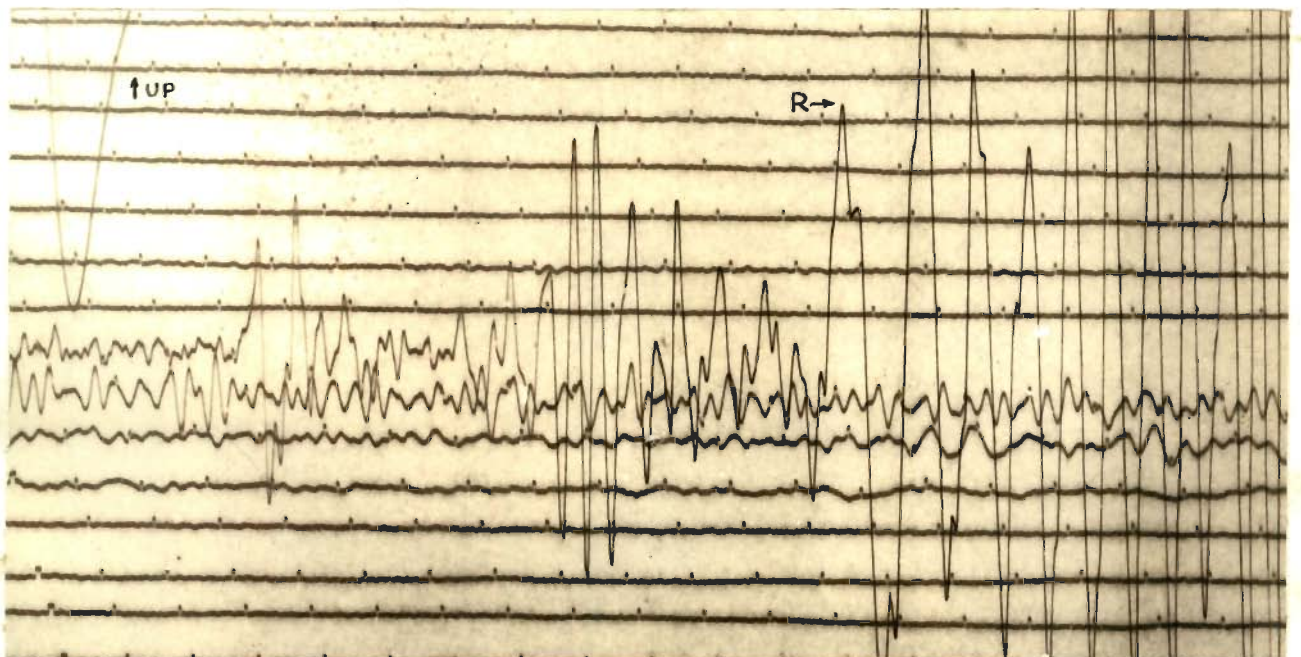
Figure 17. Relief map of Asia (based on 'Chart of the World' H.O. 1262 A published by U.S. Naval Oceanographic Office) showing the epicenter, recording stations and the great circle paths.



Hong Kong E-W Component



New Delhi E-W Component



New Delhi Z Component

Figure 18. Section of three seismograms showing typical Love and Rayleigh Wave Dispersion.

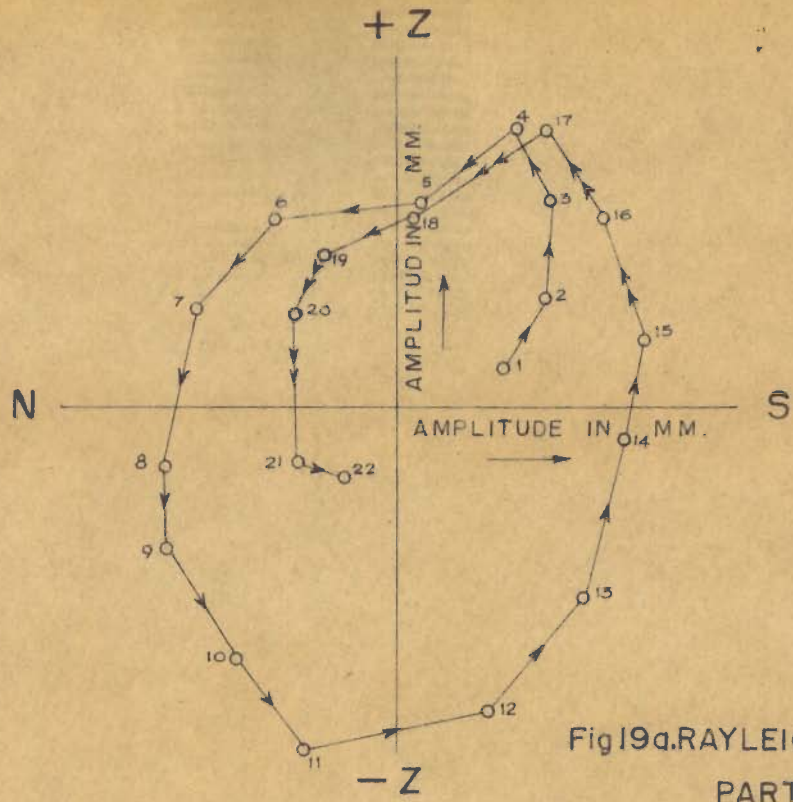


Fig.19a.RAYLEIGH WAVE -
PARTICLE MOTION

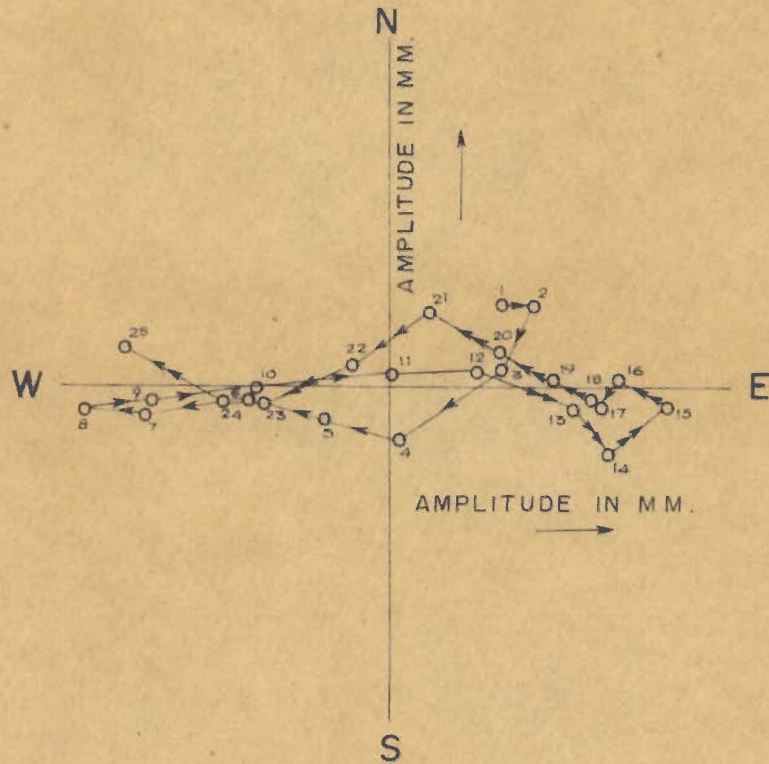


Fig.19 b.LOVE WAVE - PARTICLE MOTION

Table - 9
Particulars of W.W.S.S. Stations (Chapter III Part I)

Station	Latitude	Longitude	Type of instrument	Period of the Seismo-meter	Period of the Galvano-meter	Mag. at 30 sec period
			Long period	sec	sec	
Seoul (SEO)	37 34 00 N	126 58 00 E	N-S, E-W, Z	30	100	1,500
Hong Kong (HKG 45)	22 18 13 N	114 10 19 E	do	30	100	750
Shillong (SHL 105)	25 34 00 N	91 53 00 E	do	30	100	3,000
New Delhi (NDI 75)	28 41 00 N	77 13 00 E	do	30	100	1,500
Quetta (QUE 92)	30 11 18 N	66 57 00 E	do	30	100	3,000

The epicenter lies almost due north of Hong Kong and New Delhi and the great circle paths to these stations extend an angle of $3\frac{1}{2}^{\circ}$ and 26° respectively with N-S line (Figure 17). Hence E-W component seismograms have been used for Love wave dispersion studies, where they are recorded as a continuous train of waves with gradually decreasing period. No sudden change is observed corresponding to the onset time of Rayleigh waves in the vertical component seismogram. Figure 18 shows the seismograms and Figure 19 particle motion plotting.

The travel paths from epicenter to the recording station (Figure 17) are entirely continental since the epicenter lies on 100 fathom depth contour i.e. well within the continental shelf. Group velocities for both, Rayleigh and Love waves, are determined by Ewing and Press (1952) method. Crest and trough numbers are plotted against the arrival times. Period is obtained from the slope of these graphs and group velocities are obtained by dividing the epicentral distance by travel time. Since the operating characteristics of all the recording instruments are same, no phase corrections are applied to the travel times. Tables 10 and 11 give the group velocities, thus calculated for the Rayleigh and Love waves.

Table-10

Group velocities of Rayleigh waves

Epicenter Hong Kong		Epicenter Seoul		Epicenter Quetta		Epicenter Shillong		Epicenter New Delhi	
Period	Group velo- city (km/ sec)	Period	Group velo- city (km/ sec)	Period	Group velo- city (km/ sec)	Period	Group velo- city (km/ sec)	Period	Group velo- city (km/ sec)
sec		sec		sec		sec		sec	
60.0	3.76	52.6	3.76	66.0	3.71	58.5	3.60	71.0	3.76
55.8	3.74	41.7	3.62	55.0	3.61	50.3	3.46	61.5	3.67
49.7	3.72	34.7	3.49	46.0	3.53	46.0	3.37	52.0	3.62
44.0	3.66	30.0	3.34	39.3	3.38	35.0	3.17	45.4	3.49
39.4	3.58	24.9	3.20	34.7	3.23	28.0	3.02	38.0	3.35
33.7	3.45	22.2	2.98	32.0	3.09	25.5	2.94	33.6	3.20
28.9	3.34	19.5	2.92	27.5	2.96	24.0	2.89	29.8	3.04
26.3	3.23	18.5	2.85	24.3	2.82	20.5	2.85	23.2	2.89
22.6	3.02			20.0	2.79	18.5	2.80	18.7	2.76
20.8	2.93			17.2	2.68	13.0	2.68	15.2	2.81
18.0	2.85			16.0	2.58				
17.0	2.77								
13.0	2.73								

Table 11

Group velocities of Love waves			
Epicenter to Hong Kong		Epicenter to New Delhi	
Period in sec	Group velocity km/sec	Period in sec	Group velocity km/sec
68.0	4.18	58.0	3.90
60.0	4.10	53.5	3.85
50.6	3.97	46.7	3.70
45.0	3.92	41.0	3.63
39.4	3.83	36.0	3.56
33.7	3.69	34.2	3.49
29.3	3.54	29.9	3.36
24.0	3.38	27.0	3.32
20.8	3.27	23.6	3.23
19.1	3.17	20.9	3.16
18.8	3.08	18.9	3.03
16.0	2.96	18.0	2.96
15.0	2.90		

3.3 .2 THEORETICAL MODEL:

For comparison of the observed dispersion curves, a model with two layer crust overlying a homogeneous, semi-infinite elastic half space is found most suitable. Earlier work carried out in Eurasia supports the existence of both the granitic and basaltic layers. Nagmune (1956) and Shechkov (1964) have specifically mentioned that dispersion of Love and Rayleigh waves for the continental regions of Eurasia agreed with theoretical dispersion curves calculated for a two layer crust and not for a single layer crust. Similar are the findings of Tandon (1954), Kovach (1959), Saverensky and Shechkov (1961), Zverev (1962), Arkhangel'skaya (1964) and others. These conclusions are based upon the results obtained from explosion seismology, surface wave dispersion and body wave travel time studies. While in some regions the granitic layer is found to be thicker than the basaltic layer and in other areas the reverse is true; in large number of cases they are found to be of equal thickness. According to Riznichenko (1958), the roots of Tien - Shan Hercynian belt are mainly due to a thicker basaltic layer (30 km of basaltic layer and 20 km of granitic layer); while in the Alpidic belt of U.S.S.R., the granitic layer extends to 30 km in portions of West Turkmania and 40 km in North Pamir and the corresponding thicknesses of basaltic layers are only 20 and 30 km. From these considerations, a model of two-layer crust with equal thicknesses of granitic and basaltic layer is considered to be most suitable.

Theoretical dispersion curves have been computed for Rayleigh waves with different crustal thicknesses from the parameters determined by Stoneley (1955) for a three layer earth model using the following Jeffereys-Bullen layer parameters:

$$\begin{aligned} \alpha_1 &= 5.598 \text{ km/sec} & \beta_1 &= 3.402 \text{ km/sec} \\ \alpha_2 &= 6.498 \text{ km/sec} & \beta_2 &= 3.741 \text{ km/sec} \\ \alpha_3 &= 6.110 \text{ km/sec} & \beta_3 &= 4.340 \text{ km/sec} \\ \rho_1 &= 2.65 \text{ gm/cc} \\ \rho_2 &= 2.85 \text{ gm/cc} \\ \rho_3 &= 3.40 \text{ gm/cc} \end{aligned}$$

These layer parameters are in close agreement with the ones reported by Bune and Butovskya (1955), Rozova (1936) and others for Central Asia. Stoneley (1955) has considered three cases: $H_2 = H_1$, $H_2 = \frac{1}{2}H_1$ and $H_2 = \frac{1}{3}H_1$; where H_1 is the thickness of the granitic layer and H_2 that of the basaltic layer. (The details of the computation are given in Appendix I).

Love wave dispersion has not been computed for the same model. Dorman (1959) has computed dimensionless parameters for Love wave for a number of models. His case 201 with the following parameters has been used for the computation of theoretical dispersion curves for comparison with the observed dispersion curves:

$\beta_1 = 3.40$ km/sec	$\rho_1 = 2.74$ gm/cc	H/2
$\beta_2 = 3.83$ km/sec	$\rho_2 = 3.00$ gm/cc	H/2
$\beta_3 = 4.50$ km/sec	$\rho_3 = 3.30$ gm/cc	∞

The details of computation for different crustal thicknesses are given in Appendix II.

These theoretical models have been extensively used and found suitable by Russian workers for comparing the observational dispersion data in Eurasia. For example Saverensky and Shechkov (1961) found these models most appropriate for Rayleigh and Love wave observational group velocity dispersion data in Siberia and far east. Shechkov (1961, 1964) has used these models for comparing dispersion character along various paths in Eurasia and further assured the suitability of these models by confirming the findings by Deep Seismic Sounding data.

3.3 .3 INTERPRETATION AND DISCUSSION:

Figure 20 shows the observed dispersion and theoretical dispersion curves for Rayleigh waves. For periods greater than 30 sec, the Seoul and Hong Kong data fall between the theoretical curves for $H = 35$ km and $H = 37$ km. New Delhi and Quetta data lie on the 45 km curve. The scatter is less than 0.05 km/sec. Shillong data lie slightly below the 45 km curve for periods greater than 40 sec. The scatter in the short-period range is most probably due to the presence of different sections of sedimentary layers and due to the waves arriving along paths other than the great circle.

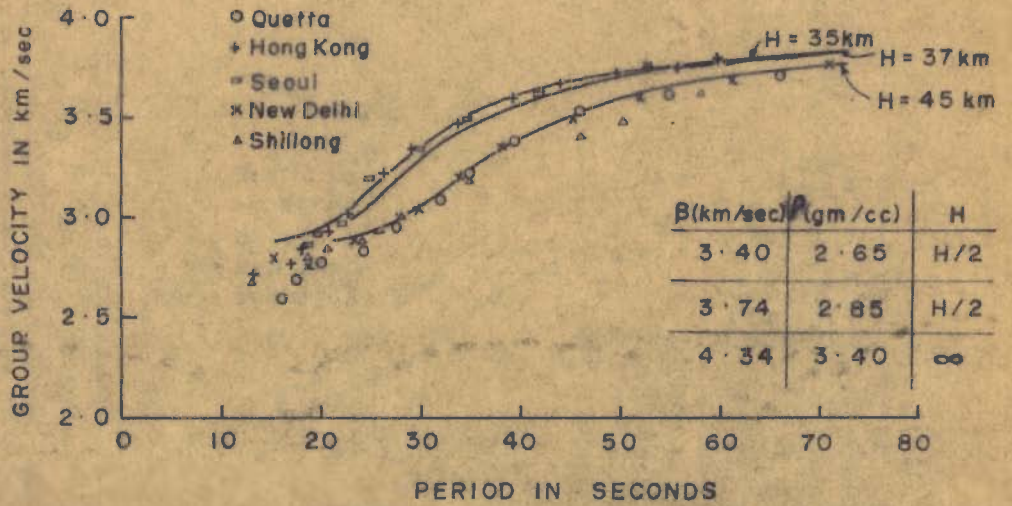


Fig. 20. RAYLEIGH WAVE DISPERSION - 25th AUGUST 1964

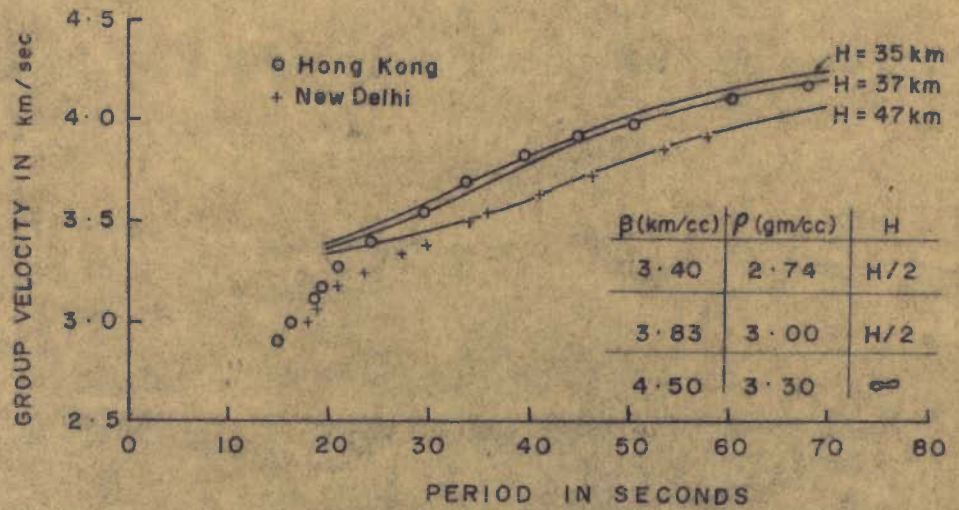


Fig. 21. LOVE WAVE DISPERSION - DORMAN CASE 201

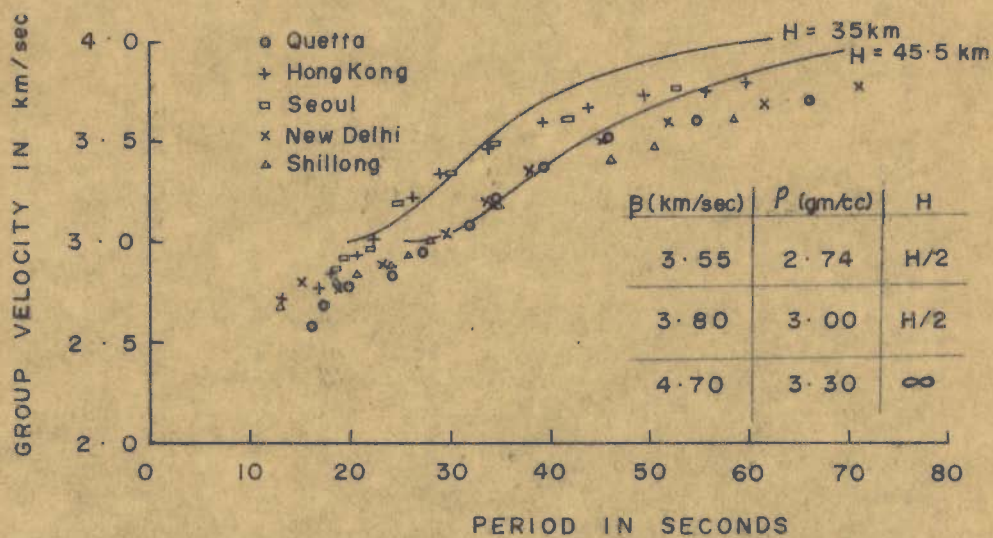


Fig. 22. RAYLEIGH WAVE DISPERSION - DORMAN CASE 8007.

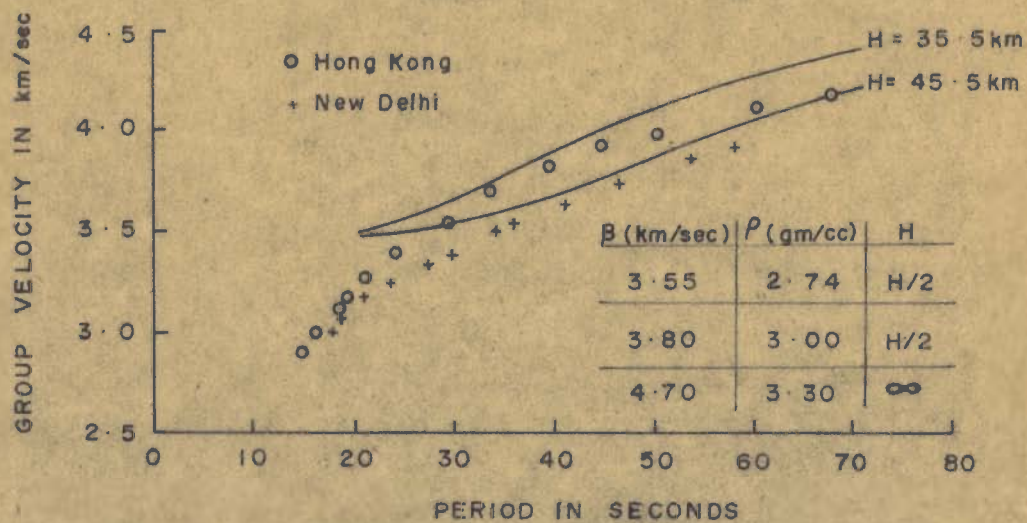


Fig. 23. LOVE WAVE DISPERSION - DORMAN CASE 208.

For Love wave dispersion in Figure 21 we observe that the Hong Kong data for periods of 30 sec and above lie between the theoretical curves for $H = 35$ km and $H = 37$ km while New Delhi data is in close agreement with the curve for $H = 45$ km.

The fact that the observed dispersion data is divided in two groups, one agreeing with a smaller crustal thickness of 35-37 km as recorded at Seoul and Hong Kong and the other with a larger crustal thickness of 45 km as recorded at Shillong, New Delhi and Quetta, is well established.

Tandon and Chaudhury (1963) have found an average crustal thickness of 45 km between Novaya Zemlya and New Delhi by studying the dispersion of Rayleigh waves generated from high yield nuclear explosions. The section through Novaya Zemlya and New Delhi is practically the same as the one between the epicenter of the earthquake under study and New Delhi. They have compared the observed Rayleigh wave dispersion with Dorman Case 8007 which has been used by Kovach (1959) for comparison of the observed dispersion between the Aleutians and Lwiro. Between Sinkiang and Uppasala, Kovach (1959) found an average crustal thickness of 45.5 km by comparing the Love wave dispersion with Dorman case 208 which has the same layer parameters as Dorman case 8007 for Rayleigh waves. Saha (1965) has also reported an average crustal thickness of 45 km between New Delhi and Novaya Zemlya from M_2 wave dispersion. However, it may be pointed out that the Rayleigh wave dispersion data show a better fit with theoretically computed curves

after Stoneley (Figure 20) than with Dorman case 8007 (Figure 22) and Love wave dispersion data have a better fit with Dorman case 201 (Figure 21) than Dorman case 208 (Figure 23).

Figure 17 is a relief map of Asia and shows the great circle paths between the epicenter and the recording stations. The waves recorded at Shillong and New Delhi pass through the high mountain regions of the Himalaya and Tibet Plateau and those recorded at Quetta pass through the Hindu Kush mountains and Plateau of Pamir whereas those recorded at Seoul and Hong Kong do not pass through high Mountain regions. Figure 24 shows 125 times vertically exaggerated elevations along the great circle paths shown in Figure 17. The average elevation between the epicenter and Quetta and New Delhi is of the same order and for Shillong it is slightly more. It is expected that the average crustal thickness obtained from Shillong data will be more than those obtained from New Delhi and Quetta and this is confirmed by Shillong data which lie beneath the 45 km for periods greater than 40 sec (Figure 20).

Rayleigh waves penetrate effectively to about one-third of their wave length. The total section through which the wave penetrates affects the group velocity. This limits the suitability of a particular wave length in studying a crust of a definite thickness. For investigations in the average crustal thickness range of 35-55 km, Rayleigh waves with periods between 25-45 sec are most suitable, because their

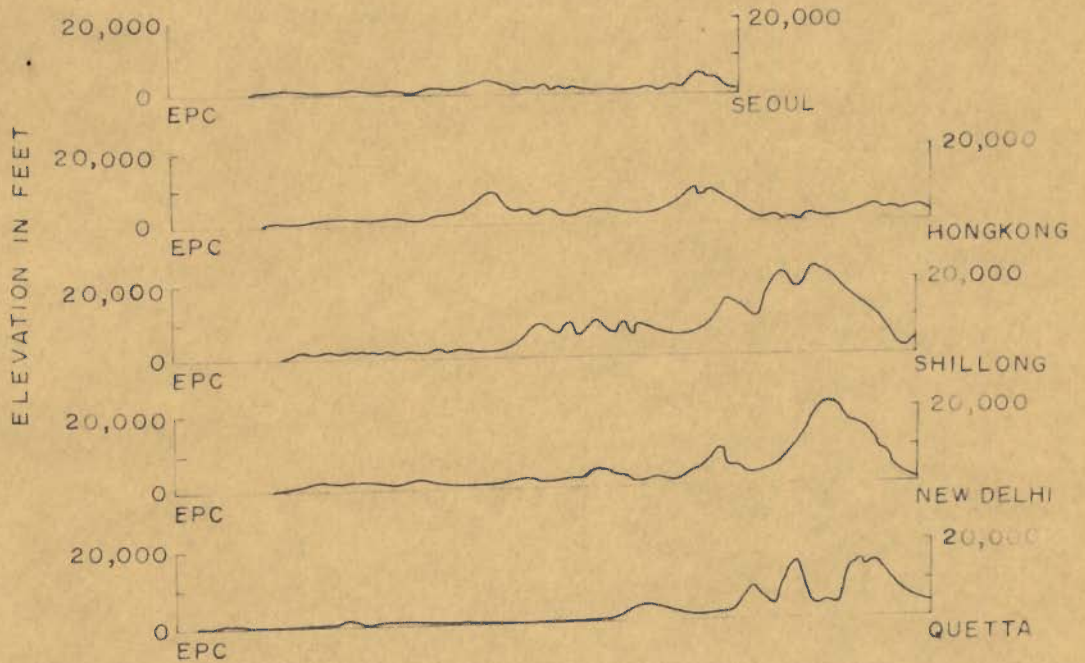


Fig. 24. TOPOGRAPHY BETWEEN EPICENTER AND RECORDING STATIONS, VERTICAL EXAGGERATION 125 TIMES

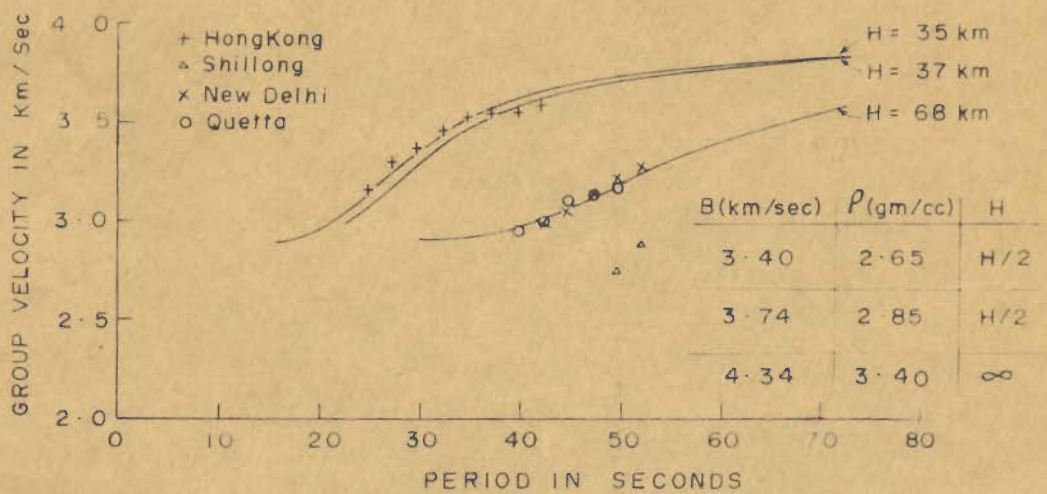


Fig. 25. RAYLEIGH WAVE DISPERSION

depth of penetration would ^{be} of the same order. This is evident from the theoretical dispersion curves in Figure 20. For $H = 35$ km and $H = 45$ km curves, the group velocity difference is a maximum of 0.275 km/sec for 30-35 sec, 0.175 km/sec for 25 sec and 45 sec periods and only about 0.1 km/sec for 22.5 sec and 60 sec periods. Same is true for the observed group velocities also. Hence more weight has to be given to the observations in the period range of 25 to 45 sec in obtaining conclusions by comparison with the theoretical curves. Also, in 25-45 sec period range, due to greater depth of penetration, the effect of the sediments becomes negligible, which otherwise reduces the group velocity in the shorter period range with smaller depths of penetration.

The average crustal thickness in the northern region of Figure 17 is about 35-37 km as obtained from the Seoul data and also reported by Shechkov (1961, 1964), Saverensky and Shechkov (1961) and Arkhangel'skaya (1964). These findings are based on detailed surface wave dispersion studies for a number of earthquakes. The high mountain regions are confined between latitude 26°N and 40°N , constituting about one-fourth of the total path traversed by the waves recorded at Shillong, New Delhi and Quetta. This quarter segment is responsible for increasing the average crustal thickness for the total path by about 8-10 km, giving an average crustal thickness of 45 km for New Delhi, Shillong and Quetta paths.

It is therefore evident that the total crustal thickness under the Tibetan Plateau and the Himalaya should be of the order 65-70 km to account for a difference of 8 to 10 km in the average values of the thickness of the crust.

The waves recorded at Hong Kong do not pass through these high mountain regions and consequently the observed dispersion data fall in between the curves for $H = 35$ km and $H = 37$ km.

Rayleigh wave group velocities are also calculated separately for the high mountain regions only. In Figure 17 an arc is drawn cutting epicentral distances equal to Seoul from the remaining four stations. This arc just separates the elevated Tibet Plateau and Himalaya from the rest. Graphs are plotted between different periods of the Rayleigh waves and the corresponding travel times for all the stations. The epicentral distance of Seoul is subtracted from the epicentral distances of the other stations. Travel times for different periods corresponding to the remaining distances are found from these graphs and the group velocities are calculated (Table 12). These group velocities are plotted in Figure 25 where points for New Delhi and Quetta fall around the theoretical curve for 68 km crustal thickness while those for Hong Kong fall around curves for 35 and 37 km. However, Shillong points lie below the theoretical curve for 68 km indicating a higher crustal

Table-12

Group velocities of Rayleigh waves and corresponding crustal thicknesses.

Period sec	Hong Kong-Seoul		New Delhi-Seoul		Quetta - Seoul		Shillong-Seoul	
	Gr. Vel. km/sec	H km	Gr. Vel. km/sec	H km	Gr. Vel. km/sec	H km	Gr. Vel. km/sec	H km
52.5			3.27	66.5				
50.0			3.22	66.2	3.19	69.0	2.87	-
47.5			3.16	66.7	3.16	66.7	2.74	-
45.0			3.04	68.6	3.11	67.2		
42.5	3.56	39.8	2.99	69.9	3.00	69.4		
40.0	3.54	37.8			2.95	70.4		
37.5	3.53	36.1						
35.0	3.52	34.5						
32.5	3.48	33.4						
30.0	3.36	34.3						
27.5	3.30	33.4						
25.0	3.18	34.9						

thickness as pointed out earlier. Table 12 also gives the computed crustal thickness corresponding to these group velocities using Stoneley's (1955) case I with $H_1 = H_2$. For this case the group velocity minimum occurs at $KH_1 = 2.2$ (K is the wave number) and the corresponding C/ρ_1 value is 0.77 and hence the table could not be used for group velocities less than 2.88 km/sec. The crustal thickness values are found to be consistent in the 25 to 42.5 sec range for Hong Kong and in the 40 to 52.5 sec range for New Delhi and Quetta. These calculations support earlier findings.

3.4

PART II

3.4.1 OBSERVATIONAL DATA:

For this study, particular epicenters and the recording stations are chosen so that travel paths pass through region 12 of Santô's (1965-B) division of Eurasia. Also, care has been taken that a major portion of the total path corresponds to region '12'. Only seismograms where well developed Rayleigh waves in the 30th sec to 45 sec period range are observed are analysed. Group velocities have been determined by Sato's (1958) method described in the second chapter. Table 13 gives the particulars of the earthquakes and recording stations used for this study and Figure 26 shows the corresponding great circle paths plotted on Santô's (1965) division pattern of Eurasia. The group velocity dispersion curves are shown in Figures 27, 28 and 29.

Table-13

Details of the paths (Figure 26) studied.

Path	Epicenter	Origin time (G.M.T.)	Recorded at	Epicentral distance km
a	45.8 N 150.8 E	10 58 09.1	New Delhi	6,556
b	34.9 N 138.0 E	23 41 58.3	New Delhi	5,767
c	29.1 N 140.8 E	21 36 05.0	New Delhi	6,111
d	24.2 N 125.2 E	16 12 41.5	New Delhi	4,767
e	29.1 N 140.8 E	21 36 05.0	Lahore	6,278
f	22.2 N 145.9 E	14 21 04.8	New Delhi	6,847
g	22.5 N 121.3 E	17 19 25.9	Lahore	4,720
h	22.2 N 145.9 E	14 21 04.8	Quetta	7,767
i	38.6 N 22.4 E	09 47 30.3	Shillong	6,538
j	43.0 N 41.0 E	18 27 18.4	Shillong	4,229
A	22.4 N 93.6 E	15 58 46.5	Anpu	2,890
B	43.5 N 146.8 E	00 40 36.4	Hong Kong	3,806

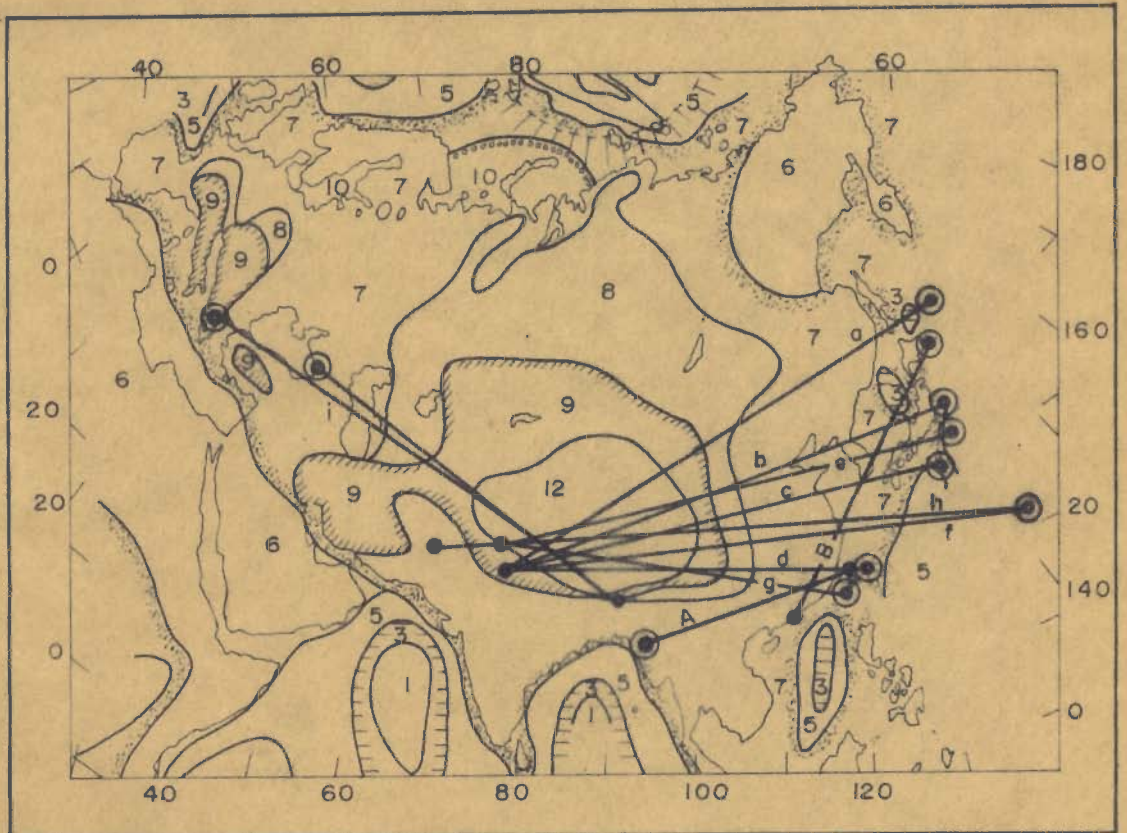


Fig. 26. RAYLEIGH WAVE PATHS STUDIED FOR THE
REGION 12

● Recording station

⊙ Epicenter

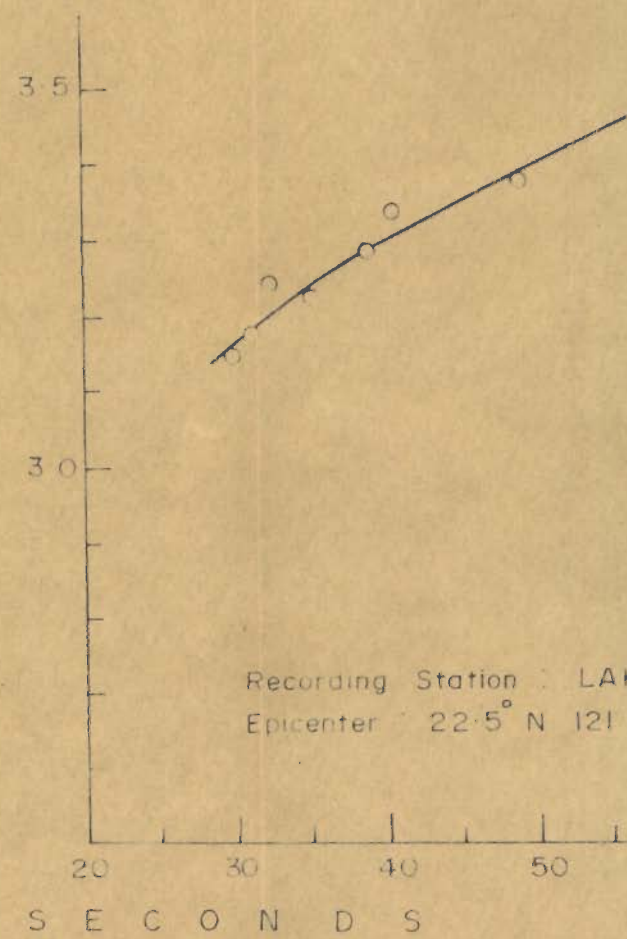
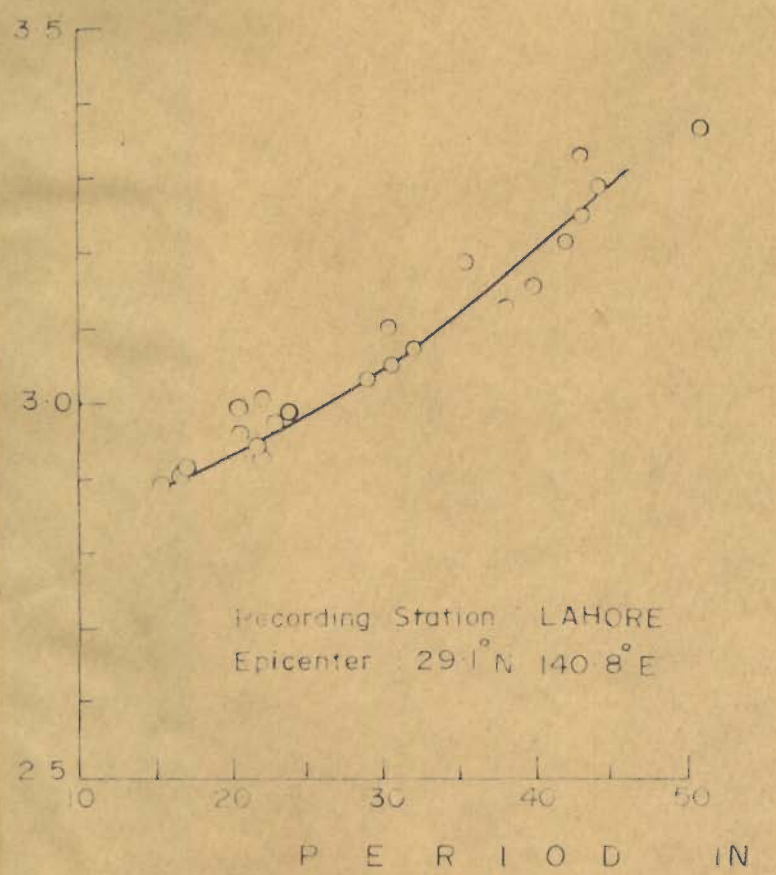
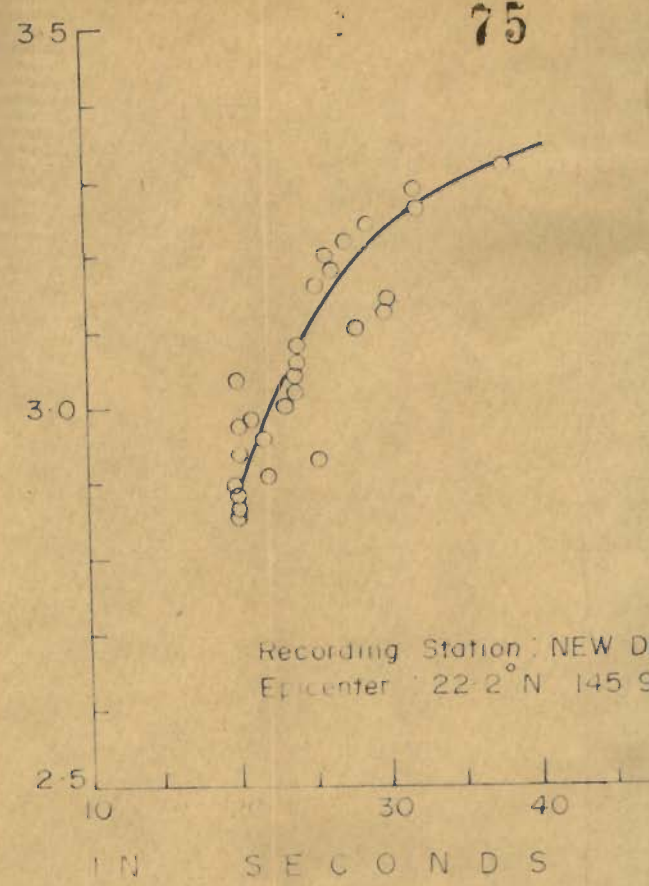
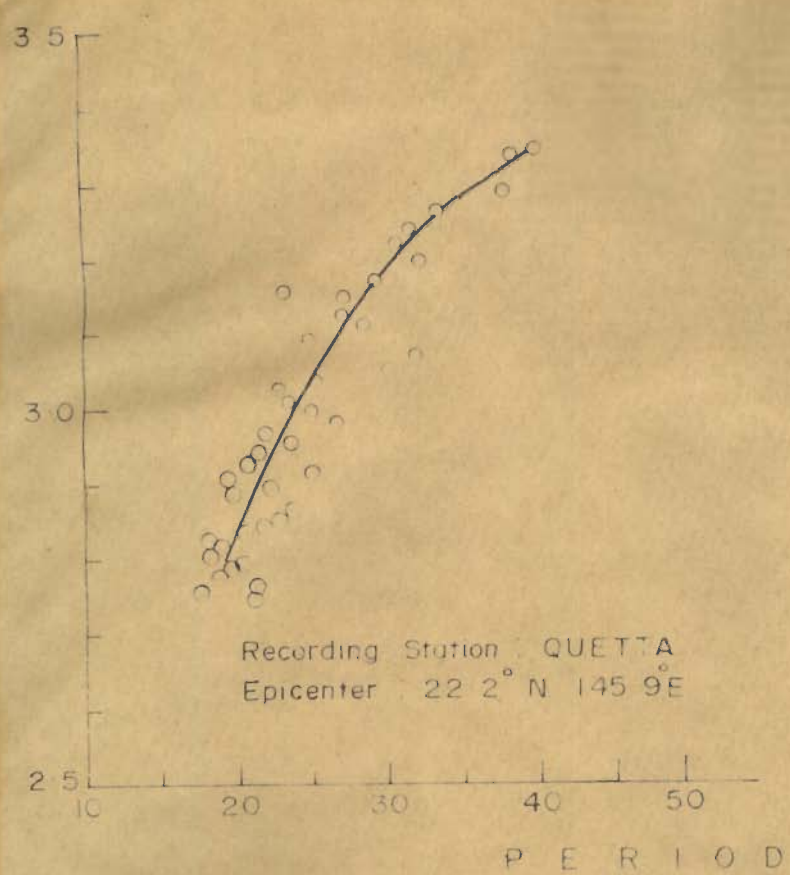


Fig. 27.

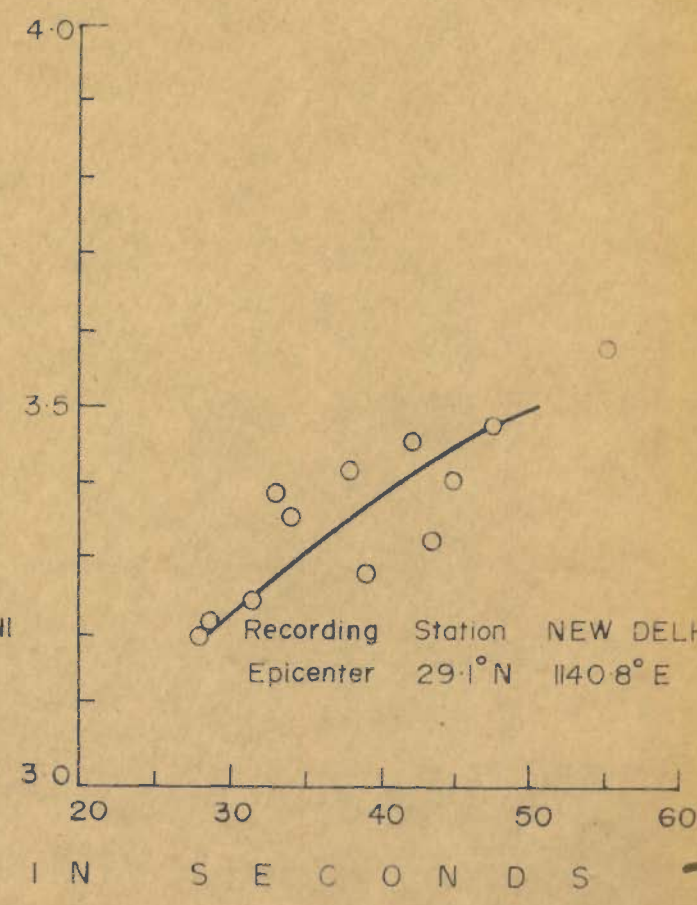
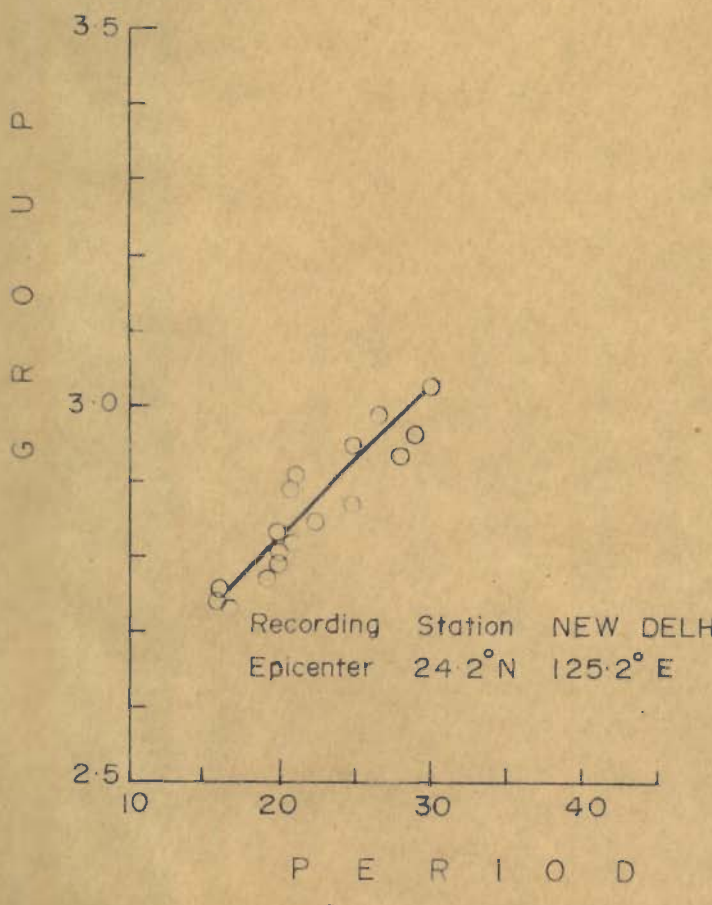
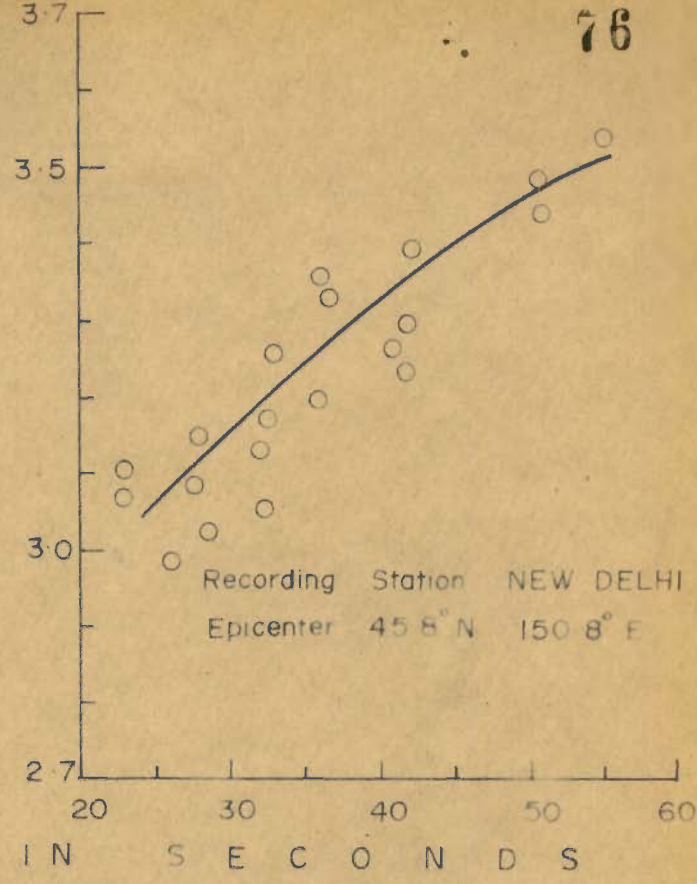
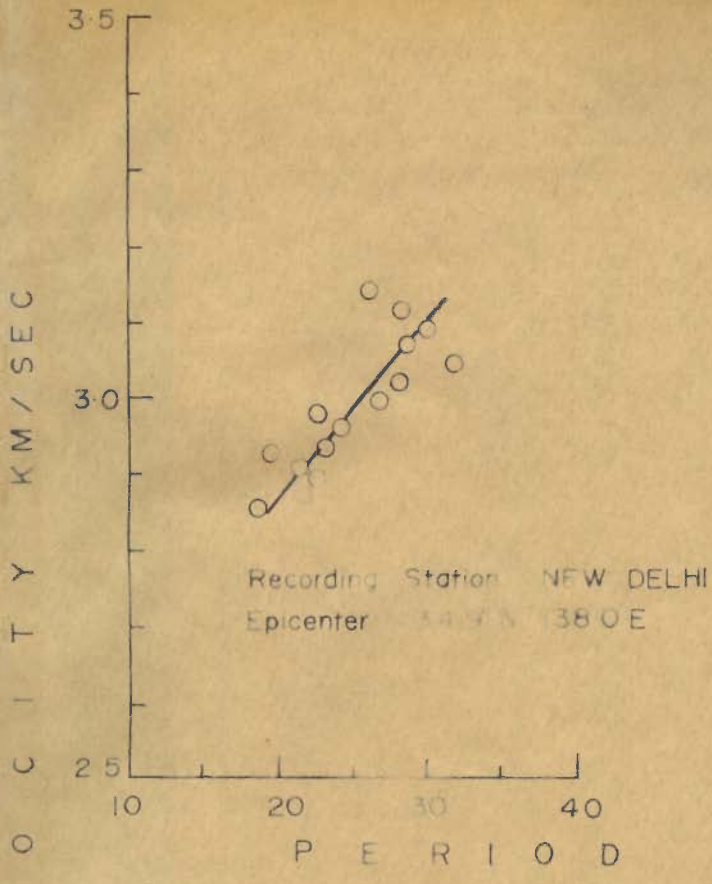


Fig. 28.

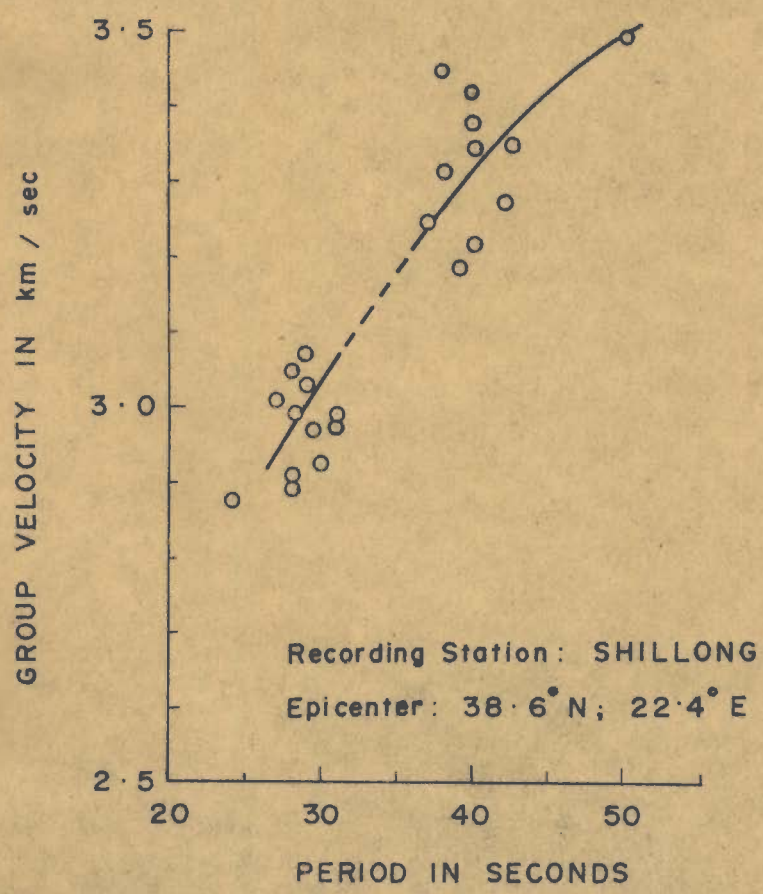
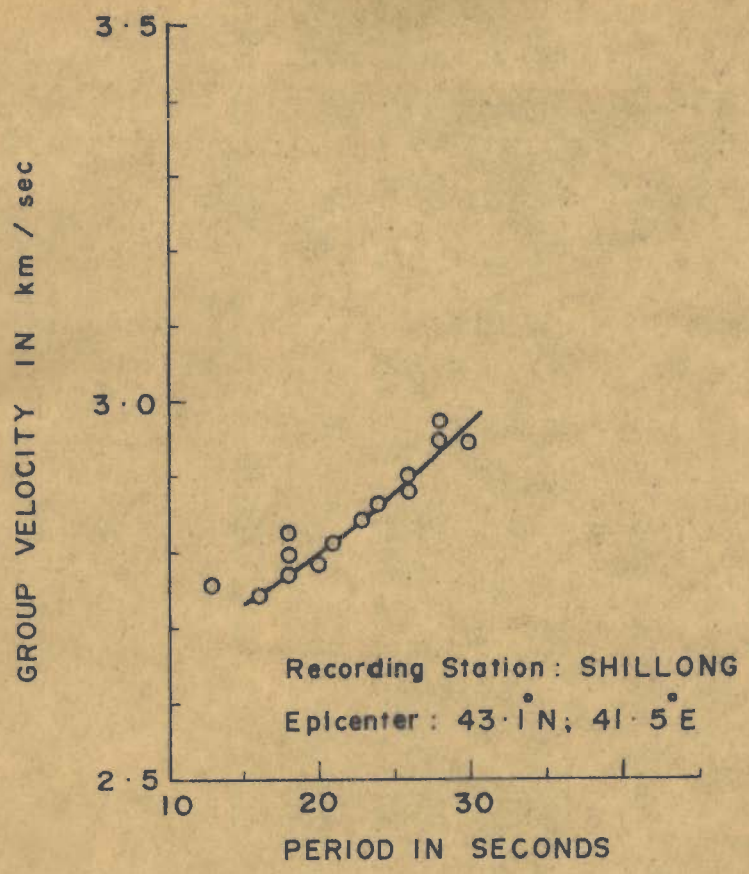


Fig. 29.

3.4 .2 COMPUTATION OF GROUP VELOCITIES FOR REGION '12'

The great circle paths used in the study are plotted on an equal area projection map (Figure 26). Distances corresponding to each region, $\Delta 1$, traversed by a particular path have been calculated. The travel time for each region 1 (except region 12) is obtained by dividing the regional distance $\Delta 1$ by the corresponding standard Rayleigh wave group velocity for a particular period, say 30 sec and added. Let us call it T_a (it does not include the travel time for region 12). Next, from the observed dispersion curve, group velocity V_o is obtained for 30 sec period and by dividing the total epicentral distance by it, the observed travel time T_o is found out. The difference ($T_o - T_a$) corresponds to the travel time in region 12 and by dividing the epicentral distance $\Delta 12$ by ($T_o - T_a$), group velocity in region 12 is obtained. The same procedure is repeated for 35 sec, 40 sec and 45 sec periods also. The computation is detailed in Table 14 for the seismogram written at Quetta for path 'h' in Figure 26. The epicentral distance of 7764 km is divided into ~~four~~^{six} parts i.e. 524 km in region 3, 986 km in region 5, 2527 km in region 7, 370 km in region 8, 585 km in region 9 and 2772 km in region 12. The calculated travel times of 30 sec period are 135.7, 269.5, 752.1, 114.2 and 191.2 sec for regions 3, 5, 7, 8 and 9 respectively. The total calculated travel time T_a for these regions adds up to 1462.7 sec. The observed group velocity for 30 sec period is 3.18 for this path and the corresponding travel time for the whole path is 2442 sec.

Table-14

Calculation of Rayleigh wave group velocities for region 12

Recording station : Quetta; Epicenter : 22.2°N, 145.9°E; Epicentral distance: 7,764 km

Period sec	Calculated travel time ($\frac{\Delta i}{V_i}$) for different segments (other than 12) from standard dispersion curves (Santô 65) in sec. Δ in km.					$T_a = \frac{\Delta i}{V_i}$ sec	Obs. gr. vel. V_o km/sec	Obs. tr. time (T_o) $\frac{\Delta}{V_o}$	Travel time for 12th region ($T_o - T_a$) sec	Gr. Vel. for 12th region $V_{12} = \frac{\Delta_{12}}{(T_o - T_a)}$ km/sec
	Δ_3	Δ_5	Δ_7	Δ_8	Δ_9					
	524	986	2527	370	585					$\Delta_{12}=2772$ km
30	135.7	269.5	752.1	114.2	191.2	1463	3.18	2442	979	2.833
35	133.7	261.6	721.9	108.8	177.8	1404	3.27	2375	971	2.857
40	132.9	257.4	703.9	105.4	172.1	1372	3.34	2325	953	2.910

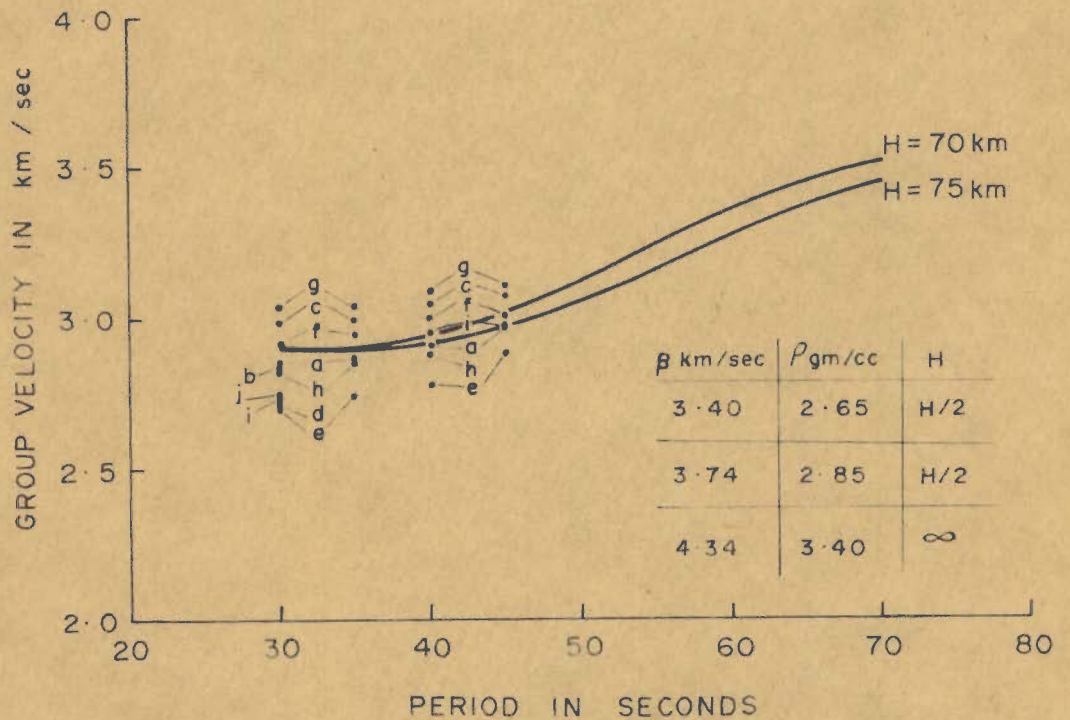


Fig. 30. RAYLEIGH WAVE GROUP VELOCITIES FOR REGION 12 FOR PATHS a TO j (Fig. 26)

105611

The remaining time ($T_o - T_a$) = 979.3 sec is for region 12 and the resulting group velocity is 2.833 km/sec for region 12. As detailed in table 14, the group velocities for 35 sec and 40 sec in region 12 are found to be 2.857 km/sec and 2.910 km/sec respectively for this path. Similar calculations are carried out for all the paths studied and the results are tabulated in Table 15. The group velocities obtained in region '12' are plotted in Figure 30.

3.4 .3 COMPARISON WITH THEORETICAL DISPERSION CURVES AND DISCUSSION:

As discussed in Part I of this chapter, Stoneley's (1955) theoretical Rayleigh wave dispersion curves for a three layer earth model are found to be most suitable for comparison with the observational data. In Figure 30, the theoretical dispersion curves computed for crustal thicknesses of 70 and 75 km are also plotted (Details of computation are given in Appendix I). The observed dispersion data indicates an average crustal thickness of 70 km for region 12. Maximum scatter is observed for 30 sec period. This scattering decreases with the increase of period and is minimum for 45 sec period. A major contribution to this scattering is probably due to the varying thicknesses of sedimentary layers along different sections of region 12. With the increase of period the wavelength increases and the waves penetrate deeper. This reduces the effect of sedimentary layers on the dispersion considerably.

Table-15

Rayleigh wave group velocities for region 12 along sections a to j (Figure 26) for different periods.

Sl. No.	Path No.	GR. VELOCITIES FOR			
		30 sec	35 sec	40 sec	45 sec
		Km/sec	Km/sec	Km/sec	Km/sec
1	NDI - a	2.862	2.877	2.907	2.980
2	NDI - b	2.835			
3	NDI - c	2.985	3.006	3.054	3.076
4	NDI - d	2.723			
5	LAH - e	2.711	2.750	2.782	2.878
6	NDI - f	2.922	2.952	3.000	
7	LAH - g	3.060	3.069	3.095	3.113
8	QUE - h	2.833	2.857	2.877	
9	SHL - i	2.740		2.956	3.082
10	SHL - j	2.745			

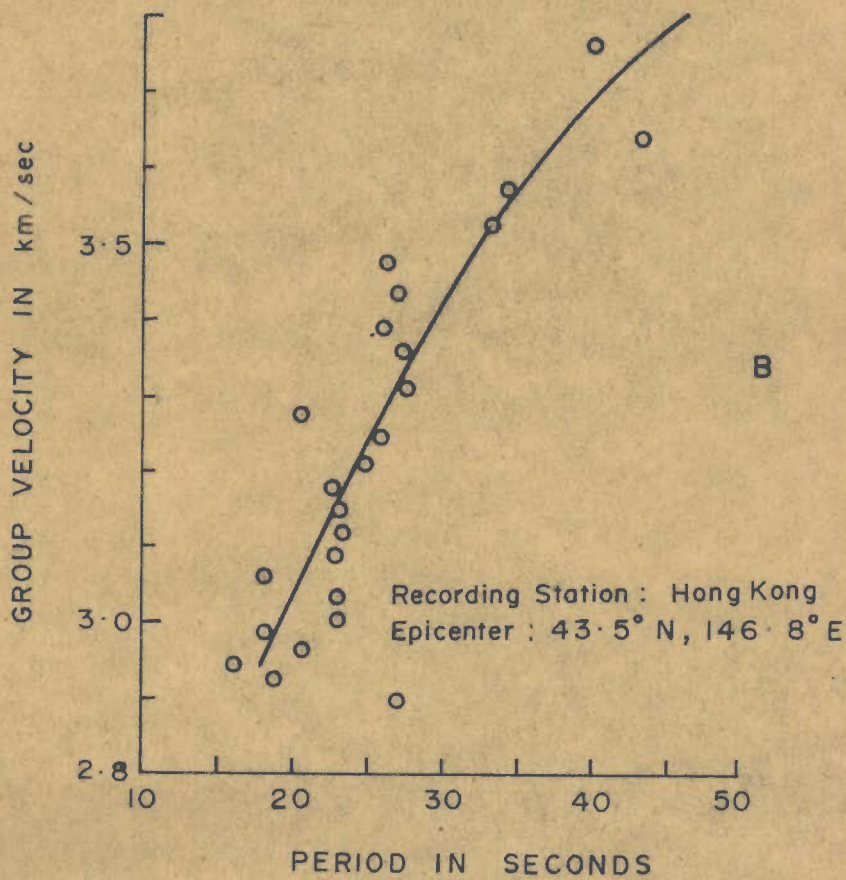
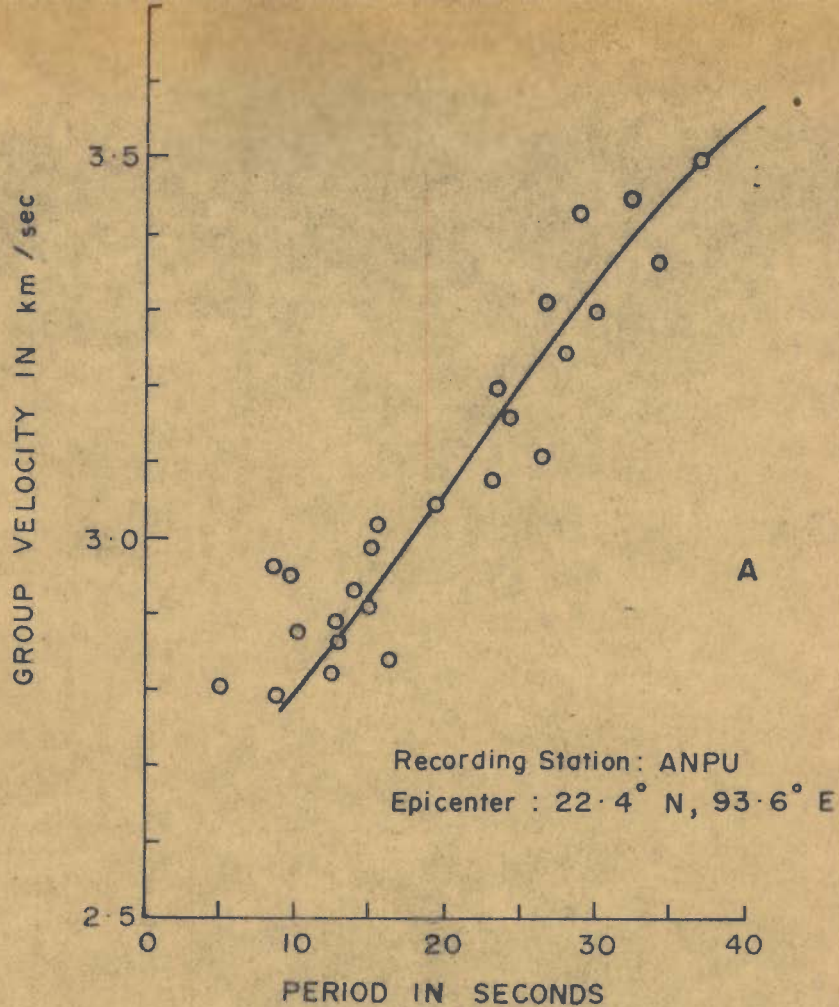


Fig. 31.

Group velocity dispersion along a number of paths not ~~not~~ crossing the region 12 but confining to Eurasia only was also studied. Path numbers A and B (Figure 26, Table 13) are two such examples. Path number A lies entirely in region 7 and the observed group velocity of 3.36 km/sec (Figure 31-A) for 30 sec period at Anpu tallies with Santo's value of standard Rayleigh wave dispersion curve for region 7. Similarly path B includes region 3 and 7 and the calculated travel time of 1130 sec for 30 sec period is in close agreement with the observed travel time of 1113 sec (Figure 31-B; observed group velocity at Hong Kong for 30 sec period is 3.42). This attests Santo's (1965) division of Eurasia and the suitability of the method used for calculating the group velocities for region 12. It also indicates the necessity of dividing region 12 into further sub~~/~~-regions.

In general, the investigations carried out in Part II substantiate the earlier finding of an average crustal thickness of 70 km for region 12 in Part I.

3.5 CONCLUSIONS:

Surface wave group velocities along various sections in Himalaya and Tibet Plateau region have been investigated and the observed dispersion is compared with theoretical dispersion curves computed for suitable earth models. The study indicates the necessity of further sub-dividing Santô's region 12 and reveals that:

1. Roots exist for Himalaya and the neighbouring Tibet Plateau region.
2. Airy's theory of Isostatic compensation holds good and there is general validity of Isostasy for region 12.
3. An average crustal thickness of 70 km is obtained for region 12 and the dispersion data supports equal thicknesses of granitic and basaltic layers.

CHAPTER-IV

LATERAL VELOCITY GRADIENTS AND GLOBAL SEISMICITY

LATERAL VELOCITY GRADIENTS AND GLOBAL SEISMICITY

4.1 INTRODUCTION:

Geographic distribution of seismicity all over the world has been extensively studied by Gutenberg and Richter. They have sought the possible correlation between seismicity and active volcanoes, gravity anomalies & major morphological structural categories like oceanic ridges, island arcs, arcuate mountain ranges, continental block structure etc. McDonald (1963) observes that on ^{an} average, gravity and heat-flow investigations reveal that the mass and radioactivity per unit area are equal under the continents and oceans. He also reviews that a global representation of the anomalies in heat flow and gravity fields shows many similarities and horizontal gradients in both fields are correlated with earthquake zones. A special mention may be made of Japan which has a very high seismicity and where extensive work has been carried out to correlate seismicity with other geophysical parameters. Recently Omote et al (1966) have discussed the seismicity of Japan and its correlation with crustal structure, heat flow, short period geomagnetic variations, folding ratio of the tertiary formations etc.

Lateral elastic wave velocity gradients on the global basis have been not yet studied. Such a study was not possible in the absence of any work dealing with the global distribution

of elastic wave velocities. Investigations carried out in the second chapter of this thesis regarding the divisioning of Eurasia into regions of similar group velocity characteristics of Love waves and its attestation of Santô's (1965-B) work makes it possible to study the lateral velocity gradients in the upper 50 ~~to 60~~ km section of earth. In the present chapter these gradients have been studied and their possible correlation with the global seismicity has been sought.

4.2 VELOCITY DIVISION PATTERN AND SHALLOW FOCUS EARTHQUAKES:

It is ~~We have~~ found in the second chapter that Love wave division pattern is in good agreement with the Rayleigh wave division pattern and both of these studies support the existence of extremely low velocities in the Himalaya and Tibet Plateau region, the presence of thick soft sedimentary layers in the sea around Novaya Zemlya and Baltic sea etc. Therefore, it seems justified to assume that in other regions of the world also, the Rayleigh wave divisioning studies carried out by Santô and Satô (1966) which includes Eurasia, Africa, Atlantic Ocean and Indian Ocean would be supported by Love wave studies. This Rayleigh wave division pattern hence depicts, in general, the seismic wave velocity distribution in upper 40-50 km section of the earth - which corresponds to the effective depth of penetration of the Rayleigh waves of 30 sec period.

A very good example to support the above statement is available from Herrin and Taggart's (1962) investigations of Pn velocities for the United States. Figure 32 represents the calculated apparent Pn velocity contours at the interval of 0.1 km/sec velocity variation. According to their assumptions the contour map represents the picture of compressional wave velocities at the top of the mantle. The contours in Figure 32 are closer on the Pacific coast side of U.S than on the Atlantic coast side. The same feature is very well exhibited in Santô's (1968) latest study of lateral variation of Rayleigh wave group velocities for North America. His division pattern is reproduced in Figure 33.

Santô and Satô's (1966) division pattern and standard dispersion curves are shown in Figures 34 and 35. The regions of highest group velocity are given a number '0' and that of lowest velocity a number '12' for the same period. Region '0' corresponds to the ocean deeps and '12' to the high mountain ranges. Regions from '0' to '12' correspond to successively decreasing group velocities. Figure 36 shows the travelling paths of Rayleigh waves on which the divisioning is based.

According to Gutenberg (1956), the average annual release of seismic energy by earthquakes is of the order of 10^{25} ergs. Nearly 80% of this energy is released in the upper 60 km of earth, 17% between 60 km and 300 km and the remaining

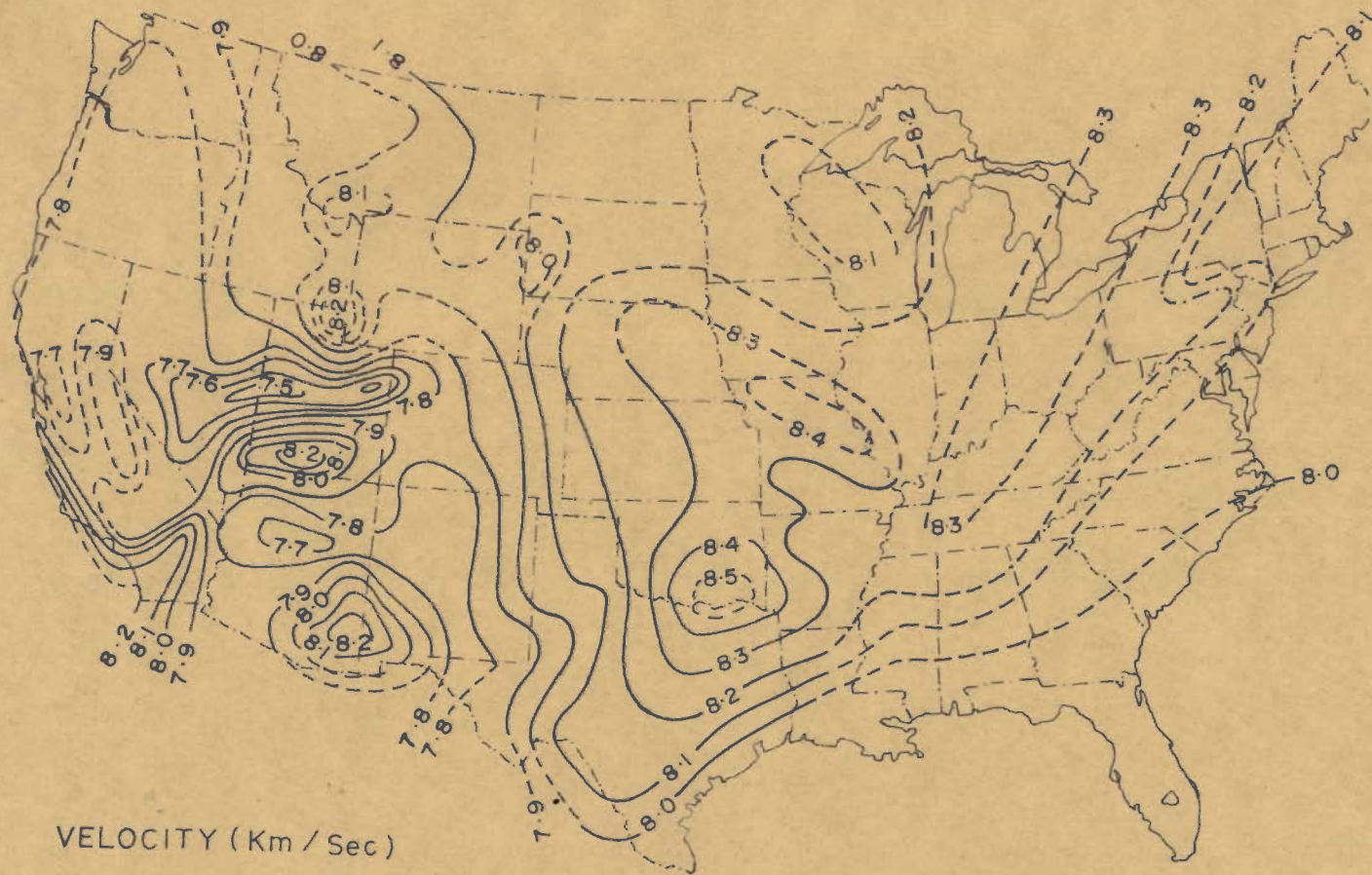


Fig. 32. APPARENT P_n VELOCITIES IN THE UNITED STATES
(HERRIN AND TAGGART - 1962)

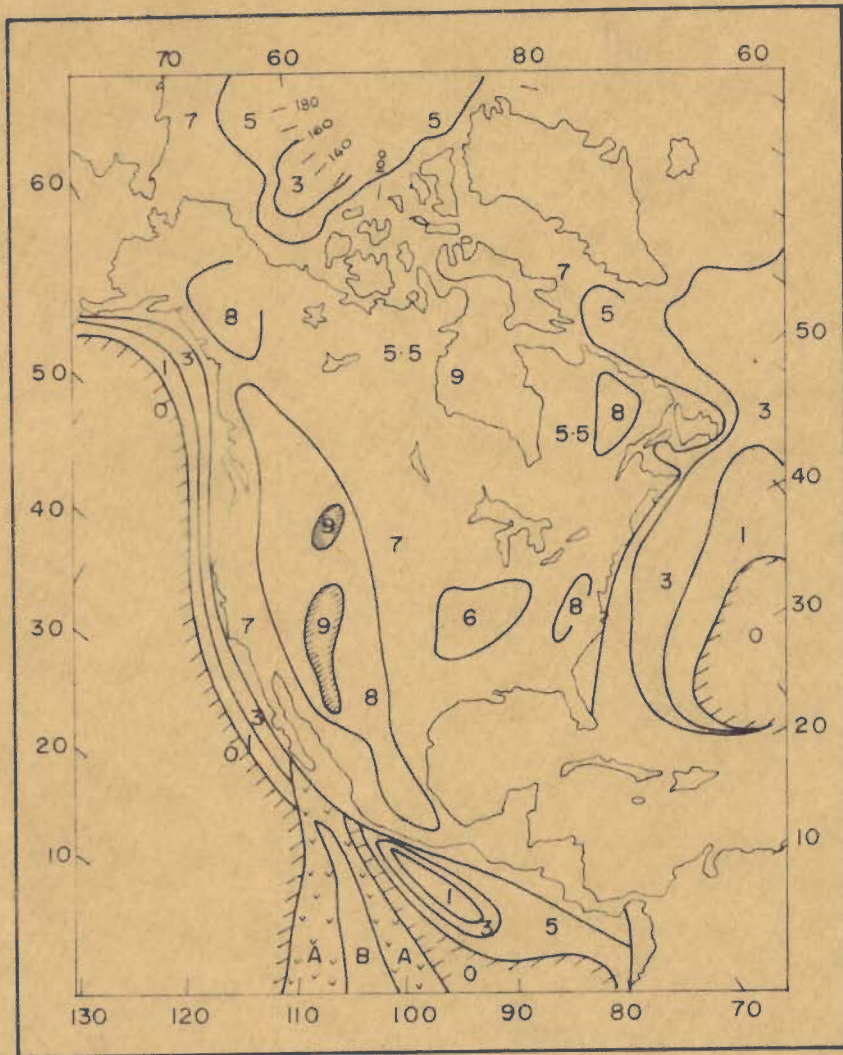


Fig. 33. RAYLEIGH WAVE DIVISIONING OF UNITED STATES AND SURROUNDINGS (SANTO - 1968)

3% between 300 km and 700 km. Gutenberg (1956) further observed that nearly 90% of total seismic energy is released through the earthquakes having magnitude 7 and above. In Figure 34 the epicenters of shallow focus earthquakes of magnitude 7.0 to 7.7 for the period 1918 to 1946, 7.7 and above for the period 1904 to 1946 and 8.6 and above (Table 16) for the period 1897 to 1956 are also plotted (data from "Seismicity of the earth and related phenomena" by Gutenberg and Richter and "Elementary Seismology" by Richter). Figure 34, hence, depicts the trend of global seismic energy release. In Figure 34, the Rayleigh wave divisioning including the major seismic belts namely the Circum-Pacific belt and its complex branches, the Alpidic belt and Pamir-Baikal zone and the mid-Atlantic ridges as well as the stable African mass has been also marked.

4.3 LATERAL VELOCITY GRADIENTS IN ACTIVE AREAS:

A careful examination of Figure 34 reveals that all regions of high seismic activity correspond uniquely to the zones of sharp velocity changes. The epicenters in Circum-Pacific belt correspond to rapid increase in velocity from '7' to '3', '1' and '0'; whereas the epicenters of the Alpidic belt harmonize with the transition zone of velocity increase from region '12' to '9' and '7'.

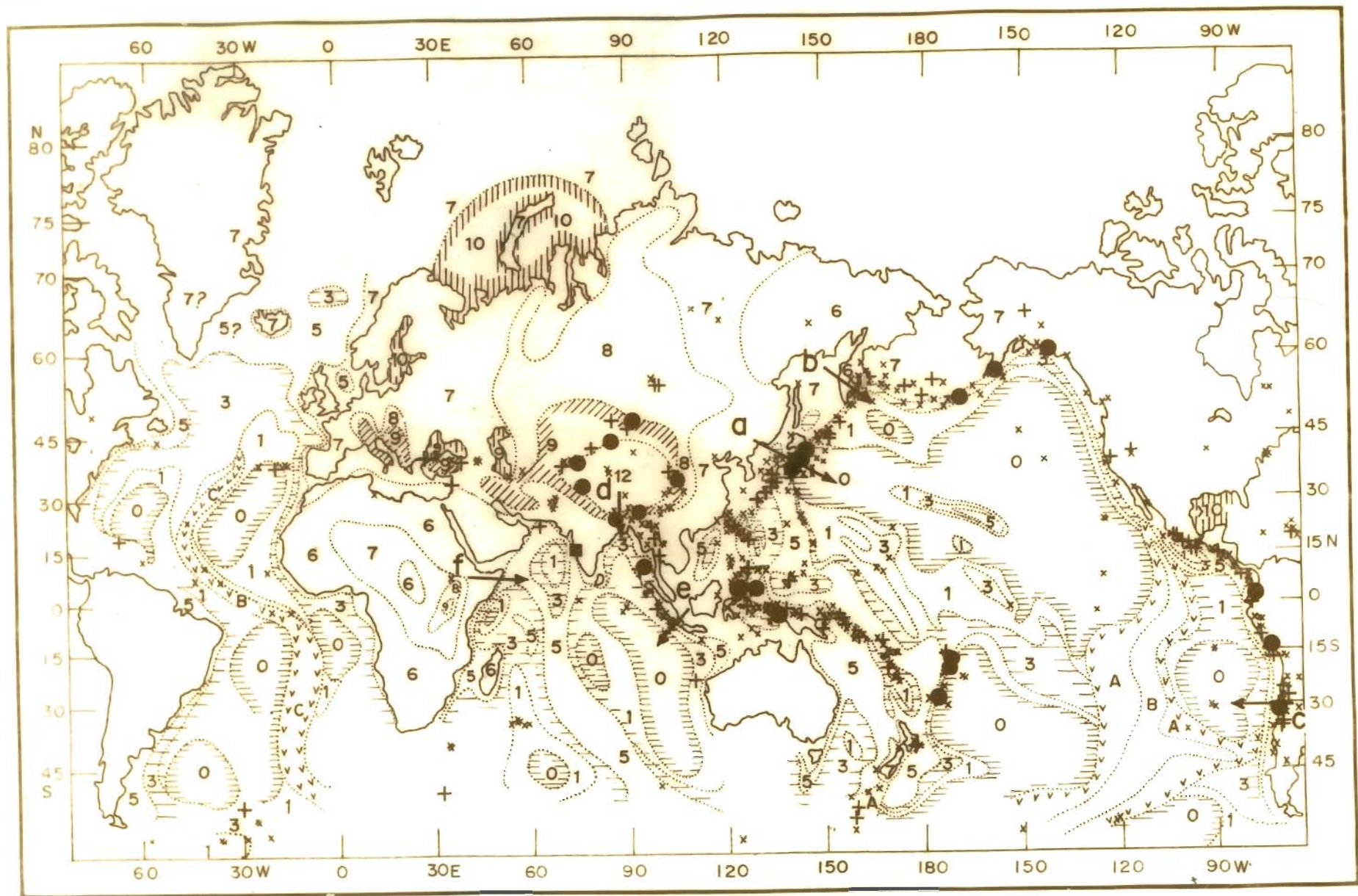
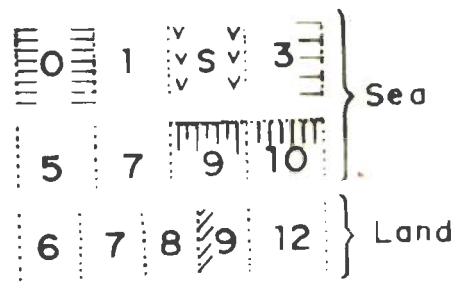
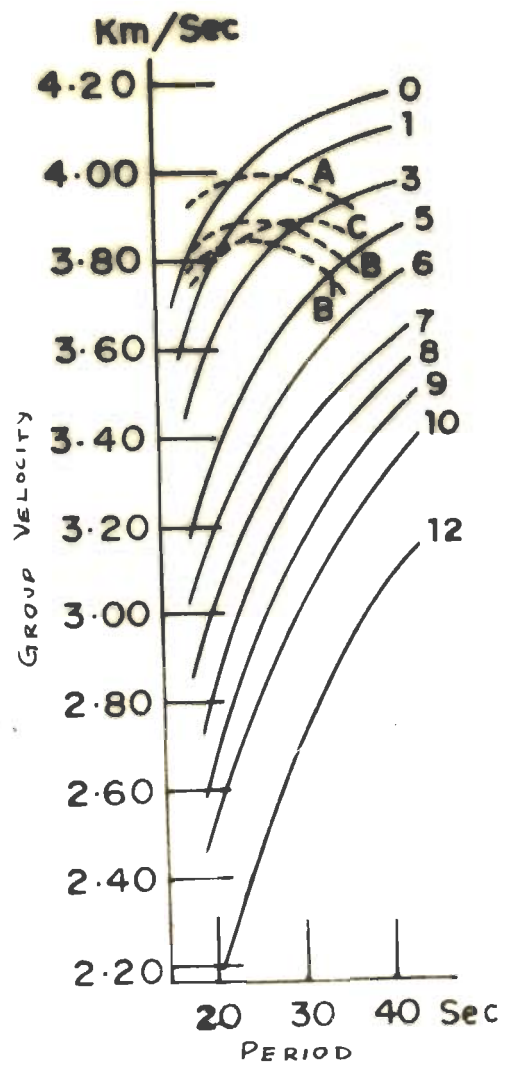


Figure 34. Map showing shallow global seismicity (data from "Seismicity of the earth and associated phenomenon", 1949 edition), Rayleigh wave division map (Santô and Satô - 1966), earthquakes of magnitude 8.6 and above (Elementary Seismology - 1958 edition) and sections 'a' to 'f'.

List of earthquakes; Magnitude 8.6 and above (Richter-1956)
From 1897 - 1956.

Date	Origin time G.C.T.	Latitude	Longitude	Magnitude
1897 June 12	11:06 ±	26 N	91 E	8.7±
Aug 5	00:12 ±	38 N	143 E	8.7±
Sept 20	19:06	6 N	122 E	8.6±
Sept 21	05:12 ±	6 N	122 E	8.7±
1899 Sept 10	21:41	60 N	140 W	8.6
1902 Aug 22	03:00	40 N	77 E	8.6
1905 April 4	00:50.0	33 N	76 E	8.6
July 23	02:46.2	49 N	98 E	8.7
1906 Jan 31	15:36.0	1 N	81½ W	8.9
Aug 17	00:40.0	33 S	72 W	8.6
1911 Jan 3	23:25:45	43½ N	77½ E	8.7
1917 May 1	18:26.5	29 S	177 W	8.6±
June 26	05:49.7	15½ S	173 W	8.7
1920 Dec 16	12:05:48	36 N	105 E	8.6
1929 Mar 7	01:34:39	51 N	170 W	8.6
1933 Mar 2	17:30:54	39¼ N	144½ E	8.9
1938 Feb 1	19:04:18	5¼ S	130½ E	8.6
Nov 10	20:18:43	55½ N	158 W	8.7
1941 June 26	11:52:03	12½ N	92½ E	8.7
1942 Aug 24	22:50:27	15 S	76 W	8.6
1950 Aug 15	14:09:30	28½ N	96½ E	8.7
1952 Mar 4	01:22:43	42½ N	143	8.6



- x Magnitude 7-7.7, 1918-1946
- + Magnitude 7 3/4 or over, 1904-1946
- Magnitude 8.6 or over, 1897-1956
- The Koyna earthquake epicentre 10th December 1967

Figure 35. Standard Rayleigh wave group velocity dispersion curves used for divisioning and legend to Figure 34.

Let us, now, examine these velocity gradients quantitatively. In Figure 37, sections of Figure 34 at 'a' to 'f' are drawn. For example, section across 'b' in Figure 34 starts from region '7' and then passing through '5', '3' and '1' terminates in '0' region. The distances along this section in various zones are calculated and are plotted on the abscissa against the corresponding group velocities (for 30 second period from Figure 35) on the ordinate. A smooth curve is drawn through the mid-points of these distances and rate of change of group velocity/km is calculated which gives gradients.

Section 'a' is across Japan which is known for its very high seismicity. Region '7' continues from Mongolia to Japan Sea and extends till the eastern Pacific coast of Japan, which is the boundary between '7' and '0' regions. This transition corresponds to a very high velocity gradient. It is striking that epicenters around Japan cluster on its eastern Pacific coasts and not on its western Japan Sea coasts.

Section 'b' across Kamchatka is another typical example. Proceeding from the Okhotsk Sea along the arrow to Kamchatka Peninsula and then to the Pacific Ocean, there is a gentle gradient from region '7' to '6' ($0.49 \cdot 10^{-3} \text{ sec}^{-1}$) and then a steep gradient from '6' to '3' ($1.62 \cdot 10^{-3} \text{ sec}^{-1}$)



Figure 36. Paths used for Rayleigh wave divisioning (Figure 34 Santô and Satô - 1966)

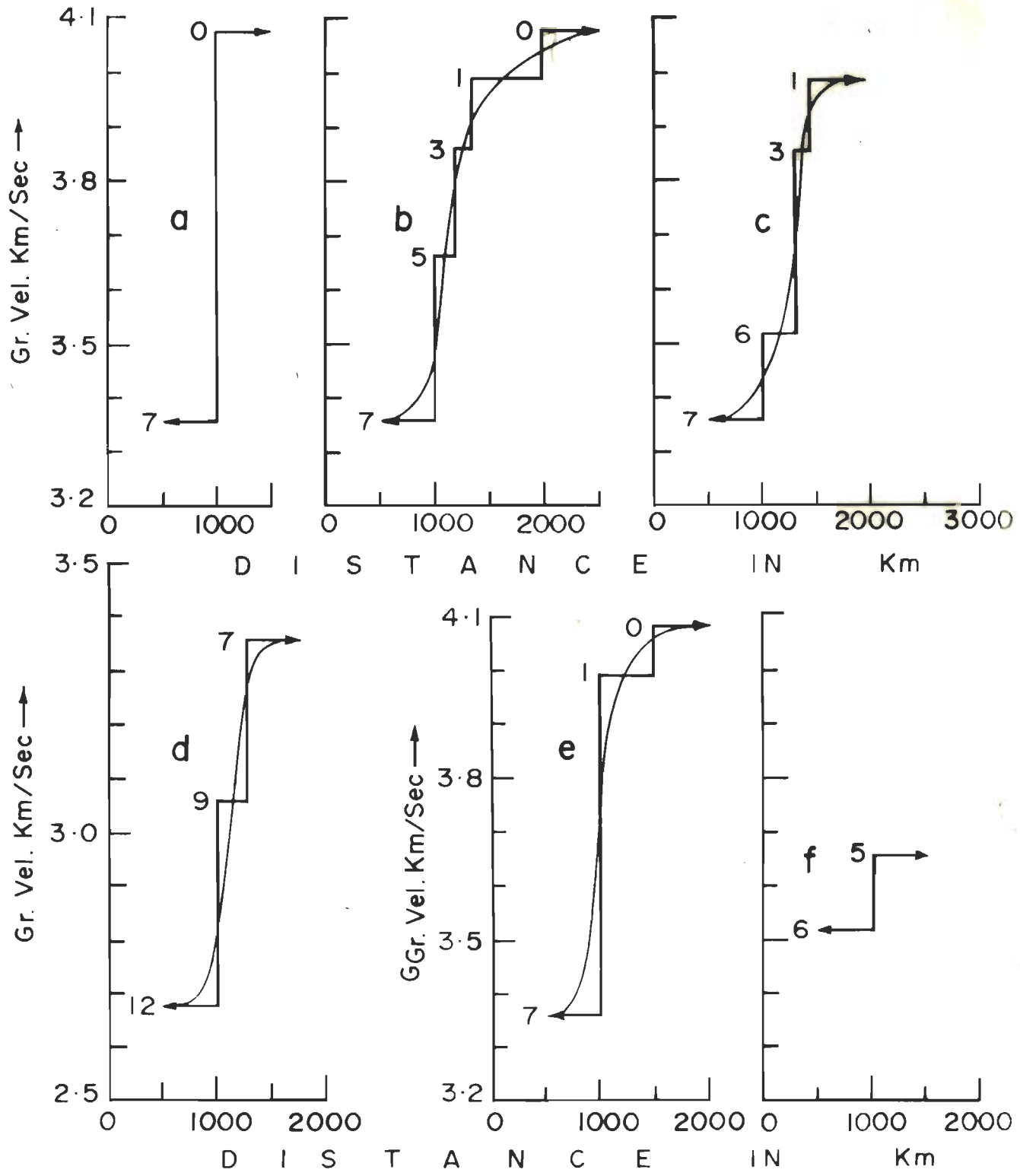


Figure 37. Velocity variations along sections 'a' to 'f' of Figure 34.

and '3' to '1' ($1.08 \cdot 10^{-3} \text{ sec}^{-1}$). As evident from Figure 34, seismicity is highest in this section in the transition zone '6' to '3' of highest velocity gradient.

Section 'c' on the Pacific coast line of South America also confirms the same trend for the circum Pacific belt. Along the arrow, there is high velocity gradient from '7' to '5' ($1.77 \cdot 10^{-3} \text{ sec}^{-1}$) and '5' to '3' ($1.25 \cdot 10^{-3} \text{ sec}^{-1}$) and low gradient from '3' to '1' ($0.33 \cdot 10^{-3} \text{ sec}^{-1}$) and '1' to '0' ($0.15 \cdot 10^{-3} \text{ sec}^{-1}$). Here also we find that high seismicity conforms to high velocity gradients.

The Himalaya arc is the most well defined and seismically active among the Asiatic arcs of the Alpid belt, and the lowest group velocities have been observed in the Himalaya and Tibet Plateau regions. These velocities increase rapidly from '12' to '9' and '7' in the encompassing areas. Section 'd' is across Assam; where some of the biggest earthquakes have occurred. Velocity gradients ($1.58 \cdot 10^{-3} \text{ sec}^{-1}$ from '12' to '9' and $1.25 \cdot 10^{-3} \text{ sec}^{-1}$ from '9' to '7') are very high along this section.

Section 'e' is across Sumatra - another active region of the Alpid belt. Epicenters in this region cluster on the Indian Ocean coast of Sumatra where the velocity gradient is high ($1.25 \cdot 10^{-3} \text{ sec}^{-1}$) and not on the Borneo side coast which does not exhibit any velocity variation.

4.4 CORRELATIONSHIP WITH DISTRIBUTION OF EARTHQUAKES OF MAGNITUDE 8.6 and ABOVE:

All major shallow earthquakes of magnitude 8.6 and above during 1897 - 1956 (data from the "Elementary Seismology" by C.F. Richter) uniquely have their epicenters in the regions of high velocity gradients. The parameters of these earthquakes are given in table 16 and their epicenters have been plotted by closed circles in Figure 34.

In Circum-Pacific belt these epicenters are confined to regions of highest velocity gradients. Three out of these 14 epicenters of the Circum-Pacific belt crowd in Japan where the observed velocity gradient is highest (transition from '7' to '0'). Aleution Islands region which is seismically very active presents another interesting example. Here also the epicenters are restricted to areas where '7' and '0' regions come very close. The two epicenters, north east of New Zealand in the Kermadec Island region also lie on the junction of region '5' and '0'.

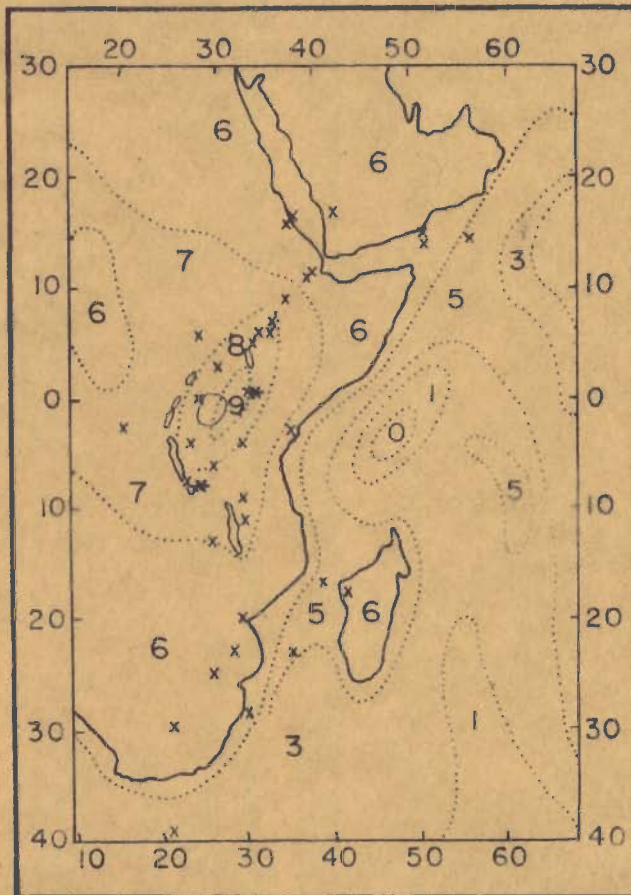
In Alpidic belt, 7 of the 8 epicenters lie in the Himalaya and Tibet Plateau region, which has the highest wave velocity gradients in the belt. It is remarkable that out of these 7 epicenters, 6 are on the boundary of region '12' and '9' and none in the central part of region '12'. Section 'a' and 'c' of Figure 2 represent the velocity gradients corresponding to these high magnitude earthquakes of the Circum-Pacific belt and section 'd' for the Alpidic belt. They are of the order of $1.5 \cdot 10^{-3} \text{ sec}^{-1}$.

4.5 VELOCITY GRADIENTS IN INACTIVE AREAS:

So far, seismically active regions of the world have been examined. Now, let us consider some of the comparatively inactive regions. Section 'f' is on the eastern coast of Africa near the Gulf of Aden. There is no concentration of the regional contours. The only transition encountered along this section is from region '6' to region '5' indicating a very low velocity gradient. Consequently, no earthquake epicenters have been reported in this region. Africa as such has a low seismicity and all the reported earthquakes in this region have shallow focus and low magnitude (Figure 38). These epicenters mostly lie around lakes Victoria, Tanganyika and Nyasa, where the regional velocity contours are comparatively less sparse. This typical example exhibits that even in comparatively less seismic areas, the seismicity is confined to regions of relatively high velocity gradients.

4.6 IMPORTANCE OF THE CORRELATION:

Table 17 gives the gradients encountered along the various sections discussed. All the major seismic events are well defined by high gradients. There are places of very high gradients; for example Pacific coasts of Kamchatka ($1.62 \cdot 10^{-3} \text{ sec}^{-1}$) and Mexico ($2.00 \cdot 10^{-3} \text{ sec}^{-1}$) which are seismically very active but no earthquake of magnitude of the order of 8.6 has occurred there during the last seven decades. Earthquakes of very high magnitude are likely to occur at such places. Seismically active regions where the



* Magnitude 7.0-7.7

x Magnitude 6.0-6.9

Fig. 38. SHALLOW SEISMIC ACTIVITY (RICHTER-58)
AND RAYLEIGH WAVE DIVISION (SANTÔ
AND SATÔ - 66) OF A PART OF AFRICA

Table-17

Velocity gradients along sections 'a' to 'f' of Figure 34.

Section	Transition between the regions.	Corresponding velocity gradient 10^{-3} . sec. ⁻¹	Remarks
a	7 - 0	Extremely high	There is an abrupt change in velocity from region '7' to '0'. The seismicity is very high at the junction accounting for 3 out of 14 epicenters (1897 - 1956) in the Circum-Pacific belt of magnitude 8.6 and above.
b	7 - 6	0.49	More epicenters are in zone '3' - which is a narrow strip between region '6' and '1'.
	6 - 3	1.62	
	3 - 1	1.08	
c	7 - 5	1.77	The seismicity decreases from the coast towards ocean with the gradient. The three big earthquakes; one of mag. 8.6 (17th August 1906) and two of mag. 8.3 (1st December 1928 and 6th April 1943) had their epicenters in the area corresponding to gradients of 1.77 and 1.25.
	5 - 3	1.25	
	3 - 1	0.33	
	1 - 0	0.15	

contd. . . .

Table-17 Continued

Section	Transition between the regions.	Corresponding velocity gradient 10^{-3} . sec. ⁻¹	Remarks
d	12 - 9 9 - 7	1.58 1.25	A typical section of the Alpidic belt showing a sudden increase in velocity from region '12' of the lowest velocity. Six out of eight epicenters (1897 - 1956) of magnitude 8.6 and above of the Alpidic belt lie on the boundary of region '12' and '9'.
e	7 - 1 1 - 0	1.26 0.18	Another section of Alpidic belt. Epicenters are crowded on the boundary of region '7' and '1'.
f	6 - 5	Very low	No earthquake of magnitude of the order of 7 has been reported along this section. Region '6' and '5' extend on the two sides of the boundary.

gradients are high, say $1.5 \cdot 10^{-3} \text{ sec}^{-1}$ and above, but no major earthquake of magnitude of the order of 8.5 or above has occurred, are prone to such events.

The importance of the correlation is immediately realized while considering the relatively higher western coast marginal activity, than the eastern coast of the stable Peninsular shield of India. Along western coast epicenters of low magnitude earthquake are more often located around Bombay than any where else. Recently the Koyna earthquake (Figure 34) ^{of} magnitude 6.2 (Narain and Gupta 1968) occurred in the same region. This specific localization of seismic activity is expected from the velocity gradients. On western coasts of the shield, the velocity gradients are higher than the eastern coast, and are highest near Bombay, where the regional oceanic contours '1' and '3' come close to shield area of '7'. Keeping in view the relatively higher velocity gradients, Koyna region was prone to earthquake occurrence and the impounding of the reservoir seems to have triggered the event (Discussed in detail in the next chapter).

Among the continents, South America and Australia have been not yet divided into different regions of similar group velocity dispersion character. It is expected, from the observed seismicity trend of the three continents, that for South America, where the seismicity is relatively much higher on the western coasts than their eastern

coasts; the regional contours would be concentrated on its Pacific Ocean coasts and would be comparatively sparse on its Atlantic coasts. Whereas for Australia, which has only a few scattered epicenters of low magnitude, there will be no rapid changes at all, and the whole area would belong to region '6' and '7' corresponding to very low velocity gradients; if any; similar to Africa.

4.7.CONCLUSIONS:

In this chapter, a new type of fundamental correlationship between seismicity and surface wave velocity variations has been formulated. In effect, these velocity gradients connect directly the elastic parameters with seismicity.

The results of the study conclude that:-

1. Regions of high seismicity correspond invariably to regions of steep wave velocity gradients.
2. All earthquakes of magnitude 8.6 and above, during the last six decades, occurred only in regions having gradients of $1.5 \cdot 10^{-3} \text{ sec}^{-1}$ and upward.
3. The Pacific coasts of Kamchatka and Mexico are very potential regions for high magnitude

(8.5 and above) earthquake occurrence in view of their gradients above $1.5 \cdot 10^{-3} \text{ sec}^{-1}$, and absence of such activity during last 6 - 7 decades.

4. Divisioning pattern for South America is predictable to have concentration of regional contours on the Pacific coast and their relative sparseness on Atlantic coast side. Australia is expected to have low velocity gradients like Africa.

5. As expected from gradients, for India, seismicity is highest on its northern borders along the foot hills of Himalaya. The relatively higher gradients on the western coast of stable Deccan Shield of India help in comprehending the specific localization of seismic activity in region around Bombay coasts.

CHAPTER-V

A STUDY OF KOYNA EARTHQUAKE

CHAPTER-V

A STUDY OF KOYNA EARTHQUAKE

5.1 INTRODUCTION:

While discussing the lateral velocity variations in the previous chapter, it has been noticed that for India the gradients are highest along its northern boundary in the foot hills of Himalaya including Assam and Indogangetic planes, being of the order of $1.5 \cdot 10^{-3} \text{ sec}^{-1}$. In this region, which constitutes a part of the Alpidic belt, lie the epicenters of some of the largest known earthquakes. Some of these have been described in detail by Oldham (1899, 1928), Middlemiss (1910), Brett (1935), Auden et al (1939), Kingdon-Ward (1951), Rao, M.B.R. (1953), Tandon (1954) and others.

Himalaya is separated from the Deccan shield by Indogangetic planes having thick sedimentary layers. The Deccan shield is a continental old land and Archean rocks are exposed over more than half of the area. The remaining is covered by basaltic lava flows, known as the Deccan Traps of Cretaceous - Eocene age. The Deccan shield is one of the nearly non-seismic shield and in the central part, the Bellary earthquake of 1843 and the Coimbatore earthquake of 1900 are the only conspicuous seismic events during the known history. However, as is the case with most of the stable shield areas of the world, marginal activity along the western and the eastern coast has

been reported in the past. A review of the earthquake catalogues prepared by Oldham (1882) and Kelkar (1968) shows the occurrence of 23 earthquakes of moderate intensity (upto 7 on M.M. scale) during the last 370 years on the western coast. On the eastern coast of the shield, the activity has been much less compared to the western coast and only about 10 mild local tremors have been reported during the said period, This behaviour is the expected one considering the comparatively higher lateral velocity gradients on the western coast as compared to the eastern coast.

The Koyna earthquake of December 10, 1967 is of particular interest in view of its occurrence in nearly non-seismic Deccan shield of India and the proximity of the epicenter to the Koyna Dam and Shivajisagar Lake area. Narain and Gupta (1968-a, 1968-b) have assessed the magnitude of the earthquake by using the instrumental data and field investigations and have pointed out the possible association of the seismic activity in this region with the Shivajisagar Lake reservoir. Guha et al (1968) have shown an increase in the seismic activity of the Shivajisagar Lake area following the impounding of the reservoir in 1963. They have worked out the parameters of this earthquake using the data of four nearby observatories. A magnitude of 7 has been assigned by them to this earthquake and they consider it to be an isolated event, unconnected with the earlier seismic activity of the region. Tandon and Chaudhury (1968) have independently determined the parameters of this

earthquake using the data of additional twentyone Indian seismological observatories and have worked out the fault plane solution using the P wave data. They also consider it to be an isolated event. A detailed report dealing with the earthquake effects, geology of the region and the seismic history has been prepared by the Geological Survey of India (1968). Based upon the field investigations and felt reports, they have drawn elliptical isoseismals with the major axis running slightly west of the N-S direction.

In this chapter the data now available from these reports, analysis of the seismograms of different observatories over the world and field investigations carried by the author for this earthquake are discussed.

5.2 ORIGIN TIME AND EPICENTER:

The parameters of the earthquake have been independently determined by the following three agencies:

Agency	Epicenter	Origin time G.M.T.			Depth of focus
		h	m	s	km
Central Water and Power Research Station (C.W.P.R.S.)	17° 31.1' N, 73° 43.9' E	22	51	17.0	12
India Meteorological Department (I.M.D.)	17° 22.4' N, 73° 44.8' E	22	51	19.0	8
United States Coast and Geodetic Survey (U.S.C.G.S.)	17° 39.6' N, 73° 55.8' E	22	51	24.3	33 (Restricted)

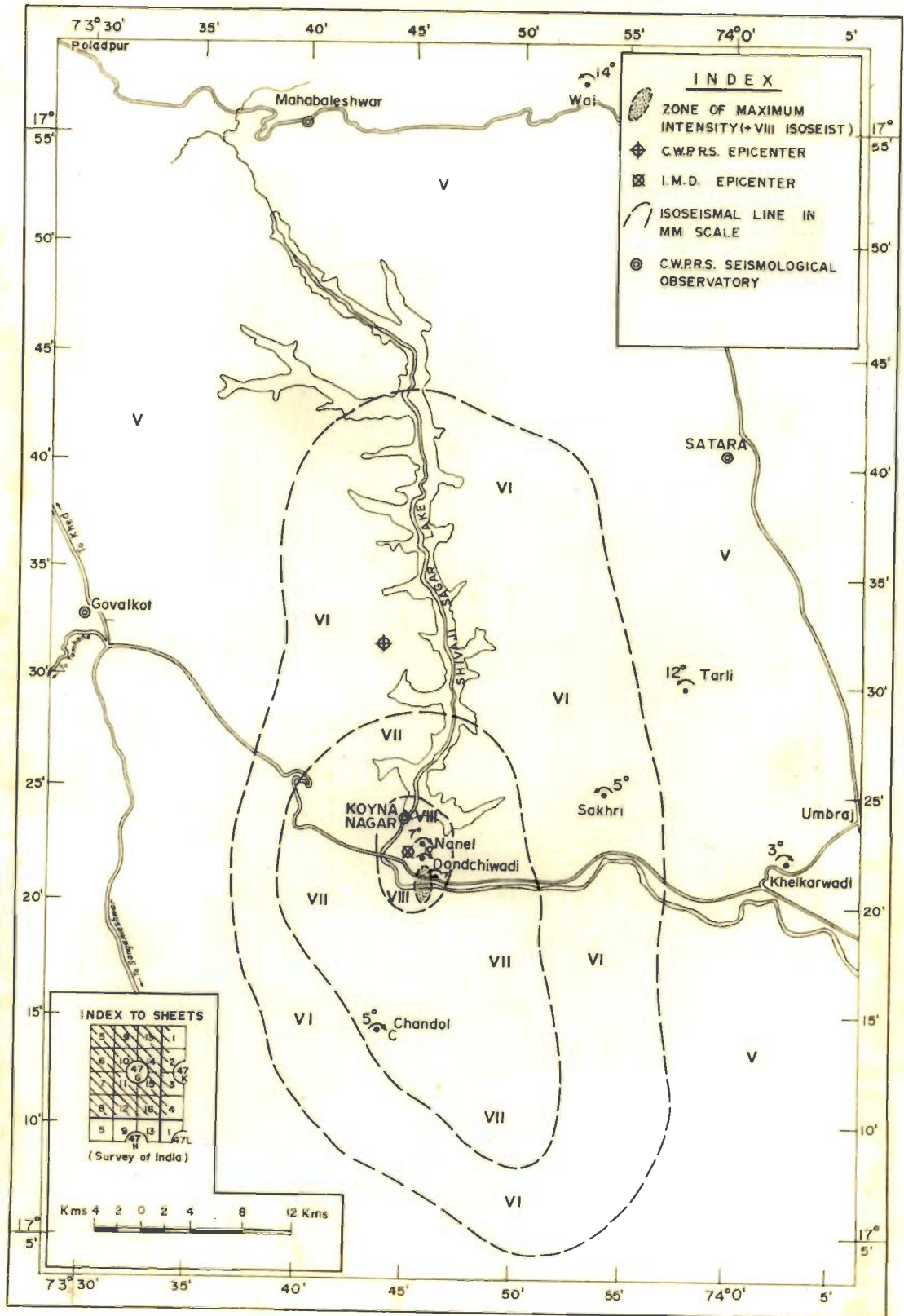


Figure 39. Map of the Koyna region showing the location of the various observatories, two epicenters, isoseismals and the rotational displacements.

Table-18

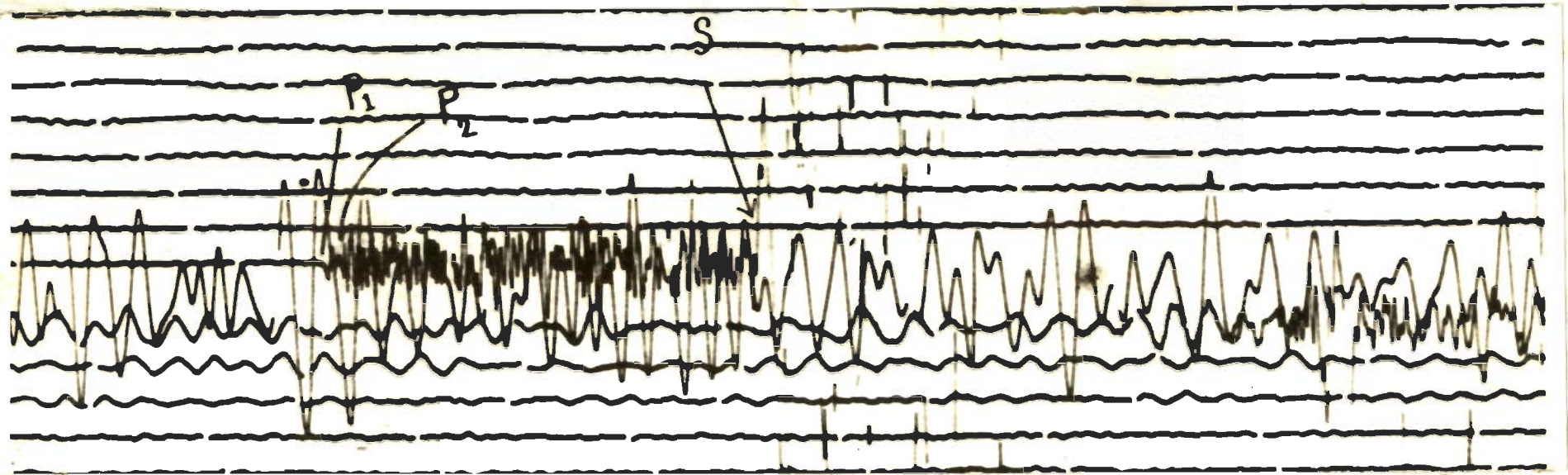
P wave residual time (observed - calculated) for Indian observatories with respect to I.M.D. origin time.

Magnification and the period are mentioned where available.

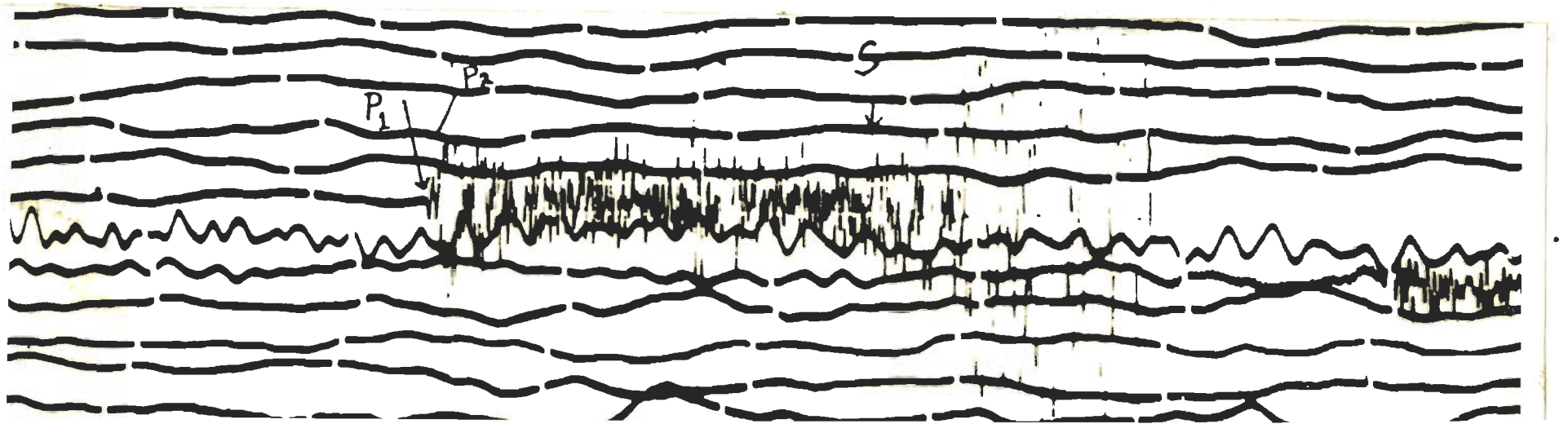
Station	O - C sec	Equipment	Magnifi- cation	Period sec
Poona	- 0.6	Benioff	50,000	1.0
Goa	+ 0.1	Sprengnether	5,000	7.4
Gauribidanur	- 0.6	Benioff	1,83,000	1.0
Madras	+ 0.3	Sprengnether		
Kodaikanal	- 0.4	Benioff	1,00,000	1.0
Vijag	+ 0.8	Sprengnether	6,000	1.65
Trivandrum	+ 2.9	Sprengnether	2,500	7.1
Delhi	- 0.5	Benioff	50,000	1.0
Rohtak	+0.6	Electromagnetic (I.M.D.)		
Sonepat	+ 0.8	Electromagnetic (I.M.D.)		
Bokaro	+ 1.4	Sprengnether	5,000	7.3
Dehra Dun	+ 0.5	Sprengnether	1,500	15
Bhakra	0	Electromagnetic (H)	5,600	1
Mukerian	0	Hagiwara Electromagnetic seismograph	1,00,000	
Pong	+ 0.7	Hagiwara Electromagnetic seismograph	1,00,000	
Jwalamukhi	+ 0.4	Hagiwara Electromagnetic seismograph	1,00,000	
Calcutta	+ 2.1	Sprengnether	1,000	7
Dalhausi	0	Hagiwara Electromagnetic seismograph	1,00,000	
Chatra	0	Benioff		
Shillong	- 3.3	Benioff	2,00,000	
Port Blair	- 4.7	Benioff		

At C.W.P.R.S., Guha et al (1968) have determined the origin time using the data of four nearby seismological observatories at Koyna, Govalkot, Satara and Mahabaleshwar (Figure 39). The four observatories are situated within a few tens of kilometers and are equipped with sensitive vertical component short-period Benioff seismometers ($T_0 = 1$ sec; $T_g = 1$ sec; Mag. 11,000), running at 60 mm/min paper speed. These observatories, being located so close to the focus, have picked up the very first arrivals and the origin time corresponds to the initiation of the seismic event.

At I.M.D., Tandon and Chaudhury (1968) have determined the origin time, using the data of the additional twentyone Indian seismological observatories. Poona is nearest among them - at a distance of 110 km. It has been observed that on the seismograms of Indian observatories which are equipped even with sensitive short-period Benioff seismometers; the initial P wave motion has been very feeble and is followed by discrete large movements within next few seconds. Seismograms of New Delhi and Meerut clearly show the multiplicity of this earthquake (Figures 40, ~~41~~). The I.M.D. origin time works out to be two seconds later than the C.W.P.R.S. origin time. Apparently the distances of these observatories had been too large for the first feeble motion to be picked up everywhere. Table 18 shows the residuals (observed - calculated) for Indian observatories with respect to India Meteorological Department's origin time. All observatories equipped with sensitive short-



New Delhi



Meerut

Figure 40. Sections of seismograms of New Delhi and Meerut supporting the multiple shock hypothesis.

period Benioff seismometers show a negative residual and others equipped with less sensitive seismographs show positive residual. The total positive residual is 10.6 sec and negative 10.1 sec. This suggests that the stronger second event which was taken as the first motion at the observatories operating less sensitive seismometers, should have occurred about 3-4 sec after the initiation of the activity.

U.S.C.G.S., using data from 115 stations all over the world, reports a still later origin time. Obviously the first arrivals were not recorded by many far off stations and the least square fit gave a late origin time. Tandon and Chaudhury (1968) have given the residual (observed - calculated) travel times with respect to I.M.D. origin time for observatories in different parts of the world. It is interesting to note that at most of the 188 stations it is positive and the total positive residual adds up to 300.9 sec, while the total negative residual is only 68.2 sec. For the Assam earthquake of August 15, 1950; Tandon (1954) has given similar residuals. Adding up a total positive residual of 51.1 sec is found and a negative residual of 34.1 sec for 61 stations distributed all over the world. The great circle paths for most of the far off observatories would not differ much for the two epicenters (Assam earthquake of August 15, 1950 and Koyna earthquake of December 10, 1967). Since the same Jeffreys-Bullen travel time tables are used,

the much larger positive residual compared to the negative residual for the Koyna earthquake confirms that the first arrivals have been missed at most of these observatories.

The I.M.D. epicenter lies about 15 km away, almost in the south, of the C.W.P.R.S. epicenter (Figure 39). The cracks developed in the ground are oriented mostly in N-S direction and same is the direction of the major axis of the elliptical isoseismals. Guha et al (1968) in their report have pointed out that there is a general tendency of the tremors in this region to start at about 20 km upstream in north of the dam and then the epicenters of these tremors continue to shift towards south. This cycle has repeated in the past. All these considerations lead to the most obvious conclusion that the Koyna earthquake could have been a series of events closely spaced in time which started at the focus and origin time determined by C.W.P.R.S. continuing towards south, the India Meteorological Department's focus being a later stronger event of this series.

A similar observation has been made by McEvelly and Casaday (1967) in their study of the 1965 earthquake sequence near Antioch - California, where the shocks migrated to the south and then eventually returned to the initial focal region. This phenomenon they have explained in terms of the progression of the local region of stress release along a zone of weakness.

5.3 FIELD EVIDENCE:

Figure 39 depicts the isoseismals, reproduced from the report of Geological Survey of India on the M.M. scale. The I.M.D. epicenter lies very close to the zone of maximum intensity of + VIII. A very significant and interesting observation has been made in terms of the recorded rotational displacements. G.S.I. (1968) has reported seven such well documented and precisely measured rotational displacements (Table 19). Picture 42 shows one such typical displacement recorded and photographed by the author. The sense and the amount of these rotational displacements has been plotted on Figure 39.

Table-19

List of the places where rotational movements have been measured with magnitudes and directions.

Place	Rotation	Recorded by
Sakhri	5° Anticlock-wise	Geological Survey of India
Tarli	12° "	"
Wai	14° "	"
Nanel	7° Clock-wise	"
Dondchiwadi	10° "	"
Chandol	5° "	"
Khelkarwadi	3° "	"
Dondchiwadi	7° Anticlock-wise	The author



Figure 41. Rotational movement registered on a pillar on Helwak
Chiplun road-Near Dondchiwadi

The displacements on the eastern side of the line joining the C.W.P.R.S. epicenter and the zone of maximum intensity are all anticlock-wise (with the exception of the observation at Khelkarwadi) and clock-wise on the western side. Such a rotational movement is in agreement with the expected displacements considering the C.W.P.R.S. focus as the initiating point of the Koyna earthquake event which continued upto the meizoseismal area.

5.4 FAULT PLANE SOLUTION:

In Figure 42, the sense of first motions has been plotted on Byerly's extended distance projection. Data permits the drawing of only one plane separating the compressions and dilatations on the two sides. This plane strikes $N 32^{\circ} W$ and is nearly vertical. Out of 52 stations only 5 are inconsistent with this plane. Even among these 5, the reported dilatations at WRA (Warramunga) is well surrounded by compressions. This indicates that the plane drawn is consistent with the observations. This plane, which is an arc of a very large circle, could be the fault plane or the auxiliary plane.

The following facts support $N 32^{\circ} W$ to be the fault plane:

- i. Elliptical trend of the isoseismals with major axis $N 12^{\circ} W$.
- ii. Near N-S direction of most of the cracks developed in the epicentral region.

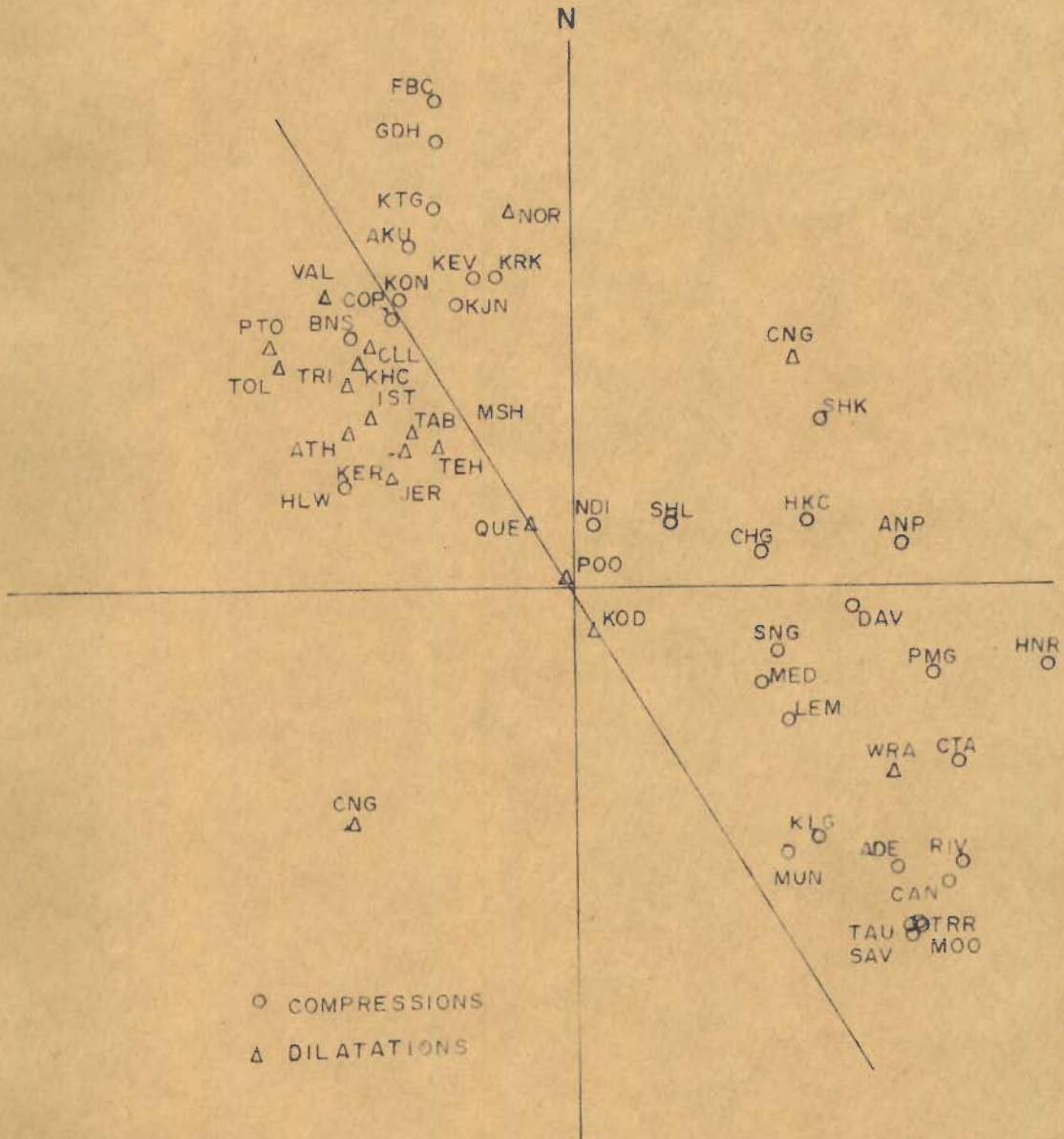


Fig. 42. FAULT-PLANE SOLUTION BASED ON SENSE OF P WAVE MOTION PLOTTED ON BYERLY'S EXTENDED DISTANCE PROJECTION

- iii. The line joining C.W.P.R.S. focus (beginning of the seismic event) and the I.M.D. focus (end of the seismic event) also orients in $N 7^{\circ} W$ direction.

Distribution of compressions on north-eastern side and rarefactions on the south-western side indicates that the north-eastern side has gone down with respect to the south-western side.

While plotting the P wave data for fault plane solution the observations at Addis Ababa, Bangui, Nairobi and Durham have been omitted in view of their anomalously high 'O-C' residuals compared to the other residuals at similar epicentral distances. Tandon and Chaudhury (1968) have also suggested a fault plane solution from P wave data. According to them, fault is ^a sinistral strike-slip fault striking $N 026^{\circ} E$ and dipping at an angle of 66° in $N 296^{\circ} E$ direction. The plane striking $N 293^{\circ} E$ is given as the auxiliary plane. They have drawn two circles to have the three African stations in the overlap of these circles. It has been pointed out that at these stations the anomalously high positive residuals are due to missing of the first initial motion.

5.5 CORRELATION BETWEEN WATER LEVELS IN THE RESERVOIR AND SEISMIC ACTIVITY:

Prior to the construction of the Dam, no seismological observatory was operating in the immediate vicinity of the Koyna region. However, Guha et al (1968) have mentioned

that the inhabitants and engineers engaged in the construction of the Dam report rare occurrences of very feeble tremors. An examination of the seismograms written by a sensitive Benioff seismograph operating since 1951 at Poona, at a distance of 120 km from the Dam site, also reveals a rare occurrence of tremors for this region in the said period. Soon after the impounding of Koyna reservoir in 1962, the reports of earth tremors near the Dam site began to be prevalent. Guha et al (1966) located the foci of these tremors at a depth of about 4 km and attributed crustal adjustments within the Deccan lava flows due to water loading to be their cause. The Koyna earthquake of December 10, 1967 has been considered as an isolated event unconnected with the earlier seismic activity of the region by Guha et al (1968), Tandon and Chaudhury (1968) and Geological Survey of India (1968). It was earlier pointed out by Narain and Gupta (1968-b) that the earthquake is of very shallow focus and its magnitude is of the order of 6 and not 7 as reported by Guha et al (1968) and Tandon and Chaudhury (1968). Narain and Gupta had also mentioned that the highest magnitude for tremors in the region till March, 1966 was of the order of 4, the September 13, 1967 and December 10, 1967 earthquakes had magnitudes of the order of 5 and 6 respectively and that all these events appeared to be connected.

In Figure 43, the inflow hydrograph of the Shiva-jisagar Lake, the water levels in the reservoir and the weekly frequency of the earth tremors recorded at the Koyna Nagar seismological observatory have been reproduced from the report of Guha et al (1968) for the period between June, 1963 and December, 1967. As mentioned before, the near absence of seismic activity in the region prior to the impounding of the reservoir is note worthy. Moreover, a careful examination of Figure 43 indicates that every year, following the rainy season the seismic activity increases. The maximum of the enhanced seismic activity, which occurs after a certain lag of time seems to correspond and depend on the height of water level in the reservoir and the duration for which it is retained. The data for the last five rainy seasons give five such examples. Out of these five, the following two are very conspicuous. Water was retained above 2,140 ft level for a long time during August, 1965 to October, 1965 and high seismic activity was reported during November, 1965. So far highest water level was retained for the longest time during August, 1967 to December, 1967 and this appears to be responsible for the maximum reported seismic activity of the August, 1967 to December, 1967 period. Whenever the water level has crossed the 2,140 ft mark and has been retained for a long time, the seismic activity has considerably increased with a certain lag of time. The absence of seismic activity before filling the reservoir and these examples indicate a correlation between the reservoir levels and the seismicity of the region.

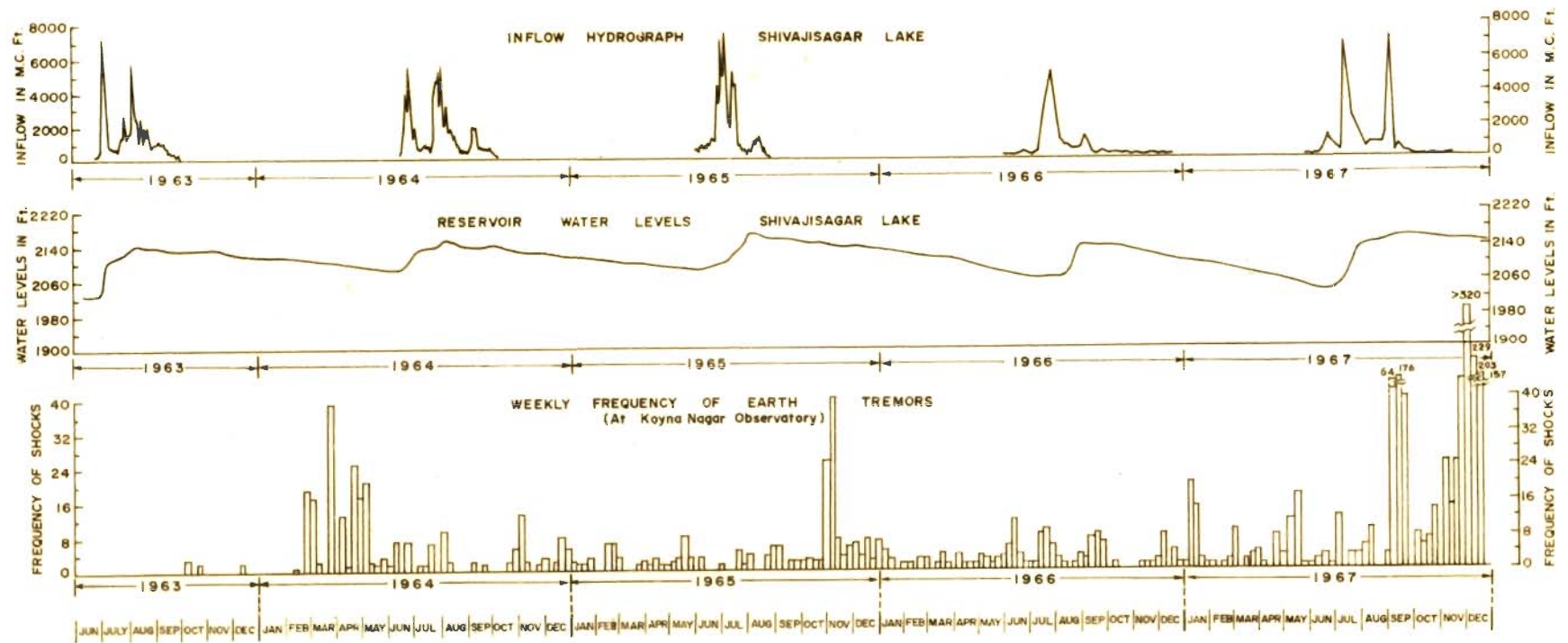


Figure 43. Inflow hydrograph, reservoir water level in the Shivajisagar Lake and the seismic activity in the Koyna region (Guha et al 1968).

5.6 OTHER EXAMPLES OF THE ASSOCIATION OF SEISMIC ACTIVITY WITH WATER RESERVOIRS:

Association of seismic activity with filling of the reservoir has been reported elsewhere also. Rothe (1968) has cited a number of these examples. Carder (1945) reported several hundred felt earthquakes and thousands recorded by seismographs in the vicinity of Lake Mead of Boulder Dam, Colorado, following its filling in 1935. Burst of seismic activity succeeding the overfilling was particularly remarkable in 1940, 1941 and 1942. At Kariba Dam of Rhodesia, forming the largest artificial lake in the world, seismic activity followed the impounding. In this case shocks up to the magnitude 6 occurred. In Monteynard Dam (French Alps), a close relationship between the frequency of the shocks and water level of its reservoir was observed. The occurrence of few mild shocks and a destructive earthquake of magnitude 6.3 has been associated with the filling of a large artificial lake at Kremasta Dam in Greece. Fluctuations in the level of Marathon Dam lake, also in Greece, have been followed by quite marked seismic activity. Some activity was also reported after the construction of Contra Dam in Switzerland. Adams (1968) has found a threefold increase in seismic activity at Mangla Dam in Pakistan. Evans (1966, 1967), has put forward the classic example of Rocky Mountain Arsenal near Denver where a deep well was used for disposal of waste fluids. Otherwise a

nonseismic area, Denver experienced several hundred tremors. The frequency of these tremors was found to be high during the months of high injection and vice-versa.

5.7 FORESHOCKS AND AFTERSHOCKS OF KOYNA EARTHQUAKE:

Figure 44 shows the frequency magnitude relation for the aftershocks of the earthquake (data - preliminary report on 'Koyna earthquake of December 10, 1967 from the teleseismic array at Gauribidanur, Mysore, operated by Bhabha Atomic Research Center). Fortysix aftershocks having magnitude above 4.0 recorded during the next three days have been divided into five groups (Table 20) of magnitude interval of half. The shocks falling in each group are numbered and their average magnitude has been calculated. The magnitude distribution of the sequence has been fitted with a function of the type $\text{Log } N = a + b.M$ and the value of b has been found to be $- 0.8$.

Table 20

Mag. Group	Total No. (N)	Average Mag.
4 to 4.5	26	4.3
4.6 to 5.0	10	4.8
5.1 to 5.5	8	5.3
5.6 to 6.0	2	5.6
6.1 to 6.5	1 (Main shock)	6.3

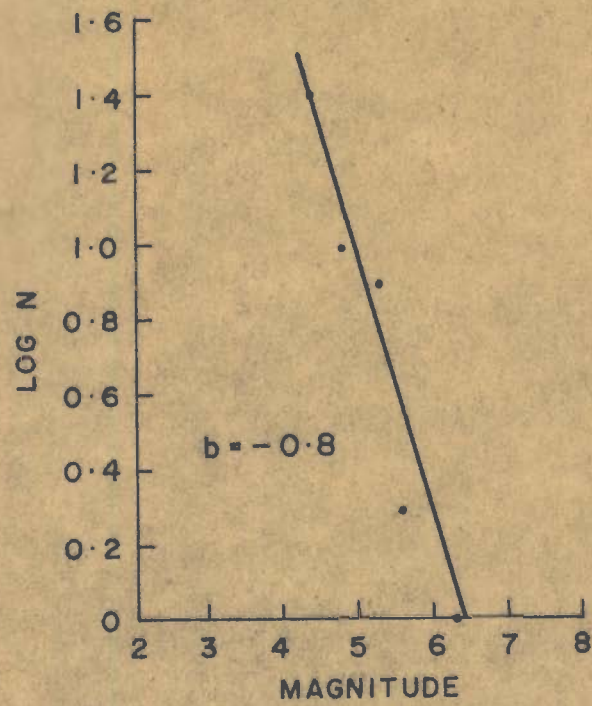


Fig. 44. FREQUENCY-MAGNITUDE RELATION FOR THE AFTERSHOCK SEQUENCE OF DECEMBER 10, EARTHQUAKE

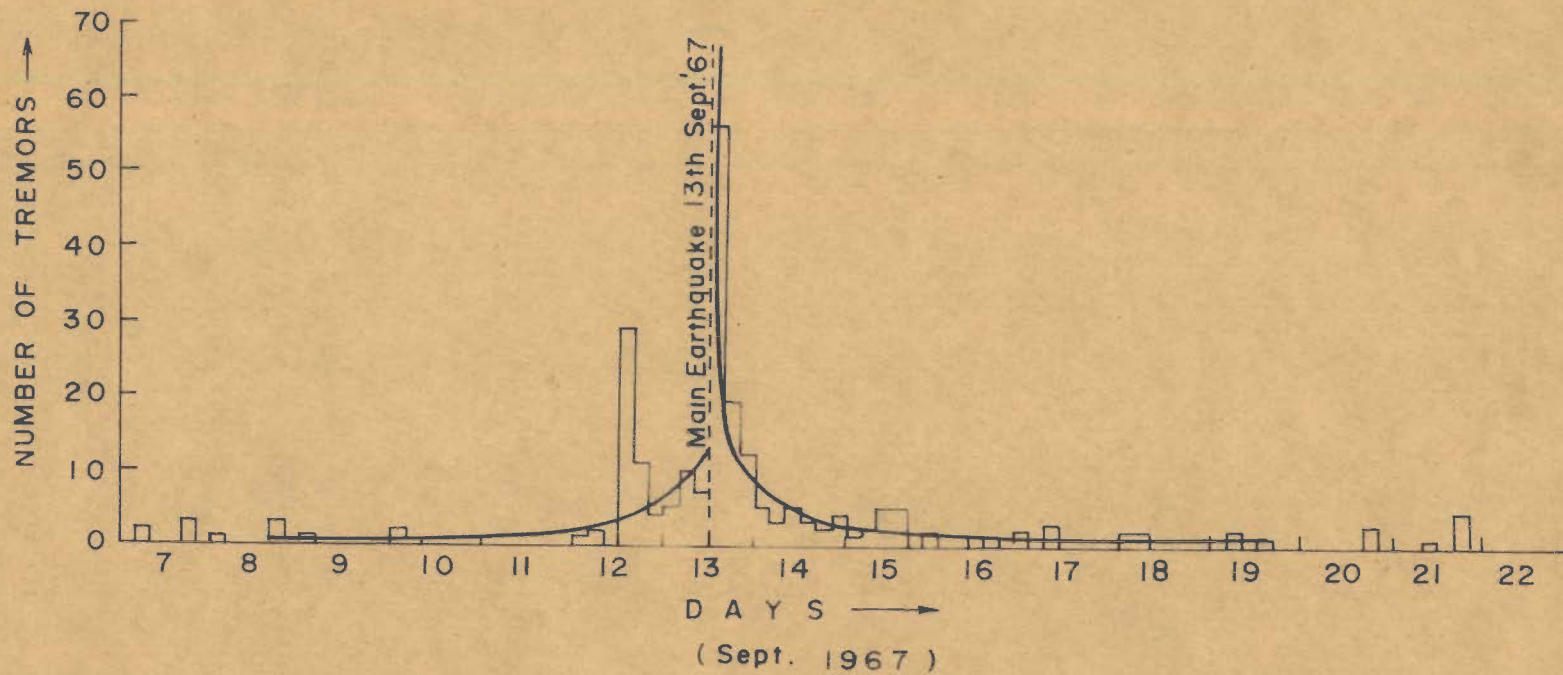


Fig. 45. FORESHOCK - AFTERSHOCK SEQUENCE FOR THE KOYNA EARTHQUAKE OF SEPTEMBER 13, 1967 (GUHA et al 1968)

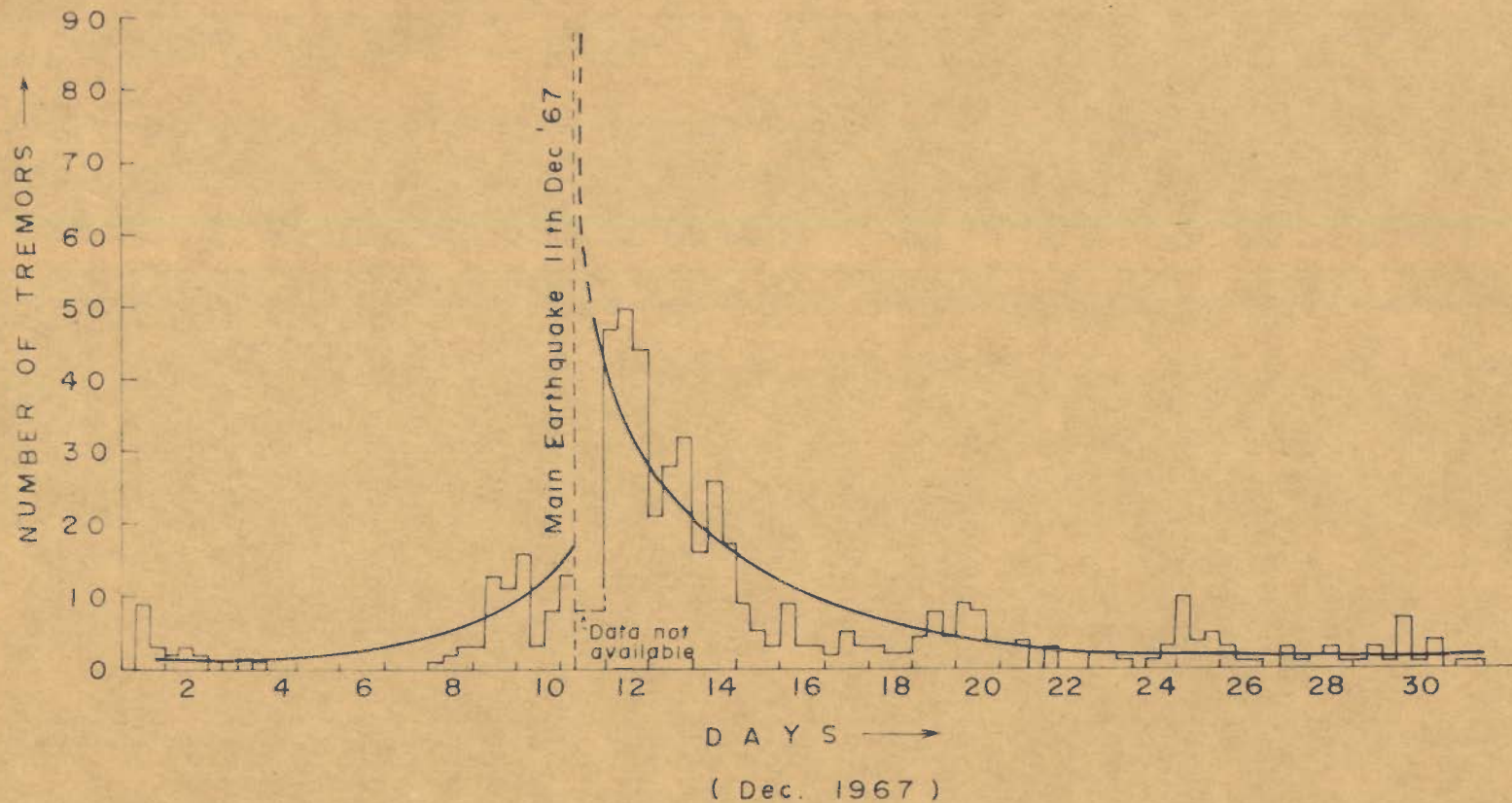


Fig. 46. FORESHOCK - AFTERSHOCK SEQUENCE FOR
 THE KOYNA EARTHQUAKE OF DECEMBER 10, 1967
 (GUHA et al 1968)

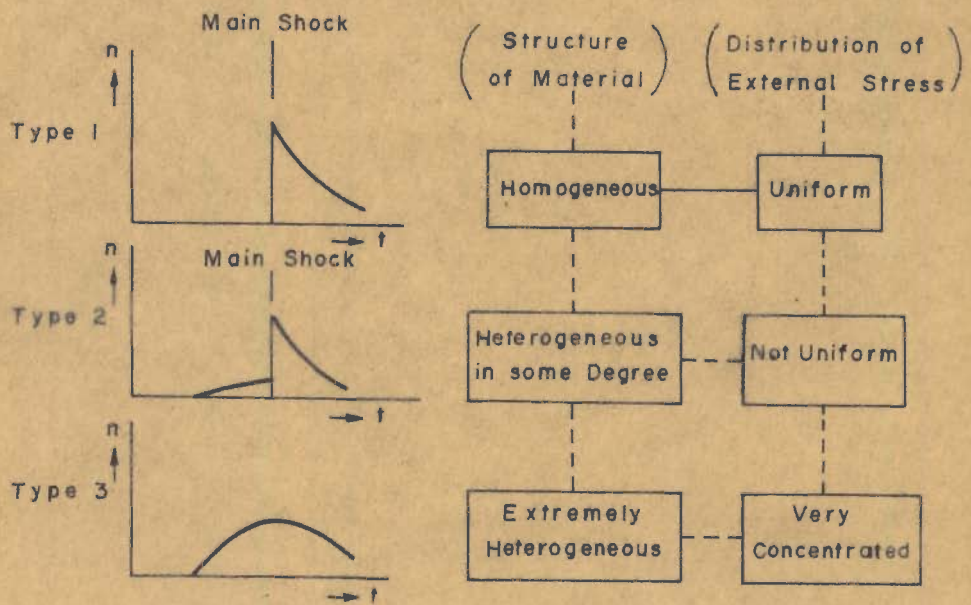


Fig. 47. MOGI'S (1963) THREE TYPES OF EARTHQUAKE SEQUENCES AND THEIR RELATIONS TO THE STRUCTURES OF THE MATERIALS AND THE APPLIED STRESSES

Figures 45 and 46 give the foreshock and aftershock patterns (Guha et al, 1968) of the two major seismic events i.e., September 13, 1967 and December 10, 1967 earthquakes of the Koyna region. It is remarkable to note that the two patterns are identical. The frequency of the foreshocks increases steadily, then there is a sudden rise in their number at the time of main shock and then their frequency diminishes exponentially.

Mogi (1963) has studied the foreshock and aftershock patterns experimentally on models in the laboratory and has compared them with the natural earthquake occurrences. He has broadly classified these patterns into three types (Figure 47). His second pattern is similar to the observations in the Koyna region. It is interesting to note that out of 1,500 earthquakes studied by Mogi in Japan, only 4% fall in the second category. They are also found to be confined in certain localities only. It is very important that the occurrence of the foreshocks is not accidental and has a general tendency to be limited to certain regions attributed to the local mechanical structure. With the increase of stress in the heterogeneous structure of the region, its concentration increases highly at many irregular points and the local fractures occur at such weak points. Hence the regions where earthquakes are preceded by foreshocks are deduced to be moderately fractured regions. In case of such occurrences in Japan, the spatial distribution of the regions to some degree

agrees with the geographic distribution of quaternary volcanoes and volcanic regions in Neogene. It is striking that the Koyna region is also heterogeneous to some extent and has evidences of volcanic activity in the geological past.

In his recent work, Scholz (1968) attributes the dependence of $|b|$ value on the percentage of the existing stress within the rock sample to the final breaking stress. According to him, at low stress levels microfractures occur due to the frictional sliding on pre-existing cracks and crushing of pores. This situation is similar to the occurrence of shallow volcanic earthquakes having high $|b|$ values of 2 to 3. Between 30 to 50 percent of fracture strength, few microfractures are detected. After 50 percent, microfracture rate increases continuously till final rupture occurs and the $|b|$ value decreases with increasing relative stress from 1 to 0.3. For a single component mean stress, values are confined between 0 to 1 corresponding to non-volcanic earthquakes in seismology. In the study of Californian earthquake sequences McEvilly and Casaday (1967) and McEvilly et al (1967) have pointed out that for the sequences with low $|b|$ value the largest aftershock magnitude is at least 0.9 times that of mainshock and for higher values of $|b|$ the magnitude of largest aftershock is about 0.6 - 0.7 times the magnitude of the main-shock. This does not hold good for Koyna sequence where although, $|b|$ value is high (i.e. 0.8), the magnitude of largest aftershock (5.6) is 0.9 times the main shock magnitude (6.3).

It is likely that the earthquake sequences belonging to type 2 mechanism in the moderately heterogeneous regions of non-uniform distribution of external stresses are characterised by a high $|b|$ value along with a high largest aftershock magnitude, ratio.

Besides the two major events of September 13 and December 10, 1967 the third biggest earthquake of Koyna region in the immediate past was that of November 11, 1965. The foreshock and aftershock pattern for this earthquake is also identical. It is also noticeable that number of foreshocks increases with the magnitude of the main shock. The December 10, 1967 (Mag. of the order of 6) had 18 foreshocks, the September 13, 1967 (Mag. of the order of 5) had 12 foreshocks and November 11, 1965 (Mag. of the order of 4) had only 8.

The pattern established for Koyna region by the 3 major events discussed above indicates a correlation between the frequency of foreshocks and the corresponding probable maximum magnitude of the earthquake. It looks possible to work out an empirical relationship from which it should be possible to predict the maximum expected magnitude by a detailed study of these foreshock patterns, corresponding to a certain seismic activity level.

5.8 CONCLUSIONS:

The Koyna earthquake sequence has been studied in detail. Following significant conclusions are drawn:

1. The C.W.P.R.S. epicenter and origin time correspond to the initiation of the seismic event, which 3-4 sec later had a larger burst of energy near I.M.D. epicenter and in the meizoseismal region of + VIII intensity.
2. Fault plane solution based on P wave data indicates a near vertical movement on a plane striking NNW, with north-eastern side going down with respect to south-western side.
3. Seismicity in Koyna region increases with the increase of water level in the reservoir with certain lag of time.
4. The aftershocks of the December 10, earthquake are related by a function of the type $\log N = a + b.M$ the value of $|b|$ being - 0.8.
5. The foreshock - aftershock patterns of the two major events in the Koyna region are identical and correspond to type 2 of Mogi's model. This is a typical feature of the earthquakes of moderately fractured region. The geological history of the regions of such earthquake occurrences in Japan is similar to that of Koyna region.
6. The increase in the number of foreshocks correlates directly with the magnitude of the main shock in this region. Prediction of maximum expected magnitude related to certain seismic activity level seems possible through a more detailed study.

CHAPTER VI
SUMMARY AND CONCLUDING REMARKS

CHAPTER VI

SUMMARY AND CONCLUDING REMARKS.

6.1 SUMMARY:

In Chapter I, the importance of Seismology and its contributions in the investigation of earth's physical properties has been emphasized and the major discoveries are briefly reviewed. Some of the new applications of seismology in the prediction of earthquakes, detection of nuclear explosions and exploration of moon have been also commented upon.

Valuable information is obtained from surface wave dispersion studies. It provides an alternative method to body waves for studying the velocity distribution in the earth, gives information about the density distribution and in principle, a single surface wave dispersion seismogram for a particular path contains all the information necessary for structural interpretation along it.

Previous work on surface wave dispersion studies is briefly surveyed. It is observed that most of the earlier observational work was confined to studying the dispersion along a few paths and comparing it with the theoretical dispersion curves. In the later work during 1960's, the installation of W.W.S.S.S. gave impetus to surface wave investigations

and studies were conducted along a number of paths criss-crossing a particular region in different directions. From this, evolved the 'crossing path technique'. Using this technique global investigations were carried out for divisioning it into different regions of similar group velocity dispersion characteristics. However, all this work was confined to Rayleigh waves only.

In Chapter II, the necessity of examining Rayleigh wave divisioning by Love waves is pointed out. Compared to Rayleigh waves, the observation of Love waves is difficult. Keeping in view the geographical distribution of epicenters in the Circum-Pacific and Alpidic belts and location of W.W.S.S.S. in Europe and South Asia - giving an opportunity to study purely continental paths, Love wave dispersion for the fundamental mode has been investigated in Eurasia. It is found possible to divide Eurasia into different regions of similar Love wave group velocity dispersion characteristics and the divisioning is in agreement with Rayleigh wave divisioning based on wave lengths in the same range. Observation of extremely low group velocities necessitated the creation of a new region '13' in Himalaya and Tibet Plateau area.

In Chapter III, the origin of the concept of isostasy, Airy's and Pratt's hypotheses and the investigations carried out regarding the roots of mountains have been briefly reviewed. Himalaya - the highest mountains and the neighbouring Tibet Plateau, where lowest group velocities for Rayleigh and Love

waves were delineated in Chapter II, are found to be the least explored regions. In view of the absence of facilities for carrying out deep seismic sounding, surface wave dispersion studies and the comparison of the observed dispersion curves with theoretical curves computed for suitable earth models for crustal investigations in this region is the most suitable method. Consequently, Rayleigh and Love wave group velocity dispersion along a number of paths crossing region '12' in various directions has been studied. For comparison a three layer earth model with equal thicknesses of granitic and basaltic layers is found to be appropriate as indicated by earlier dispersion studies and deep seismic sounding investigations in Eurasia. This investigation indicates the existence of roots and an average crustal thickness of 70 km for Himalaya and Tibet Plateau region.

In Chapter IV, a new significant correlation has been sought between global seismicity and lateral elastic wave velocity gradients. The attestation of Rayleigh wave divisioning of Eurasia by Love waves in Chapter II has been emphasized and it is postulated that similarly the Rayleigh wave divisioning in other parts of the world would also be valid for Love waves. Since the divisioning patterns are based on Rayleigh waves penetrating effectively to outer 40 to 50 km section of the earth, it is argued that the division pattern, in general, depicts the seismic wave velocity distribution in the upper 50 km section of the earth. This statement is supported by the apparent Pn velocity distribution investigated for United States.

It is observed that 90% of the total seismic energy is released through shallow focus earthquakes of magnitude 7 and above. On the Rayleigh wave division map of Eurasia and Africa; Indian, Atlantic and the Pacific Oceans, the epicenters of shallow focus earthquakes of magnitude 7 and above are plotted for the last 70 years. The lateral group velocity gradients along a number of sections have been also determined. It is found that regions of high seismicity invariably correspond to regions of steep velocity gradients. All epicenters for earthquakes of magnitude 8.6 and above lie in regions having gradients of the order of $1.5 \cdot 10^{-3} \text{ sec}^{-1}$ and above. On the basis of seismicity, the Rayleigh wave division pattern for South America and Australia, where such investigations are not yet carried out; is predicted. Also on the basis of very high velocity gradients, some regions prone to very high magnitude earthquake occurrence are indicated. The Koyna earthquake of December 10, 1967 and the relatively higher seismic activity on the western coasts of India compared to eastern coasts is comprehended in view of comparatively higher velocity gradients on western coasts.

In Chapter V, the data now available on Koyna earthquake is discussed. The different origin times and epicenters given by various agencies have been explained. Field observations, different origin times and epicenters given by India Meteorological Department and Central Water and Power Research Station, ~~field evidences~~ and nature of the seismograms for this earthquake suggest a multiple event. A fault plane solution has been

obtained by using the sense of first motions. Seismicity in Koyna region has been found to increase with the increase of water level in the reservoir and vice-versa with a certain time lag. The two major earthquakes of this region have similar foreshock - aftershock pattern, corresponding to type 2 of Mogi's models. Aftershocks of this earthquake are related by a function $\text{Log } N = a + b.M$, value of b being -0.8 . Possibility of predicting maximum expected magnitude at a certain seismic activity level of Koyna region has been also pointed out.

6.2 CONCLUDING REMARKS:

In the present course of studies, dispersion of the fundamental mode of Love and Rayleigh waves has been investigated and implied for crustal delineations and formulation of a new significant correlation between lateral velocity gradients and global seismicity. These investigations have given rise to new approaches to solve some fundamental problems and have indicated the necessity of further detailed work.

Theoretical dispersion curves based upon suitable earth models should be computed to fit in the standard Rayleigh and Love wave dispersion curves used for divisioning. The present Rayleigh and Love wave divisioning is based upon 30 sec period waves. It is important to study, how this divisioning changes when investigated for longer wave lengths

say for 100 sec period waves. Since lateral velocity gradients connect directly the elastic parameters with seismicity, it is very important to study the variation of lateral velocity gradients with depth. It is expected that the gradients would decrease and would be negligible at the depths of 700 km or so.

APPENDIX - I

APPENDIX - I

Summary of the detailed computation for plotting the Theoretical Rayleigh Wave Dispersion curves for different crustal thicknesses. Stoneley - 1955

$\alpha_1 = 5.598$ km/sec $\beta_1 = 3.402$ km/sec $\rho_1 = 2.65$ gm/cc
 $\alpha_2 = 6.498$ km/sec $\beta_2 = 3.741$ km/sec $\rho_2 = 2.89$ gm/cc $H_1 = H_2$
 $\alpha_3 = 8.110$ km/sec $\beta_3 = 4.340$ km/sec $\rho_3 = 3.40$ gm/cc

(For crustal thicknesses of 75, 70 and 68 km).

KH ₁	c/ β_1	Phase Velocity c	C/ β_2	Group Velocity C	K			Period T = 2 π /Kc		
					H = 75km	H = 70km	H = 68km	H=75	H=70	H=68
					H ₁ =H ₂ =37.5 km	H ₁ =H ₂ =35 km	H ₁ =H ₂ =34 km			
0.8	1.014116	3.7938	0.9438	3.531		0.02286	0.02353		72.4	70.4
0.9	1.004830	3.7591	0.9170	3.431	0.02400	0.02571	0.02647	69.6	65.0	63.1
1.0	0.994665	3.7210	0.889	3.326	0.02667	0.02857	0.02941	63.2	59.1	57.4
1.5	0.940890	3.5199	0.792	2.963	0.04000	0.04286	0.04411	44.6	41.6	40.5
2.0	0.900392	3.3684	0.774	2.900	0.05333	0.05714	0.05882	35.0	32.6	31.7
2.5	0.875262	3.2744	0.7778	2.910	0.06667	0.07143	0.07353	28.8	26.9	26.1
3.0	0.859668	3.2160	0.7856	2.939	0.08000	0.08571	0.08823	24.4	22.8	22.1
3.5	0.849618	3.1784	0.7929	2.966	0.09335	0.10000	0.10294	21.2	19.8	

APPENDIX - I Continued

KH ₁	c/ β ₂	Phase Velocity c	C/ β ₂	Group Velocity C	K			Period T=2 π/Kc		
					H = 45km H ₁ =H ₂ =22.5 km	H = 37km H ₁ =H ₂ =18.5 km	H = 35km H ₁ =H ₂ =17.5 km	H=45	H=37	H=35
0.4	1.041918	3.8978	1.01844	3.815		0.02162	0.02286		74.5	70.5
0.5	1.035994	3.8756	1.00559	3.762	0.02222	0.02703	0.02857	72.9	60.0	56.7
0.6	1.029605	3.8518	0.98904	3.700	0.02667	0.03243	0.03429	61.1	50.3	45.6
0.7	1.022373	3.8247	0.96826	3.622	0.03111	0.03784	0.04000	52.8	43.4	41.1
0.8	1.014116	3.7938	0.94380	3.531	0.03555	0.04324	0.04571	46.6	38.3	36.2
0.9	1.004830	3.7591	0.9170	3.431	0.04000	0.04865	0.05143	41.8	34.3	32.5
1.0	0.994665	3.7210	0.889	3.326	0.04444	0.05405	0.05714	38.0	31.2	30.0
1.5	0.940890	3.5199	0.792	2.963	0.06667	0.08108	0.08571	26.8	22.0	20.8
2.0	0.900392	3.3684	0.774	2.900	0.08889			21.0		

APPENDIX - II

Summary of the computations done for plotting the Theoretical Love Wave Dispersion curves, Dorman (1959) - Case 201.

$$\beta_1 = 3.40 \text{ km/sec} \quad \rho_1 = 2.74 \text{ gm/cm}^3$$

$$\beta_2/\beta_1 = 1.127, \quad \beta_3/\beta_1 = 1.324, \quad \rho_2/\rho_1 = 1.095, \quad \rho_3/\rho_1 = 1.204, \quad \frac{H_1}{H} = 0.5, \quad \frac{H_2}{H} = 0.5$$

$\beta_1 T/H$	U/β_1	U	Period T			
			H=75	H=45	H=37	H=35
6.251	1.228	4.175				64.4
5.815	1.22	4.148			63.3	59.9
5.145	1.191	4.049			56.0	53.0
4.644	1.168	3.971		61.5	50.5	47.8
4.249	1.1458	3.896		56.2	46.2	43.8
3.924	1.1258	3.828		51.9	42.7	40.4
3.649	1.107	3.764		48.3	39.7	37.6
3.409	1.090	3.706		45.1	37.1	35.1
3.197	1.074	3.652	70.5	42.3	34.8	32.9
3.005	1.060	3.604	66.3	39.8	32.7	30.9
2.830	1.05	3.570	62.4	37.5	30.8	29.1
2.668	1.0359	3.522	58.9	35.3	29.0	27.5
2.516	1.026	3.488	55.5	33.3	27.4	25.9
2.372	1.0172	3.458	52.3	31.4	25.8	24.4
2.235	1.010	3.434	49.3	29.6	24.3	23.0
2.103	1.003	3.410	46.4	27.8	22.9	21.7
1.975	0.9976	3.392	43.6	26.1	21.5	20.3
1.850	0.9933	3.377	40.8	24.9	20.1	
1.727	0.990	3.366	38.1	22.9		
1.605	0.9872	3.356	35.4	21.2		
1.483	0.99	3.366	32.7	19.6		
1.361	0.984	3.346	30.0			
1.238	0.9838	3.345	27.3			
1.112	0.984	3.346	24.5			
0.984	0.9841	3.346	21.7			

REFERENCES

REFERENCES

- Adams, R.D. (1968) Personal communication.
- Airy, G.B. (1855) Phil. Trans. Roy. Soc. London, 145, pp. 101-104.
- Anderson, Don L. (1965) Physics and Chemistry of the earth 6, Pergamon Press, London, pp. 1-131.
- Arkhangel'skaya, V.M. (1960) Iz. Acad. Sciences, USSR, Geophysics ser. No. 9, pp. 904-927, English translation.
- Arkhangel'skaya, V.M. (1964) Iz. Acad. Sciences, USSR, Geophysics ser. pp. 807-821. English trans.
- Auden, J.B. et al (1939) Geol. Survey of India, 73, pp.1-391. (Memoir).
- Båth, M., and Vogel, A. (1957) Geofis. Pura e appl. 38, pp. 10-18.
- Båth, M. (1959) Geofis. Pura e appl. 43, pp.131-147.
- Bhabha Atomic Research Center Trombay (1968) Koyna Earthquake of 11th December, 1967, Preliminary Technical Report No. 1.
- Brett, W.B. (1935) A report on the Bihar Earthquake and on the Measures Taken in Consequence Thereof upto the 31st Dec. 1934, Patna, Govt. Printing Office (Bihar and Orissa).
- Brilliant, R.M. and Ewing, M. (1954) Bull. Seism. Soc. Am. 44, pp. 149-158.
- Brune, J.N., Nafe, J.E., and Oliver, J.E. (1960) J. Geophys. Res. 65, No. 1 pp. 287-304.
- Bullen, K.E. (1939) Mon. Not. Roy. Astr. Soc. Geophys. Suppl. 4, pp. 579-582.
- Bullen, K.E. (1940) Bull. Seism. Soc. Am. 30, pp.235-250.
- Bullen, K.E. (1942) Bull. Seism. Soc. Am. 32, pp.19-29.

- Bune, V.I., and Butovskaya, E.M. (1955) Trudy Geofiz. Inst. Akad. Nauk. SSSR. 30, pp.142-156.
- Byerly, P. (1930) Gerlands Beitr. Z. Geophysik 26, pp.27-33.
- Byerly, P. (1938) Bull. Seism. Soc. Am. 48, pp. 2025-2031.
- Byerly, P. (1956) Advances in Geophysics, 3, pp.106-152.
- Caloi, P. (1958) Z. Geophys. 24, pp. 65-95.
- Carder, D.S. (1934) Bull. Seism. Soc. Am. 24, pp.231-302.
- Chaudhury, H.M. (1966) Ind. J. Met. Geophys. 17, pp.385.
- Carder, D.S. (1945) Bull. Seism. Soc. Am. 35, pp.175-192.
- Cisternas, A. (1961) Bull. Seism. Soc. Am. 51, pp.381-388.
- Conrad, V. (1925) Mitt. Erdb. Komm. Wien. Akad. Wiss. (N.F.) No. 59, pp. 1-23.
- Datta, A.N. (1961) Bull. of the National Institute of Sciences of India, No. 22, pp.32-41.
- Dorman, J. (1959) Geophysics, 24, pp. 12-29.
- Evans, M.David. (1966) Geotimes, 10, pp.11-17.
- Evans, M.David. (1967) Geotimes, 12, pp.19-20.
- Ewing, M. and Press, F. (1952) Bull. Seism. Soc. Am. 42, pp.149-158.
- Ewing, M. and Press, F. (1954-A) Bull. Seism. Soc. Am. 44, pp.121-147.
- Ewing, M. and Press, F. (1954-B) Bull. Seism. Soc. Am. 44, pp.471-479.
- Ewing, M., Jardetzky, W. and Press, F. (1957) Elastic Waves in Layered Media. McGraw Hill, New York.

- Ewing, J. and Ewing, M. (1959) Bull. Geol. Soc. Am. 70, pp.291-318.
- Geological Survey of India (1968) A Geological Report on the Koyna Earthquake of 11th December, 1967, Satara District, Maharashtra State.
- Guha, S.K. et al. (1966) Crustal Disturbances in the Shivajisagar Lake area of the Koyna Hydroelectric Project. Third Symposium Earthquake Engineering Roorkee, pp.399-416.
- Guha, S.K. et al. (1968) Recent Seismic Disturbances in the Koyna Hydroelectric Project, Maharashtra, India, A report by the Central Water and Power Research Station, India.
- Gupta, Harsh and Hari Narain. (1967) Bull. Seism. Soc. Am. 57, pp.235-248.
- Gupta, Harsh and Satô, Y. (1968) Bull. Earthq. Res. Inst. 46, pp. 1-12.
- Gutenberg, B. (1923) Physikalische Zeitschrift 24 Jahrgang, pp.458-459.
- Gutenberg, B. (1924) Physikalische Zeitschrift 25 Jahrgang, pp.377-381.
- ~~Gutenberg, B. (1925) Ann. d. Phys. der Erde. Borntraeger, Berlin.~~
- Gutenberg, B. (1933) Hand buch der Geophysik 2, pp.440-564. Borntraeger, Berlin.
- Gutenberg, B. (1943) Bull. Geol. Soc. Am. 54, pp.473-498.
- Gutenberg, B. (1948) Bull. Seism. Soc. Am. 38, pp.121-148.
- Gutenberg, B. (1925) Zeit. fur Geophysik, 3, pp.94-108.
- Gutenberg, B. and Richter, C.F. (1949) Seismicity of the Earth and Associated Phenomenon, Princeton Univ. Press.
- Gutenberg, B. (1951) Trans. Am. Geophys, Un. 32, pp.373-390.

- Gutenberg, B. (1956) Quart. J. Geol. Soc. London. 112, pp. 1-14.
- Hari Narain and Gupta, Harsh. (1968-a) J. Ind. Geophysical Un. 5, pp.30-34.
- Hari Narain and Gupta, Harsh. (1968-b) Nature, 217, pp. 1138-1139.
- Herrin, E. and J. Taggart. (1962) Bull. Seism. Soc. Am. 52, pp. 1037-1046.
- Jacobs, J.A. (1956) 'The Interior of the Earth' - Advances in Geophys. 3. Academic Press, New York, pp.183-239.
- Jeffreys, H. (1934) Mon. Not. Roy. Astr. Soc. Geophys. Suppl. 3, pp. 253-261.
- Jeffreys, H. (1925) Ibid, 1, pp 282-292.
- Jeffreys, H. (1939-A) Mon. Not. Roy. Astr. Soc. Geophys. Suppl. 4, pp. 498-533.
- Jeffreys, H. (1939-B) Mon. Not. Roy. Astr. Soc. Geophys. Suppl. 4, pp. 594-615.
- Kelkar, Y.N. (1968) Kesari Daily January 7th issue (In Marathi).
- Kingdon-Ward, F. (1951) Nature, 167, pp. 130-131.
- Kosminskaya, I.P. and Riznichenko, Y.V. (1964) Research in Geophysics, 2, MIT Press, pp.81-122.
- Kosminskaya, I.P. (1965) Annals of the I.G.Y. XXX, pp.182-208.
- Kovach, R.L. (1959) J. Geophys. Res. 64, pp.805-813.
- Kovach, R.L. (1965) Physics and Chemistry of the Earth, 6. Pergamon Press, London pp.251-314.
- Labrouste, Y. (1933) Soixante-sixième Congrès des Sociétés Savantes, pp.463-467.
- Lamb, H. (1903) Phil. Trans. 203, pp. 1-42.
- Love, A.E.H. (1911) Some Problems of Geodynamics, Cambridge.

- Middlemiss, C.S. (1910) Mem. Geol. Survey of India 38, pp. 1-409.
- McDonald, Gordon, J.F. (1963) Reviews of Geophysics, 1,4, pp.587-665.
- McEvelly, T.V. and Casaday, K.B. (1967) Bull. Seism. Soc. Am. 57, pp.113-124.
- McEvelly, T.V. et al. (1967) Bull. Seism. Soc. Am. 57, pp. 1221-1224.
- Mogi, K. (1963) Bull. Earthq. Res. Instt. 41, pp. 615-658.
- Mohorovičić, A. (1909) Jahrb. Meteorol. Obs. Zagreb, 9, Teil 4, Abschnitt 1, pp.63.
- Nagmune, T. (1956) Geophys. Mag. 27, pp.93-104.
- Nuttli, O. (1963) Reviews of Geophysics, I 3, pp.351-400.
- Oldham, T. (1882) Catalogue of Indian Earthquakes. Mem. Geol. Survey of India, X, p. 1883.
- Oldham, R.D. (1899) Mem. Geol. Survey of India, 29, pp. 1-379.
- Oldham, R.D. (1928) Mem. Geol. Survey of India, 46, pp. 17-147.
- Omote, S., Santô, T., Taisseyre, R. and Vesaneu, E. (1966) Bull. International Instt. of Seism. and Earthq. Engg. 3, pp. 81-101.
- Pakiser, I.C. and Steinhart. (1964) Research in Geophysics, 2, M.I.T. Press, pp. 123-147.
- Porkka, M.T. (1961) Geophysica, 7, p.151.
- Pratt, J.H. (1855) Phil. Trans. Roy. Soc. London, 145, pp. 53-55.
- Pratt, J.H. (1859) Phil. Trans. Roy. Soc. London, 149, pp.747-763.

- Press, F. (1956) Bull. Geol. Soc. Am. 67, pp. 1647-1658.
- Press, F., Ewing, M. and Oliver, J. (1956) Bull. Seism. Soc. Am. 46, pp.97-103.
- Press, F. (1960) J. Geophys. Res. 65, pp.1039-1051.
- Press, F. (1967) Geophysic, XXXII, No. 1, pp.8-11.
- Qureshy, M.N. Tectonophysics (Under publication).
- Ramachandra Rao, M.B. (1953) A compilation of papers on the Assam Earthquake of August 15, 1950, Govt. of India.
- Rayleigh, Lord. (1885) Proc. London Math. Soc. 17, pp. 4-11.
- Richter, C.F. (1958) Elementary Seismology, W.H. Freeman and Company.
- Riznichenko, Y.V. (1958) Studia Geophys. et Geodact 2, pp. 133-140.
- Röhrbach, W. (1932) Zeit. Fur Geophysik, 8, pp.113-129.
- Rozova, E. (1936) Acad. Sci. USSR. Inst. Seism. Publ. 72, pp. 28, Leningrad.
- Rothe, J.P. (1968) New Scientist, 39, No. 605, pp.75-78.
- Roy, A. and Jain, S.C. Bull. N.G.R.I. (Under publication).
- Saha, B.P. (1965) Ind. J. Met. Geophys. 16, pp. 277-280.
- Santô, T. (1960) Bull. Earthq. Res. Instt. 38, pp.219-240.
- Santô, T. (1961-A) Bull. Earthq. Res. Instt. 39. pp. 603-630.
- Santô, T. (1961-B) Bull. Earthq. Res. Instt. 39. p. 631.
- Santô, T. (1962-A) Ann. Geofis. 15, pp. 245.

- Santô, T. (1962-B) Ann. Geofis. 15, p277.
- Santô, T. (1963) Bull. Earthq. Res. Instt. 41, pp.719-741.
- Santô, T. (1965-A) Pure and Applied Geophysics, 62, pp. 49-66.
- Santô, T. (1965-B) Pure and Applied Geophysics, 62, pp. 67-80.
- Santô, T. (1966) Pure and Applied Geophysics, 63, pp. 40- .
- Santô, T. (1967) Bull. Earthq. Res. Instt. 45, p.963.
- Santô, T. (1968) Bull. Earthq. Res. Instt. 46, pp. 431-456.
- Santô, T. and Bâth, M. (1963) Bull. Seism. Soc. Am. 53, p.151.
- Santô, T. and Satô, Y. (1966) Bull. Earthq. Res. Instt. 44, pp. 939-964.
- Satô, R. (1958) Zisin, 11, p.121.
- Satô, Y. (1960) Bull. Seism. Soc. Am. 50, p.417.
- Savarensky, E.F. and Sh.S.Ragimov. (1958) Iz. Acad. Sciences, USSR, Geophysics Ser. pp. 866-869. English trans.
- Savarensky, E.F. and Shechkov, B.N. (1961) Iz. Acad. Sciences, USSR, Geophysics Ser. pp. 454-456. English trans.
- Scholz, C.H. (1968) Bull. Seism. Soc. Am. 58, pp.399-415.
- Sezava, K. (1935) Bull. Earthq. Res. Instt. 13, pp.245-250.
- Shechkov, B.N. (1964) Iz. Acad. Sciences, USSR, Geophysics Ser. pp. 183-187. English trans.
- Shechkov, B.N. (1961) Iz. Acad. Sciences, USSR, Geophysics Ser. pp. 450-452.
- Shurbet, D.H. (1960) J.Geophys. Res. 65, p.1251.

- Stoneley, R. (1925) Mon. Not. Roy. Astr. Soc.
Geophys. Suppl. 1, pp.280-282.
- Stoneley, R. (1931) Mon. Not. Roy. Astr. Soc.
Geophys. Suppl. 2, pp.429-433.
- Stoneley, R. (1948) Bull. Seism. Soc. Am.
38, pp.263-274.
- Stoneley, R. (1955) Mon. Not. Roy. Astr. Soc.
Geophys. Suppl. 7, pp.71-75.
- Tams, E. (1921) Centralblatt für Mineralogie,
Geologie und Paläontologie,
Nos. 2 & 3, pp. 44-52.
- Tandon, A.N. (1954) Ind.J. Met. Geophys, 5, pp.95-137.
- Tandon, A.N. and Chaudhury, H.M. (1963) Ind. J. Met. Geophys.
14, pp.283-301.
- Tandon, A.N. and Chaudhury, H.M. (1968) Koyna Earthquake of December,
1967. India Meteorological Dept.
Scientific Report No. 59.
- Thomson, G.A. and Talwani, M. (1964) J. Geoph. Res., 69, pp 4813-4837.
- Veitsman, P.S. and Kosminskaya, I.P. (1965) Annals of I.G.Y.
XXX, pp. 131-139.
- Wilson, J.T. (1940) Bull. Seism. Soc. Am.
30, pp.273-301.
- Wilson, J.T. and Baykal, O. (1948) Bull. Seism. Soc. Am.
38, pp.41-53.
- Woolard, G.P. (1965) Annals of the I.G.Y.
XXX, pp.168-182.
- Worzel, J.L. and Ewing, M. (1948) Geol. Soc. Am. Mem. 27.
- Zverev, Z.N. et al. (1962) Deep Seismic Sounding of the
Earth's Crust in the USSR,
Collection of papers (Gostopt-
ekhzdat, Leningrad).

CRUSTAL STRUCTURE IN THE HIMALAYAN AND TIBET PLATEAU REGION FROM SURFACE WAVE DISPERSION

BY HARSH K. GUPTA AND HARI NARAIN

ABSTRACT

Dispersion of Rayleigh and Love waves recorded at Seoul, Hong Kong, Shillong, New Delhi and Quetta by similar long-period seismographs has been studied for the Arctic region earthquake of 25th August 1964. The entire paths from the epicenter to the recording stations are continental. Waves recorded at Shillong, New Delhi, and Quetta pass through the high mountain regions of the Himalayas and Tibet Plateau while those recorded at Seoul and Hong Kong do not pass through these high mountain regions. Observed dispersion has been compared with theoretical dispersion curves computed for a three-layer earth model. This gives an average crustal thickness of about 45 km between the epicenter and Shillong, New Delhi and Quetta, 35-37 km between the epicenter and Seoul and Hong Kong and 65-70 km in the Himalayan and Tibet Plateau regions.

INTRODUCTION

Crustal structure beneath various mountain ranges and plateaus has been investigated by many workers. Roots of mountains were confirmed for the first time by Gutenberg (1933) from the study of travel times of longitudinal waves across the Alps in Europe. Byerly (1938) reported a delay of a few seconds across the Sierra Nevada for longitudinal waves. The roots were confirmed by Caloi (1958) for the Alps and by Gutenberg (1943) and Byerly (1956) for the Sierra Nevada. Later work leaves little doubt about the existence of roots for the Sierra Nevada. Studies have been carried out by Savarensky and Regimov (1958), Ewing and Ewing (1959), Press (1960), Cisternas (1961), Thompson and Talwani (1964) and others for different regions. Kosminskaya and Riznichenko (1964) have concluded that in Eurasia, in general, considerable thickening of the consolidated crust is observed in mountain regions.

By and large, seismological work seems to substantiate the Airy hypothesis of isostasy of roots under mountains. However, in certain areas seismological data suggest that the crustal thickness is the same or even less under certain mountain systems compared to the coastal plains. Pakiser and Steinhart (1964) in their report on "Explosion Seismology in the Western Hemisphere" conclude that high mountains have roots at many places while at others they do not. The crust in the Sierra Nevada thickens to more than 50 km compared with about 30 km in the Basin and Range Province to the east, whereas the crust beneath the northern Rocky mountains is thinner than the crust in the Great Plains farther east.

Our knowledge of the thickness of the crust under the Himalayas—the highest mountains in the world—and the Tibet Plateau is very limited. Stoneley (1955), Tandon and Chaudhury (1963) and Saha (1965) have attributed the higher average crustal thickness found from surface-wave dispersion studies for paths crossing the Himalayas and Tibet Plateau to greater crustal thickness beneath them, but no



FIG. 1. Relief map of Asia (based on 'Chart of the World' H.O. 1262 A published by U. S. Naval Oceanographic Office) showing the epicenter, recording stations and the great circle paths.

estimate of their thickness has been made. In the absence of data from explosion seismology and the lack of a sufficient number of seismological observatories suitably situated for profile seismological observations, the study of dispersion of surface waves and travel-time studies of body waves recorded at sparsely distributed seismological observatories remain the only methods to study the crust in these regions.

In the present work, dispersion of Rayleigh and Love waves has been studied for the earthquake of 25th August 1964, with epicenter east of Severnaya Zemlya.

Long-period seismograms from a few selected stations equipped with WWSSS instruments were obtained for these studies. These investigations indicate a crustal thickness of 65–70 km under the Himalayas and the Tibetan Plateau.

OBSERVATIONS

The WWSSS around the world are equipped with standard type of both long-period as well as short-period instruments and it is easier and more reliable to compare and study seismograms obtained at those stations. Seismological investigations of the mountain roots under the Tibetan Plateau and the Himalayas involve study of the dispersion of surface waves recorded at conveniently situated stations equipped with long-period seismographs and where the entire path is continental and where for comparison purposes, great circle paths to some recording stations go under the Tibetan Plateau and the Himalayas.

TABLE 1

Station	Type of Instrument	Period of Inst. sec.	Period of Galvo. sec.	Mag. at 30 sec.
Seoul (SEO)	Long period N-S, E-W, Z	30	100	1500
Hong Kong (HKG)	Do	30	100	750
Shillong (SHL)	Do	30	100	3000
New Delhi (NDI)	Do	30	100	1500
Quetta (QUE)	Do	30	100	3000

With these criteria in mind, the earthquake of 25th August 1964 (epicenter 78.17°N, 126.65°E; origin time 13 hrs. 47 m 20.6 s; magnitude 6.1; depth of focus 50 km-USCGS) east of Severnaya Zemlya was picked up and the long period seismograms recorded at Seoul, Hong Kong, Chiengmai, Shillong, New Delhi, Lahore and Quetta were obtained for study (Figure 1, Table 1). Chiengmai and Lahore records could not be used as they did not show proper development of surface waves.

Only vertical component seismograms have been used for Rayleigh wave dispersion studies where they are very well developed. To make sure that the first long-period waves recorded are Rayleigh waves and are not mixed with long-period *S* wave reflections, the phase difference between the vertical and longitudinal components are measured and found to be of the order of 90°. Particle motion has been also plotted from the vertical and the longitudinal components which show retrograde elliptical movement confirming the identity of the Rayleigh waves.

Love waves are very well developed at Hong Kong and New Delhi seismograms. The epicenter is almost due north and the great circle paths between the epicenter and Hong Kong and New Delhi make 8½° and 26° angles with N-S. Hence E-W component seismograms have been used for Love wave studies. Love waves are recorded as a continuous train of waves whose period gradually decreases and no sudden or erratic change is observed corresponding to the time of the onset of Rayleigh waves in the vertical component. Figure 2 shows these seismograms. Particle motion plots confirm their identity. Figures 3A and 3B show Rayleigh and Love particle motion plottings for Hong Kong.

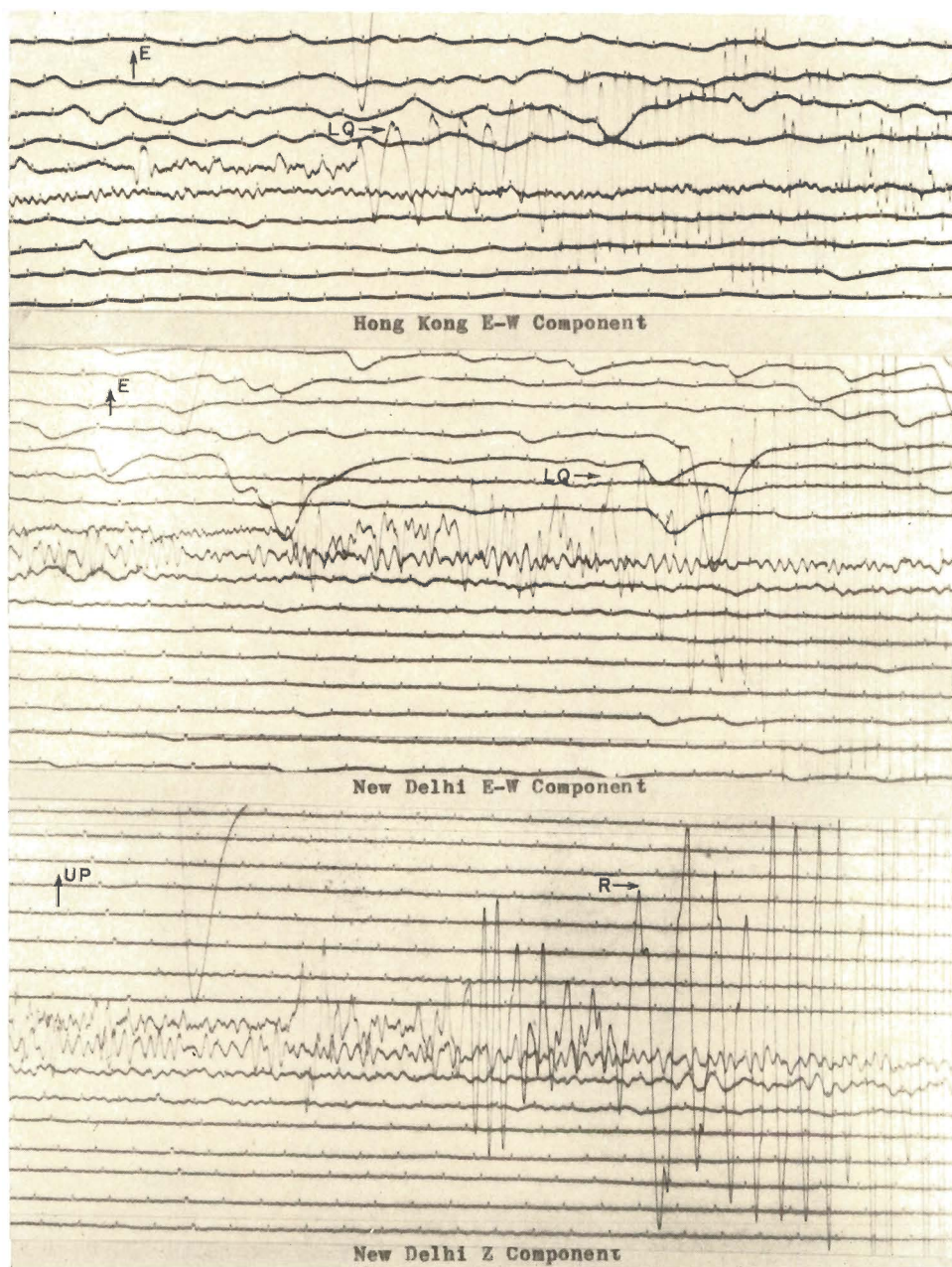


FIG. 2. Section of three seismograms showing typical Love and Rayleigh wave dispersion.

The earthquake epicenter lies on the 100 fathom depth contour i.e., well within the continental shelf. The recorded waves do not come across oceanic structure anywhere, eliminating the possibilities of significant refraction effects at the boundary between the oceans and the continents.

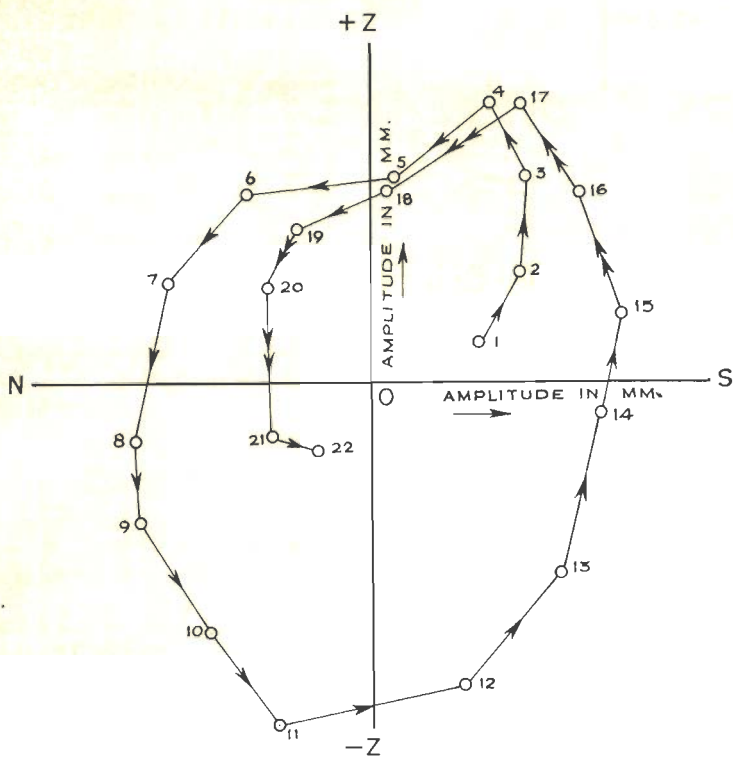


FIG. 3-A. Rayleigh wave—particle motion.

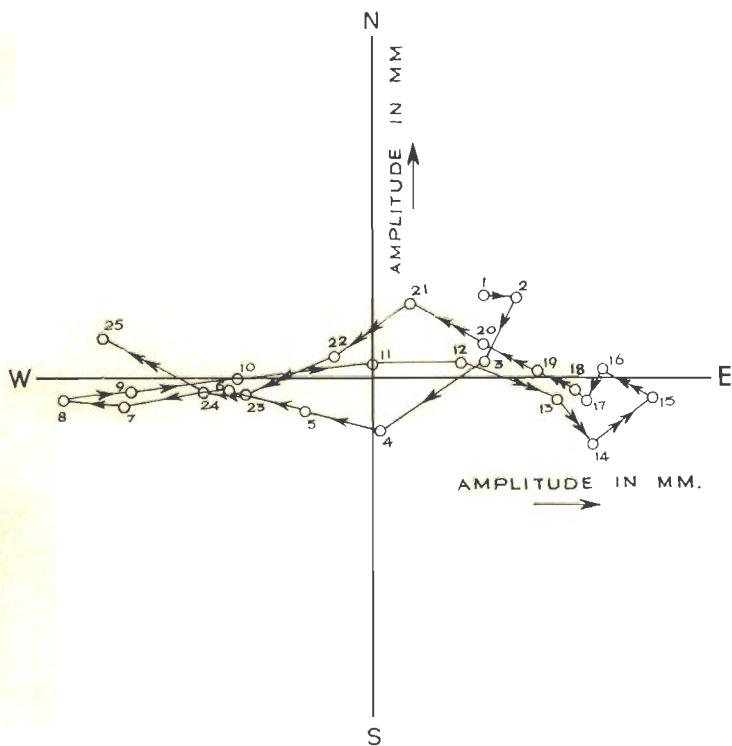


FIG. 3-B. Love wave—particle motion.

Surface-wave group velocities for both Rayleigh and Love waves are determined by the usual method of Ewing and Press (1952). Crest and trough numbers are plotted against arrival times. Slope of the graph gives period and from the known epicentral distances the group velocities are found. No phase corrections are applied

TABLE 2
GROUP VELOCITIES OF RAYLEIGH WAVES

EPC—Seoul		EPC—Hong Kong		EPC—Shillong		EPC—New Delhi		EPC—Quetta	
Period (sec.)	Group vel. (km/sec.)	Period (sec.)	Group vel. (km/sec.)	Period (sec.)	Group vel. (km/sec.)	Period (sec.)	Group vel. (km/sec.)	Period (sec.)	Group vel. (km/sec.)
52.6	3.76	60.0	3.76	58.5	3.60	71.0	3.76	66.0	3.71
41.7	3.62	55.8	3.74	50.3	3.46	61.5	3.67	55.0	3.61
34.7	3.49	49.7	3.72	46.0	3.37	52.0	3.62	46.0	3.53
30.0	3.34	44.0	3.66	35.0	3.17	45.4	3.49	39.3	3.38
24.9	3.20	39.4	3.58	28.0	3.02	38.0	3.35	34.7	3.23
22.2	2.98	33.7	3.45	25.5	2.94	33.6	3.20	32.0	3.09
19.5	2.92	28.9	3.34	24.0	2.89	29.8	3.04	27.5	2.96
18.5	2.85	26.3	3.23	20.5	2.85	23.2	2.89	24.3	2.82
		22.6	3.02	18.5	2.80	18.7	2.76	20.0	2.79
		20.8	2.93	13.0	2.68	15.2	2.81	17.2	2.68
		18.0	2.85					16.0	2.58
		17.0	2.77						
		13.0	2.73						

TABLE 3
GROUP VELOCITIES OF LOVE WAVES

Epicenter to Hong Kong		Epicenter to New Delhi	
Period in sec.	Group velocity, km/sec.	Period in sec.	Group velocity, km/sec.
68.0	4.18	58.0	3.90
60.0	4.10	53.5	3.85
50.6	3.97	46.7	3.70
45.0	3.92	41.0	3.63
39.4	3.83	36.0	3.56
33.7	3.69	34.2	3.49
29.3	3.54	29.9	3.36
24.0	3.38	27.0	3.32
20.8	3.27	23.6	3.23
19.1	3.17	20.9	3.16
18.8	3.08	18.9	3.03
16.0	2.96	18.0	2.96
15.0	2.90		

to the travel times since the operating characteristics of the instruments are similar. Tables 2 and 3 give the group-velocity data.

THEORETICAL MODEL

The next step is the comparison of the observed surface wave dispersion with theoretical dispersion curves for a suitable model. We have chosen a model with two layer crust overlying a homogeneous, semi-infinite elastic half-space.

Earlier work carried out in the Asian continent supports the existence of both the "granitic" and the "basaltic" layers. Nagmune (1956) and Shechkov (1964) have specifically mentioned that dispersion of Love and Rayleigh waves agreed for continental regions with the theoretical dispersion calculated for two layer crustal structure and not with one layer. Similar are the findings of Tandon (1954), Kovach (1959), Saverensky and Shechkov (1961), Zverev (1962), Arkhangel'skaya (1964), etc. These include results of explosion seismology, surface wave dispersion and body-wave travel-time studies. While in some regions the granitic layer is found to be thicker than the basaltic layer and in other areas the reverse is true, in a large number of cases, they are found to be of equal thickness. According to Riznichenko (1958), the roots of Tien-Shan Hercynian belt are mainly due to a thicker basaltic layer, (approximately 20 km of granitic layer and 30 km of basaltic layer), while in the Alpidic belt of the U.S.S.R., the granitic layer extends to 30 km in portions of West Turkmenia and 40 km in North Pamir, corresponding thickness of the basaltic layer being 20 and 30 km. From these considerations, a model of two-layer crust with equal thickness of granitic and basaltic layer is considered to be the most suitable choice for comparison.

Stoneley (1955) has computed Rayleigh-wave dispersion for a three-layer earth model using Jeffreys-Bullen layer parameters.

$$\begin{aligned} \alpha_1 &= 5.598 \text{ km/sec} & \beta_1 &= 3.402 \text{ km/sec} \\ \alpha_2 &= 6.498 \text{ km/sec} & \beta_2 &= 3.741 \text{ km/sec} \\ \alpha_3 &= 8.110 \text{ km/sec} & \beta_3 &= 4.340 \text{ km/sec} \\ & & \rho_1 &= 2.65 \text{ gm/c.c.} \\ & & \rho_2 &= 2.85 \text{ gm/c.c.} \\ & & \rho_3 &= 3.40 \text{ gm/c.c.} \end{aligned}$$

He has taken three particular cases: $H_2 = H_1$, $H_2 = \frac{1}{2}H_1$ and $H_2 = \frac{1}{3}H_1$ ($H_1 =$ thickness of the granitic layer and $H_2 =$ thickness of the basaltic layer). These wave velocities are in close agreement to those reported by Bune and Butovskaya (1955), Rozova (1936) etc., for central Asia.

Love-wave dispersion has not been computed theoretically for the same model. Dorman (1959) has computed dimensionless parameters for Love wave dispersion for a number of models. His case No. 201 with following parameters has been used for computing theoretical dispersion curves.

$$\begin{aligned} \beta_1 &= 3.40 \text{ km/sec} & \rho_1 &= 2.74 \text{ gm/cc} & H/2 \\ \beta_2 &= 3.83 \text{ km/sec} & \rho_2 &= 3.00 \text{ gm/cc} & H/2 \\ \beta_3 &= 4.50 \text{ km/sec} & \rho_3 &= 3.30 \text{ gm/cc} & \infty \end{aligned}$$

From these layer parameters, theoretical dispersion curves have been computed for different crustal thicknesses. These theoretical models for Rayleigh and Love-wave dispersion have been extensively used by Shechkov (1961, 1964), Saverensky and Shechkov (1961) for comparison with the observed dispersion in Eurasia.

INTERPRETATION AND DISCUSSION

Figure 4 shows the observed dispersion and theoretical dispersion curves for Rayleigh waves. For periods greater than 30 seconds, the Seoul and Hong Kong

data fall between the theoretical curves for $H = 35$ km and $H = 37$ km. New Delhi and Quetta data lie on the 45 km curve. The scatter is less than 0.05 km/sec. Shillong data lie slightly below the 45 km curve for periods greater than 40 seconds.

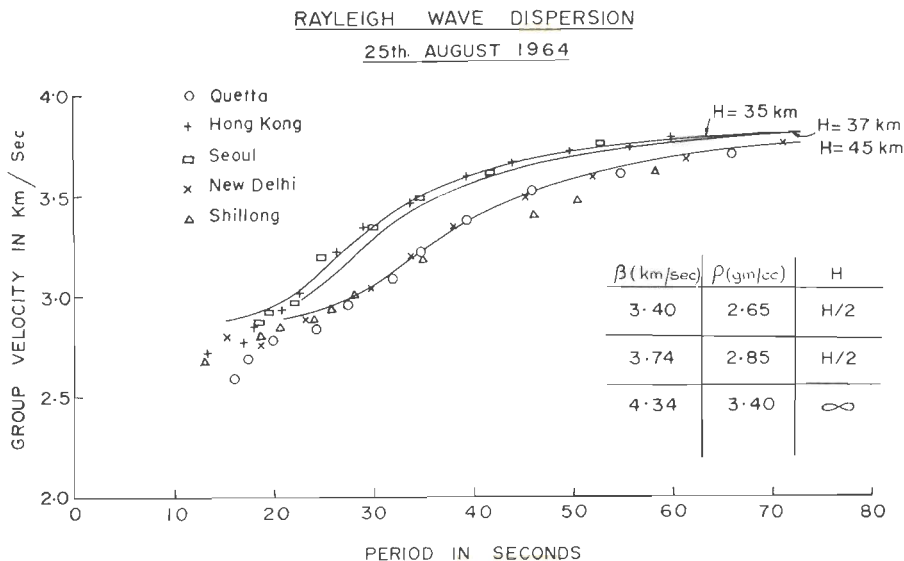


FIG. 4. Rayleigh wave dispersion—25th August 1964.

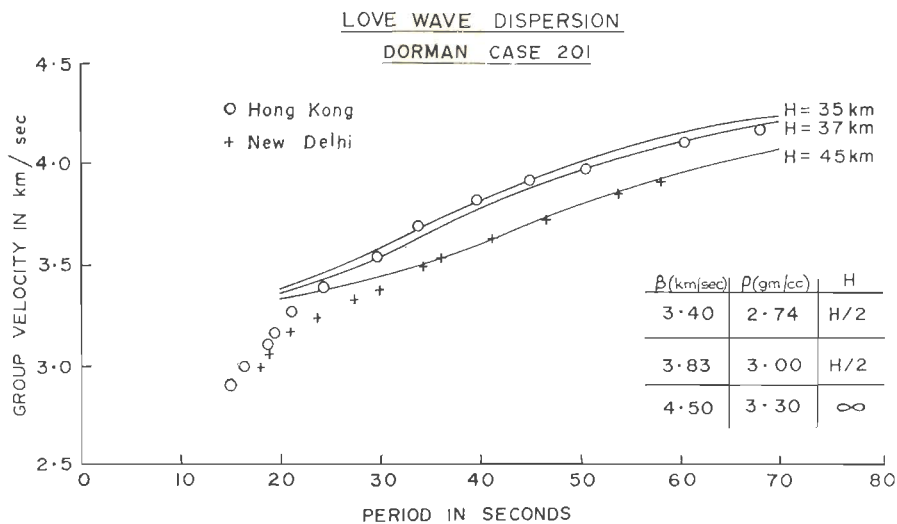


FIG. 5. Love wave dispersion—Dorman Case 201.

The scatter in the short-period range is most probably due to the presence of different sections of sedimentary layers and due to the waves arriving along paths other than the great circle.

For Love-wave dispersion in Figure 5 we observe that the Hong Kong data for

periods of 30 seconds and above lie between the theoretical curves for $H = 35$ km and $H = 37$ km while New Delhi data are in close agreement with the curve for $H = 45$ km.

The fact that the observed dispersion data are divided in two groups, one agreeing with a smaller crustal thickness of 35–37 km as recorded at Seoul and Hong Kong and the other with a larger crustal thickness of 45 km as recorded at Shillong, New Delhi and Quetta, is well established.

Tandon and Chaudhury (1963) have established an average crustal thickness of 45 km between Novaya Zemlya and New Delhi by studying the dispersion of Rayleigh waves generated from high yield nuclear explosions. The section through Novaya Zemlya and New Delhi is practically the same as the one between the

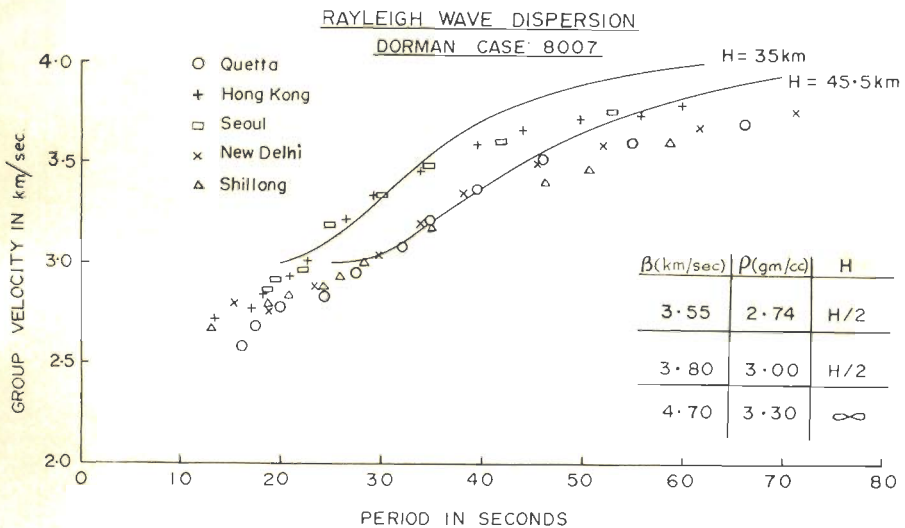


FIG. 6. Rayleigh wave dispersion—Dorman Case 8007.

epicenter of the earthquake under study and New Delhi. They have compared the observed Rayleigh-wave dispersion with Dorman Case 8007 which has been used by Kovach (1959) for comparison of the observed dispersion between the Aleutians and Lwiro. Between Sinkiang and Uppsala, Kovach (1959) found an average crustal thickness of 45.5 km by comparing the Love-wave dispersion with Dorman case 208 which has the same layer parameters as Dorman case 8007 for Rayleigh waves. Saha (1965) has also reported an average crustal thickness of 45 km between New Delhi and Novaya Zemlya from M_2 wave dispersion. However, it may be pointed out that our Rayleigh wave dispersion data show a better fit with theoretically computed curves after Stoneley (Figure 4) than with Dorman case 8007 (Figure 6) and Love wave dispersion data have a better fit with Dorman case 201 (Figure 5) than Dorman case 208 (Figure 7).

Figure 1 is a relief map of Asia and shows the great circle paths between the epicenter and the recording stations. The waves recorded at Shillong and New Delhi pass through the high mountain regions of the Himalayas and Tibet Plateau

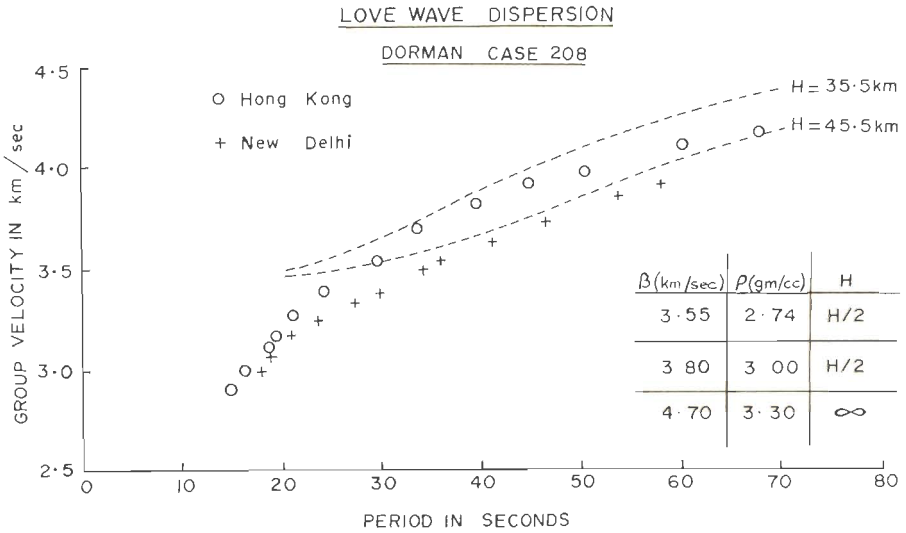


FIG. 7. Love wave dispersion—Dorman Case 208.

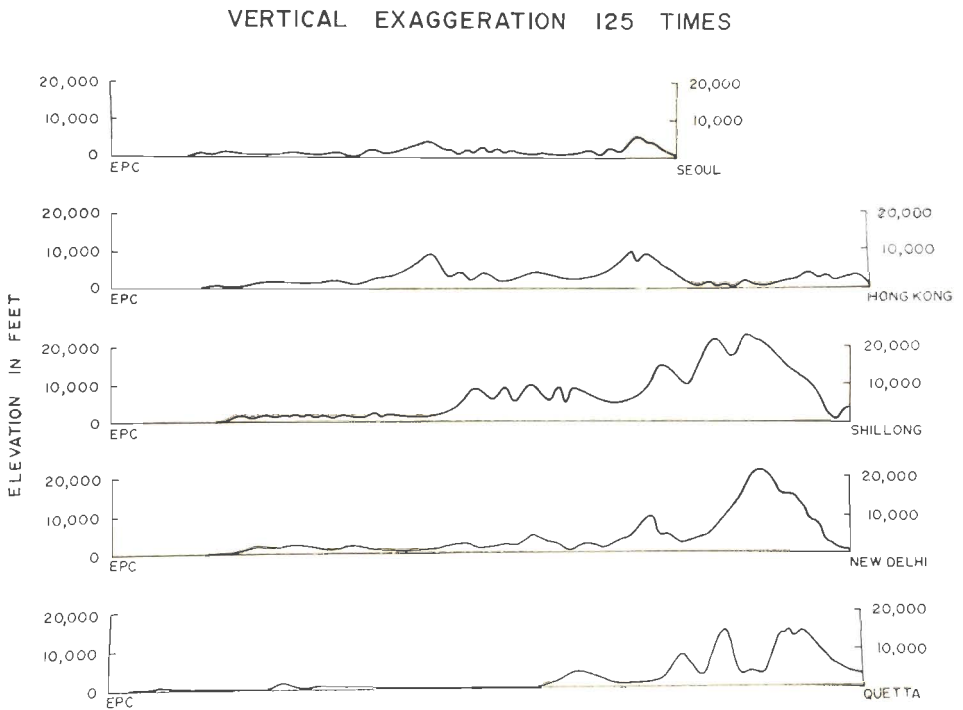


FIG. 8. Topography between epicenter and recording stations, vertical exaggeration 125 times.

and those recorded at Quetta pass through the Hindu Kush mountains and Plateau of Pamir whereas those recorded at Seoul and Hong Kong do not pass through high mountain regions. Figure 8 shows 125 times vertically exaggerated elevations along the great circle paths shown in Figure 1. The average elevation between the epicenter

and Quetta and New Delhi is of the same order and for Shillong it is slightly more. It is expected that the average crustal thickness obtained from Shillong data will be more than those obtained from New Delhi and Quetta and this is confirmed by Shillong data which lie beneath the 45 km curve for periods greater than 40 seconds (Figure 4).

Rayleigh waves penetrate effectively to about one-third of their wave length. The total section through which the wave penetrates affects the group velocity. This limits the suitability of a particular wave length in studying a crust of a definite thickness. For investigations in the average crustal thickness range of 35–55 km, Rayleigh waves with periods between 25–45 seconds are most suitable, because their depth of penetration would be of the same order. This is evident from the theoretical dispersion curves in Figure 4. For $H = 35$ km and $H = 45$ km curves, the group velocity difference is a maximum of 0.275 km/sec for 30–35 seconds, 0.175 km/sec for 25 sec and 45 sec periods and only about 0.1 km/sec for 22.5 sec and 60 sec periods. Same is true for the observed group velocities also. Hence more weight has to be given to the observations in the period range of 25 to 45 seconds in obtaining conclusions by comparison with the theoretical curves. Also in 25–45 seconds period range, due to greater depth of penetration, the effect of the sediments becomes negligible, which otherwise reduces the group velocity in the shorter period range with smaller depths of penetration.

The average crustal thickness in the northern region in Figure 1 is about 35–37 km as obtained from the Seoul data and also reported by Shechkov (1961, 1964), Saverensky and Shechkov (1961) and Arkhangel'skaya (1964). These findings are based on detailed surface-wave dispersion studies for a number of earthquakes. The high mountain regions are confined between latitude 26°N and 40°N, constituting about one-fourth of the total path traversed by the waves recorded at Shillong, New Delhi and Quetta. This quarter segment is responsible for increasing the average crustal thickness for the total path by about 8–10 km, giving an average crustal thickness of 45 km for New Delhi, Shillong and Quetta. It is therefore evident that the total crustal thickness under the Tibetan Plateau and the Himalayas should be of the order of 65–70 km to account for a difference of 8 to 10 km in the average values of the thickness of the crust.

The waves recorded at Hong Kong do not pass through these high mountain regions and consequently the observed dispersion data fall in between the curves for $H = 35$ km and $H = 37$ km.

Rayleigh wave group velocities are also calculated separately for the high mountain regions only. In Figure 1 an arc is drawn cutting epicentral distances equal to Seoul from the remaining four stations. This arc just separates the elevated Tibet Plateau and Himalayas from the rest. Graphs are plotted between different periods of the Rayleigh waves and the corresponding travel times for all the stations. The epicentral distance of Seoul is subtracted from the epicentral distances of the other stations. Travel times for different periods corresponding to the remaining distances are found from these graphs and the group velocities are calculated (Table 4). These group velocities are plotted in Figure 9 where points for New Delhi and Quetta fall around the theoretical curve for 68 km crustal thickness while those for Hong Kong fall around curves for 35 and 37 km. However, Shillong points lie below the theoretical curve for 68 km indicating a higher crustal thickness as pointed out earlier.

Table 4 also gives the computed crustal thicknesses corresponding to these group velocities using Stoneley's case I (1955) with $H_1 = H_2$. For this case the group velocity minimum occurs at $KH_1 = 2.2$ (K is the wave number) and the corresponding C/β_2 value is 0.77 and hence the table could not be used for group velocities less

TABLE 4
GROUP VELOCITIES OF RAYLEIGH WAVES AND CORRESPONDING CRUSTAL THICKNESSES

Period (sec.)	Hong Kong-Seoul		New Delhi-Seoul		Quetta-Seoul		Shillong-Seoul	
	Gr. Vel. km/sec.	H km	Gr. Vel. km/sec.	H km	Gr. Vel. km/sec.	H km	Gr. Vel. km/sec.	H km
52.5			3.27	66.5				
50.0			3.22	66.2	3.19	69.0	2.87	—
47.5			3.16	66.7	3.16	66.7	2.74	—
45.0			3.04	68.6	3.11	67.2		
42.5	3.56	39.8	2.99	69.9	3.00	69.4		
40.0	3.54	37.8			2.95	70.4		
37.5	3.53	36.1						
35.0	3.52	34.5						
32.5	3.48	33.4						
30.0	3.36	34.3						
27.5	3.30	33.4						
25.0	3.18	34.9						

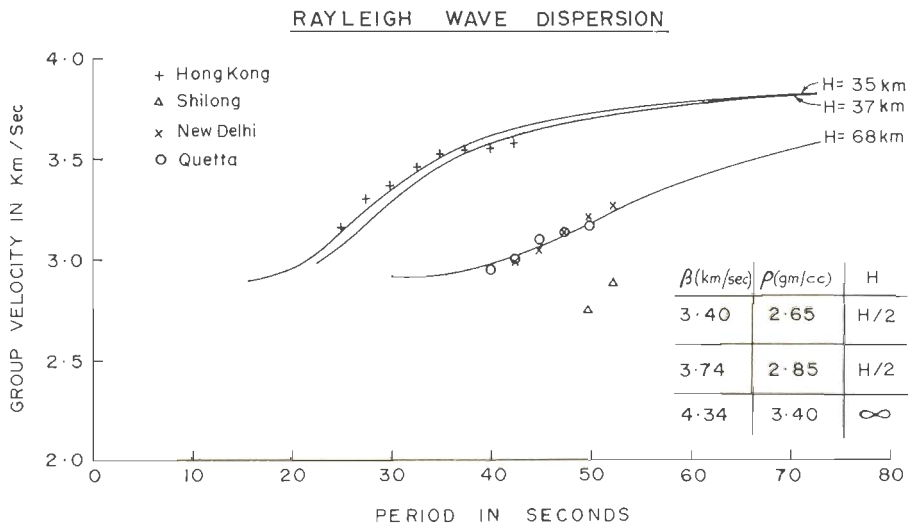


FIG. 9. Rayleigh wave dispersion.

than 2.88 km/sec. The crustal thickness values are found to be consistent in the 25 to 42.5 sec. range for Hong Kong and in the 40 to 52.5 sec range for New Delhi and Quetta. These calculations support our earlier findings.

The investigations included in this paper are consistent with an average crustal thickness of 65–70 km in the Himalayas and Tibet Plateau. These conclusions are

supported by the Profile Seismological Observations and Deep Seismic Soundings carried out by Kosminskaya *et al* (1958) and other Soviet scientists in Tien Shan and North Pamir mountain regions and where crustal thicknesses of the order of 65 km have been reported.

REFERENCES

- Arkhangel'skaya, V. M. (1964). A study of short-period surface seismic Rayleigh waves II. *Izvestiya Acad. Sci. USSR, Geophys. Ser.* 807-821. English translation.
- Bune, V. I. and E. M. Butovskaya (1955). Travel-time curves and the earth's crustal structure in central Asia according to recordings of powerful explosions. *Trudy Geofiz. Inst. Akad. Nauk. SSSR.* 30, 142-156.
- Byerly, P. (1938). The Sierra Nevada in the light of isostasy, *Bull. Geol. Soc. Am.* 48, 2025-2031.
- Byerly, P. (1956). Subcontinental structure in the light of seismological evidence. *Advances in Geophysics* 3, 106-152.
- Caloi, P. (1958). The crust of the earth, from the Apennines to the Atlantic, reconstructed in accordance with the data supplied by seismic surveys, *Z. Geophys.* 24, 65-95.
- Cisternas, A. (1961). Crustal structure of the Andes from Rayleigh wave dispersion, *Bull. Seism. Soc. Am.* 51, 381-388.
- Dorman, J. (1959). Numerical solutions for Love-Wave dispersion on a half-space with double surface layer, *Geophysics* 24, 12-29.
- Ewing, M. and F. Press (1952). Crustal structure and surface wave dispersion Pt. 2 Solomon Islands earthquake of July 29, 1950, *Bull. Seism. Soc. Am.* 42, 149-158.
- Ewing, J. and M. Ewing (1959). Seismic refraction measurements in the Atlantic Ocean basins, in the Mediterranean Sea, on the Mid-Atlantic Ridge, and in the Norwegian Sea, *Bull. Geol. Soc. Am.* 70, 291-318.
- Gutenberg, B. (1933). Der physikalische Aufbau der Erde. In *Handbuch der Geophysik* 2, 440-564 Borntraeger, Berlin.
- Gutenberg, B. (1943). Seismological evidence for roots of mountains, *Bull. Geol. Soc. Am.* 54, 473-498.
- Kosminskaya, I. P., G. G. Mikhota and Yu. V. Tulina (1958). Crustal structure of the Pamir-Alai zone from seismic depth sounding data. *Izvestiya Acad. Sci. USSR, Geophys. Ser.* 673-683, English translation.
- Kosminskaya, I. P. and Y. V. Riznichenko (1964). Seismic studies of the earth's crust in Eurasia, *Research in Geophysics*, Vol. 2. M.I.T. Press 81-122.
- Kovach, R. L. (1959). Surface wave dispersion for an Asio-African and an Eurasian path, *J. Geophys. Res.* 64, 805-813.
- Nagmune, T. (1956). On the travel time and dispersion of the surface waves, *Geophys. Mag.* 27, 93-104.
- Pakiser, I. C. and J. A. Steinhart (1964). Explosion seismology in western Hemisphere, *Research in Geophysics* Vol. 2. M.I.T. Press 123-147.
- Press, F. (1960). Crustal structure in California Nevada Region *J. Geophys. Res.* 65, 1039-1051.
- Riznichenko, Y. V. (1958). Seismische Tiefensondierungen zur Untersuchung der Erdkruste, *Studia Geophys. et Geodaet* 2, 133-40.
- Rozova, L. (1936). Construction of travel-time curves and determination of the fundamental seismic elements for Central Asia, *Acad. Sci. U.R.S.S. Inst. Seism., Publ.* 72, pp. 28, Leningrad.
- Saha, B. P. (1965). M_2 or first shear mode continental Rayleigh waves from Russian nuclear explosion of 30 October 1961, *Ind. J. Met. Geophys.* 16, 277-280.
- Saverensky, E. F. and Sh. S. Ragimov (1958). Determining the velocity of Rayleigh waves and directions to the epicenter by the nearby stations. *Izvestiya Acad. Sci. USSR, Geophys. Ser.* 866-869. English translation.
- Savarensky, E. F. and B. N. Shechkov (1961). The structure of the earth's crust in Siberia

- and in the far east from Love wave and Rayleigh wave dispersion. *Izvestiya Acad. Sci. USSR Geophys. Ser.*, 454-456. English translation.
- Shechkov, B. N. (1961). Structure of the earth's crust in Eurasia from the dispersion of the surface waves. *Izvestiya Acad. Sci. USSR Geophys. Ser.* 450-453. English translation.
- Shechkov, B. N. (1964). Seismic surface wave dispersion and Eurasian crustal structure. *Izvestiya Acad. Sci. USSR Geophys. Ser.* 183-187. English translation.
- Stoneley, R. (1955). Rayleigh waves in a medium with two surface layers, *Mon. Not. Roy. Ast. Soc. Geophys. Supp.* 7, 71-75.
- Tandon, A. N. (1954). Study of the great Assam earthquake of August 1950 and its aftershocks, *Ind. J. Met. Geoph.* 5, 95-137.
- Tandon, A. N. and H. M. Chaudhury (1963). Seismic waves from high yield atmospheric explosions, *Ind. J. Met. Geophys.* 14, 283-301.
- Thompson, G. A. and M. Talwani (1964). Crustal structure from Pacific Basin to central Nevada, *J. Geophys. Res.* 69, 4813-4837.
- Zverev, Z. N. *et al* (1962). Deep Seismic Sounding of the earth's crust in the USSR *Collection of papers* (Gostoptekhizdat, Leningrad).

NATIONAL GEOPHYSICAL RESEARCH INSTITUTE
HYDERABAD-7
INDIA

Manuscript received August 22, 1966.

3. Regional Characteristics of Love Wave Group Velocity Dispersion in Eurasia

By Harsh GUPTA,

National Geophysical Research Institute, India
and

Yasuo SATÔ,

Earthquake Research Institute.

(Read September 12, 1967.—Received Oct. 12, 1967.)

Abstract

Group velocity dispersion of Love waves has been investigated for Eurasia, which has been divided into thirteen regions according to their dispersion characteristics. Extremely low group velocities have been observed in the Himalayan and the Tibetan Plateau regions. This division is in good agreement with Santô and Satô's Rayleigh wave group velocity division for the same area.

1. Introduction

In 1965, Santô¹⁾ studied Rayleigh wave dispersion along various paths in Eurasia and he divided the continent and its surroundings into 12 regions having similar dispersion characteristics of Rayleigh wave velocity. In another similar study, Santô and Satô²⁾ extended this division for Africa, the Atlantic Ocean and the Indian Ocean. (From here onwards referred to as *Rayleigh wave division*). A sufficiently large number of earthquakes and recording stations were used by these authors to cover the regions concerned. Crampin³⁾ similarly divided Eurasia using 2nd Love and 2nd Rayleigh modes. However, the data being very scanty, Crampin's division is not very precise.

In the present work, dispersion of the fundamental mode of Love

1) T. SANTÔ, "Lateral Variation of Rayleigh Wave Dispersion Character Part II: Eurasia," *Pure and Applied Geophysics*, **62** (1965), 67.

2) T. SANTÔ and Y. SATÔ, "World Wide Survey of the Regional Characteristics of Group Velocity Dispersion of Rayleigh Waves," *Bull. Earthq. Res. Inst.*, **44** (1966), 939.

3) S. CRAMPIN, "Higher Modes of Seismic Surface Waves: Propagation in Eurasia," *Bull. Seism. Soc. Amer.*, **56** (1966), 1227.

waves is studied along various paths in Eurasia. The observed group velocity curves are found to be parallel for most of the paths. This makes it possible to utilize the crossing path technique of Santô⁴⁾ to divide Eurasia into different regions having similar Love wave dispersion characteristics and to examine whether it agrees with the *Rayleigh wave division* of Eurasia.

2. Observational Data

Compared to Rayleigh waves, which can be picked up from the long-period vertical component seismograms, observation of Love waves is difficult. This difficulty is mainly due to two reasons. Firstly, for the oceanic paths, Love waves are not very dispersive and appear somewhat like a pulse in the seismogram. Secondly, when the direction of the approach of waves at the observation station is around 45° , they are strongly affected by Rayleigh waves and we cannot measure the group velocities of Love waves for the time range in which Rayleigh waves

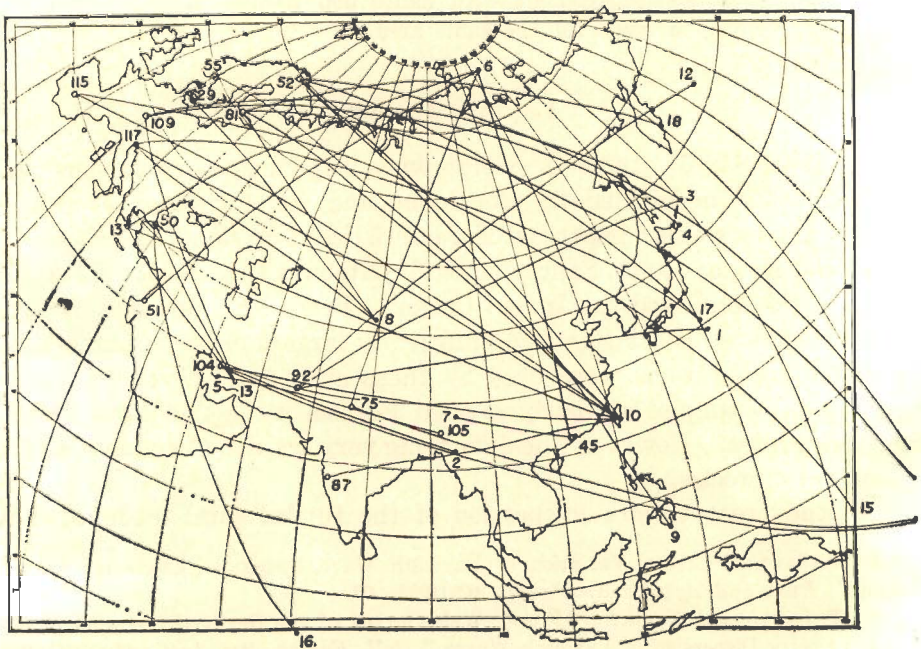


Fig. 1. Seismic stations (open circles), earthquakes (closed circles) and the wave paths.

4) *loc. cit.*, 1).

Table 1

DATA OF EARTHQUAKES USED

	D A T E	ORIGIN TIME (G.M.T.)			EPICENTRE	
		H	M	S		
1	JAN 15 64	21	36	05.0	39.1' N	140.8 E
2	JAN 22 64	15	58	46.5	22.4 N	93.6 E
3	MAY 02 64	16	11	00.2	45.5 N	150.3 E
4	MAY 31 64	00	40	36.4	43.5 N	146.8 E
5	AUG 19 64	15	20	13.9	28.2 N	52.7 E
6	AUG 25 64	13	47	20.6	78.2 N	126.6 E
7	OCT 21 64	23	09	18.8	28.1 N	93.8 E
8	MAY 04 65	08	34	39.8	41.7 N	79.4 E
9	MAY 16 65	11	35	46.0	5.3 N	125.7 E
10	MAY 17 65	17	19	25.9	22.5 N	121.3 E
11	MAY 20 65	00	40	10.9	14.7 S	167.4 E
12	MAY 23 65	23	46	12.0	52.2 N	175.0 E
13	JUNE 21 65	00	21	14.5	28.1 N	56.0 E
14	SEPT 04 65	14	32	47.9	58.2 N	152.6 W
15	SEPT 11 65	06	53	01.5	5.3 S	153.0 E
16	SEPT 12 65	22	02	34.3	6.4 S	70.8 E
17	NOV 12 65	17	52	24.1	30.5 N	140.2 E
18	NOV 18 65	21	58	12.4	53.9 N	160.7 E

Table 2

LIST OF STATIONS

	STATION		COUNTRY	LATITUDE	LONGITUDE
13	ATHENS (ATU)		GREECE	37 58 22 N	23 43 00 E
29	COPENHAGEN (COP)		DENMARK	55 41 00 N	12 26 00 E
45	HONG-KONG (HKG)		HONG KONG	22 18 13 N	114 10 19 E
50	ISTANBUL (IST)		TURKEY	41 02 36 N	28 59 06 E
51	JERUSALEM (JER)		ISRAEL	31 46 19 N	35 11 50 E
52	KEVO (KEV)		FINLAND	69 45 21 N	27 00 45 E
55	KONGSBERG (KON)		NORWAY	59 38 57 N	09 37 55 E
75	NEW DELHI (NDI)		INDIA	28 41 00 N	77 13 00 E
81	NURMIJARVI (NUR)		FINLAND	60 30 32 N	24 39 05 E
87	POONA (POO)		INDIA	18 32 00 N	73 51 00 E
92	QUETTA (QUE)		PAKISTAN	30 11 18 N	66 57 00 E
104	SHIRAZ (SHI)		IRAN	29 30 40 N	52 31 34 E
105	SHILLONG (SHL)		INDIA	25 34 00 N	91 53 00 E
109	STUTT GART (STU)		GERMANY	48 46 15 N	09 16 36 E
115	TOLEDO (TOL)		SPAIN	39 52 53 N	04 02 55 W
117	TRIEST (TRI)		ITALY	45 42 32 N	13 45 51 E

also arrive. Because of the horizontally polarized transverse locus of Love waves, horizontal component seismograms for the stations where waves arrive along one of the coordinate axes are most suitable. With this consideration in mind, seismograms of the Eurasian W.W.S.S.N. stations for 1964 and 1965 were examined. Finally 18 earthquakes recorded by 16 W.W.S.S.N. stations in Eurasia (Fig. 1.) were found suitable. Tables 1 and 2 give the data of the earthquakes and stations used in the present study. Epicentral distances and azimuthal angles are measured using standard trigonometrical relations with the help of

a computer. The shortest and the longest distances are 2142 km and 14096 km respectively. In most cases, the azimuthal angle is within $\pm 10^\circ$ of either of the coordinate axes.

However, in all cases, the horizontal component seismograms have been compared with the vertical components to confirm the identity of the Love waves. In doubtful cases, particle motion diagrams have been plotted to ensure the identity of waves. R. Sato's⁵⁾ technique has been employed for preparing the group velocity dispersion curves.

3. Standard Love Wave Dispersion Curves & Division of Eurasia

Santô⁶⁾, in his study of Love waves along various paths to Japan, summarized the Love wave dispersion into eleven categories. He has also shown the various paths around Japan which are responsible for these eleven different dispersion curves. Earthquakes with their epicentres in Northeastern India, Western China, Sinkiang Province and Northern Burma and recorded in Japan belong to dispersion curve 6. Fig. 2 shows these paths plotted on the group velocity division map.

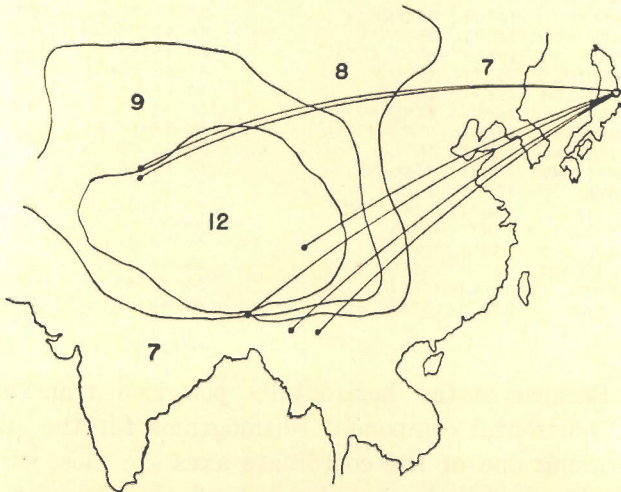


Fig. 2. Earthquakes around Himalayan and Tibetan Plateau region and their wave paths to Japan.

5) R. SATO, "On the Determination of Crustal Structure by the Dispersion Curves of Surface Waves," *Zisin*, 11 (1958), 121.

6) T. SANTÔ, "Dispersion of Love Waves along Various Paths to Japan (Part I)," *Bull. Earth. Res. Inst.*, 39 (1961), 631.

Calculations reveal that the Rayleigh waves travelling along these paths correspond to the Number 8 standard Rayleigh wave dispersion curve of Santô and Satô. Hence Santô's⁷⁾ previous Love wave dispersion curve Number 9 has been adopted as Number 8 in the present study. Similar correspondence holds as follows:

Table 3

Santô's Love wave study	Region				
	7	8	9	10	11
Present Love wave study	6	7	8	9	10

Validity of this adoption is further supported by some simple cases. For example, the earthquake of 17th May, 1965, recorded at Poona, traversed only region 7 of the Rayleigh wave division. The Love wave dispersion curve for this path is in good agreement with the adopted Number 7 Love wave dispersion curve.

For obtaining Love wave dispersion curves Numbers 0, 1, 3 and 5,

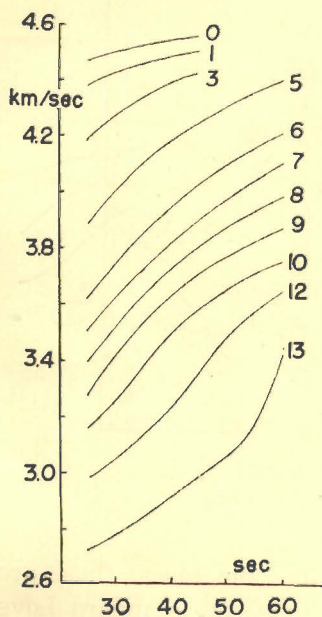


Fig. 3. Standard Love wave dispersion curves.

such paths are chosen which traverse one of these unknown regions and the other known regions i.e. 6, 7, 8, 9 or 10, on the Rayleigh wave division. Then, after subtracting the time corresponding to these known regions from the total travel time, group velocities for the unknown regions are calculated. However, curve Numbers 12 and 13 were taken to explain exceptionally low group velocities across the Himalayan and Tibetan Plateau (details given under discussion). By successive approximation the dispersion curves and the division pattern are adjusted, so that using the crossing path technique, the calculated travel time $\sum \Delta_i/u_i$ (where Δ_i is the length of a segment in region i and u_i is the corresponding group velocity), is within $\pm 1\%$ of the observed travel time for a particular period.

In all cases, these calculations are made

7) *loc. cit.*, 6).

Table 4

GROUP VELOCITIES (KM/SEC) OF LOVE WAVES FOR VARIOUS STANDARD DISPERSION CURVES AT DIFFERENT PERIODS IN SECONDS

REGION	25	30	35	40	45
0	4.46	4.49	4.52	4.54	4.55
1	4.37	4.42	4.46	4.48	4.50
3	4.18	4.27	4.33	4.39	4.42
5	3.88	4.00	4.10	4.18	4.24
6	3.62	3.74	3.86	3.94	4.02
7	3.51	3.62	3.72	3.82	3.90
8	3.39	3.52	3.63	3.73	3.81
9	3.27	3.41	3.53	3.63	3.71
10	3.16	3.26	3.38	3.50	3.58
12	2.98	3.05	3.14	3.23	3.36
13	2.72	2.77	2.85	2.91	2.98

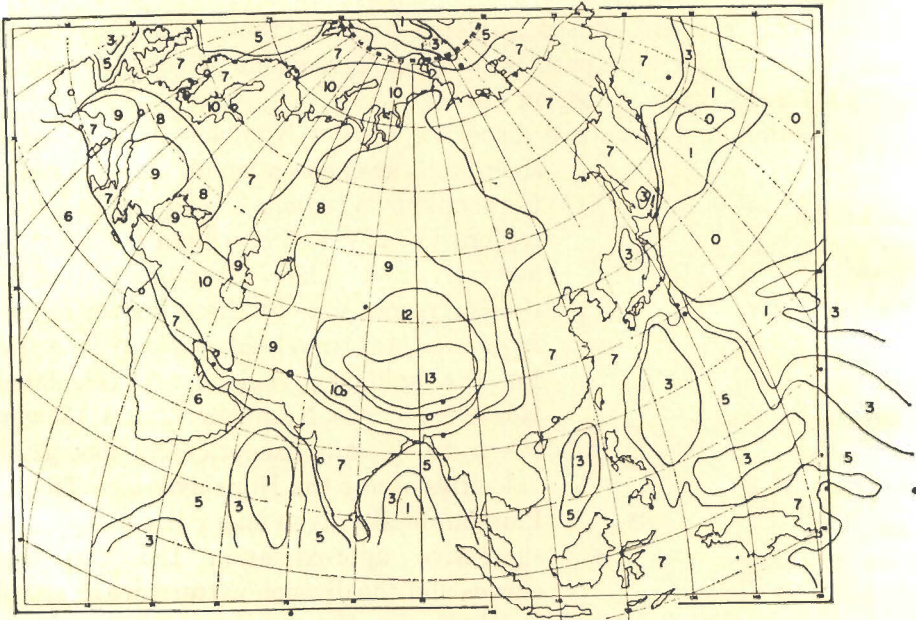


Fig. 4. Love wave division pattern of Eurasia
(Stations: open circles. Epicentres: closed circles.)

for 30, 35, 40 and 45 second periods. However, in some cases, these are extended up to 60 seconds. Fig. 3 and Table 4 show the standard Love wave group velocity dispersion curves and Fig. 4 shows the division pattern of Eurasia. Table 5 gives the frequency distribution of $(T_0 - T_c)/T_0$ for all cases.

Table 5

FREQUENCY DISTRIBUTION OF $(T_0 - T_C)/T_0$	
$[(T_0 - T_C)/T_0] \cdot 100$	NUMBER
+ 1.00	2
+ 0.75	2
+ 0.50	3
+ 0.25	6
0.00	10
- 0.25	4
- 0.50	4
- 0.75	2
- 1.00	2
SUM = 35	

4. Discussion

The basic element in this study is the areal division of Eurasia based upon the Rayleigh wave dispersion study by Santô and Satô⁸⁾. When necessary, this division has been altered so as to conform with the observed Love wave dispersion. Principally, however, the two divisions are similar, i.e. the regions with low (or high) Rayleigh wave velocities correspond to regions with low (or high) Love wave velocities.

4.1 Himalaya-Tibet Plateau region

Exceptionally low group velocities are observed in the Himalayan and the Tibetan Plateau region. For the earthquake of 17th May, 1965, the calculated travel time of Love waves at Kevo and Nurmijarvi was equal to the observed time and at Kongsberg 0.8% greater than the observed time. These paths traverse region Nos. 7, 8, 9 and 10. But the observed time of Love waves recorded at Shiraz, was 9.0% larger than the calculation, which traverse the 12th region of the Rayleigh wave division (assuming a 3.2km/sec group velocity for 40 sec. period). The identification of Love waves was indisputable. Fig. 5 shows the NS and vertical component of the seismograms and Fig. 6 the particle motion. Similarly, very low group velocities were obtained for other paths including the Himalayan and the Tibetan Plateau region. Hence, taking topography as the guiding factor, a new region No. 13 was formed for this very high mountainous region. Standard dispersion curves Numbers 12 and 13 were obtained by calculating the travel time

8) *loc. cit.*, 2).

Table 6

PATH	PERIOD SEC	TOTAL Δ	PATH LENGTH (KM) SEGMENT											
			Δ0	Δ1	Δ3	Δ5	Δ6	Δ7	Δ8	Δ9	Δ10	Δ12	Δ13	
8-29	35	4936												
	40							1934	827	1695	490			
	45													
10-52	35	7825												
	40							2564	3318		1943			
	45													
10-104	35	6815												
	40							1387	383	1770	973	619	1682	
	45													
11-81	35	14096	1445	1687	1657	1416								
	40							5933	1145		813			
	45													
16-50	35	6748												
	40				1941	1080	1972	1053			702			
	45													

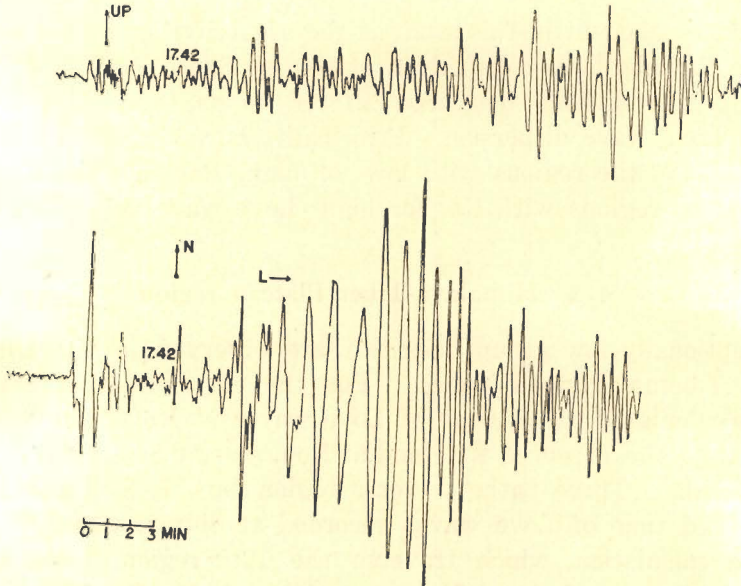


Fig. 5. Seismograms observed at Shiraz.

corresponding to these regions from the total path for different periods. Table 6 shows some examples. Very low group velocities in this region were earlier obtained by Gupta and Narain⁹⁾. Porkka¹⁰⁾, Stoneley¹¹⁾, Tan-

9) H. GUPTA and H. NARAIN, "Crustal Structure in Himalayan and Tibet Plateau Region from Surface Wave Dispersion," *Bull. Seism. Soc. Amer.*, 57 (1967), 235.

10) M. T. PORKKA, "Surface Wave Dispersion for Some Eurasian Paths. II. Love Waves," *Geophysica*, 7 (1961), 151.

11) R. STONELEY, "Rayleigh Waves in a Medium with two Surface Layers," *Mon. Not. Roy. Astr. Soc. Geophys. Supp.*, 7 (1955), 71.

TRAVEL TIME (SEC)														
SEGMENT													TOTAL	
I 0	T 1	T 3	T 5	T 6	T 7	T 8	T 9	T 10	T 12	T 13	C	O		
					520	228	476	145					1369	1366
					506	222	464	140					1332	1334
					496	217	454	137					1304	1307
					689	914		575					2178	2188
					671	889		555					2115	2123
					657	871		543					2071	2078
					373	106	501	288	197	592	2057	2055		
					363	103	488	278	192	578	2002	2002		
					356	101	477	272	184	562	1952	1955		
320	378	383	345		1595	315		241					3577	3556
318	376	378	339		1553	307		232					3505	3485
317	375	375	334		1522	301		227					3451	3438
		449	264	511	283			208					1715	1734
		444	258	500	276			201					1679	1688
		440	254	491	270			196					1651	1668

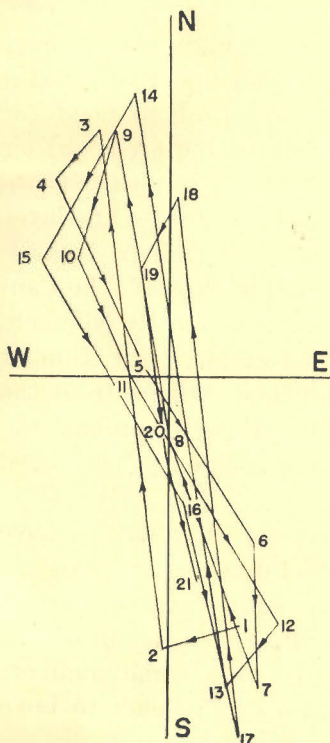


Fig. 6. Orbital motion as obtained from Fig. 5.

don and Chaudhury¹²⁾, etc. have also contributed the lower average group velocities for paths crossing the Himalayan and the Tibetan Plateau region to the thick crust beneath them.

In Fig. 4, the concentration of the regional contours towards the Indian Subcontinent and their relative sparseness to the north of the Himalayan and the Tibetan Plateau is also remarkable. This probably reflects the underground crustal structure. In the south, from the low level Indogangetic planes, the elevation increases within a very short distance to the high peaks of the Himalayas, whereas towards the north, from the plateau of Pamir the elevation decreases gradually. Hence it is likely that the crust thickens rapidly from beneath the Indogangetic planes to the high mountainous regions and thins out gradually towards the north. Another important fact is the rapid increase of the group velocities with period on curve Nos. 12 and 13 (see Fig. 3). It

12) A. N. TANDON and H. M. CHAUDHURY, "Seismic Surface Waves from High Yield Atmospheric Explosions," *Ind. J. Met. Geophys.*, 14 (1963), 283.

seems that the mountain roots in this region will affect the shorter period Love waves more than those with longer periods.

In the foot hills of the Himalayas, region 10 has been introduced and region 9 is extended to the Indogangetic planes where thick sediment is known to exist. This explains the observed dispersion of Love waves at Shillong from the earthquake of 19th Aug., 1964, and at Shiraz for the earthquake of 22nd January, 1964. Both mainly traversed the foot hills of the Himalayas. Earlier work by Chaudhury¹³⁾ also supports this extension.

4.2 Other regions

The region 6 in East Siberia in the Rayleigh wave division is not delineated by Love waves. Considering it to be region 7, the calculated time agreed with the observed time.

The existence of region 10, corresponding to the high mountainous type, in the water-covered area around Novaya Zemlya and Baltic Sea—an unexpected result according to Santô¹⁴⁾—is found to hold good for Love waves also. This region around Novaya Zemlya required further eastward extension up to the southern end of Severnaya Zemlya. These low group velocities are probably due to a thick soft sedimentary layer in the sea, similar to those reported by Shurbet¹⁵⁾ for the Gulf of Mexico.

Another change, worth mentioning, has occurred in Turkey, the Caucasian Mountains and the Persian regions. These regions (mostly Numbers 7 and 9 according to the *Rayleigh wave division*) are replaced by Number 10 to explain the Love waves recorded at Istanbul and Athens from the earthquake of 21st June, 1965. Also, in western Europe, around the Alps, Yugoslavia and Rumania, regions 8 and 9 have been extended, based upon Love wave paths crossing those regions.

The above mentioned are the major differences between the Love wave and the Rayleigh wave division pattern of Eurasia.

Since the regionalization of Eurasia by Love wave dispersion agrees reasonably well with the *Rayleigh wave division*, a comparison of the Rayleigh wave and Love wave group velocities for the same numbers is made. Table 7 shows the group velocity ratio of Rayleigh to Love

13) H. M. CHAUDHURY, "Seismic Surface Wave Dispersion and the Crust across the Gangetic Basin," *Ind. J. Met. Geophys.*, 17 (1966), 385.

14) *loc. cit.*, 1).

15) D. H. SHURBET, "The Effect of the Gulf of Mexico on Rayleigh Wave Dispersion," *J. Geophys. Res.*, 65 (1960), 1251.

Table 7

REGION	T = 30 SEC			T = 40 SEC		
	RAYLEIGH WAVE VEL	LOVE WAVE VEL	RATIO	RAYLEIGH WAVE VEL	LOVE WAVE VEL	RATIO
0	4.08	/ 4.49	= 0.91	4.16	/ 4.53	= 0.92
1	3.99	/ 4.42	= 0.90	4.06	/ 4.47	= 0.91
3	3.86	/ 4.27	= 0.90	3.94	/ 4.38	= 0.90
5	3.66	/ 4.00	= 0.92	3.83	/ 4.18	= 0.92
6	3.52	/ 3.74	= 0.94	3.71	/ 3.94	= 0.94
7	3.36	/ 3.62	= 0.93	3.59	/ 3.82	= 0.94
8	3.24	/ 3.52	= 0.92	3.51	/ 3.73	= 0.94
9	3.06	/ 3.41	= 0.90	3.40	/ 3.63	= 0.94
10	2.98	/ 3.26	= 0.91	3.30	/ 3.50	= 0.94
12	2.68	/ 3.05	= 0.88	3.06	/ 3.24	= 0.94

waves for 30 and 40 seconds period. The minimum value of this ratio is 0.88 (Region 12, period 30 sec) and the maximum value is 0.94 (Region 6~12, period 30 and 40 seconds). It is remarkable that this ratio for most of the cases is around 0.91. No such correlation could be made for Love wave dispersion curve Number 13 since this region was not delineated by Rayleigh wave study.

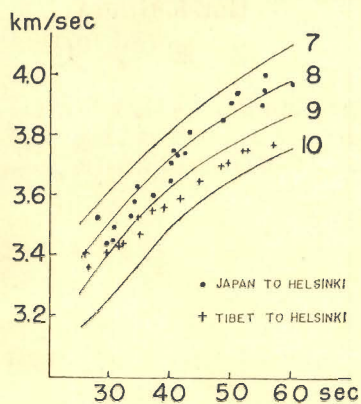


Fig. 7. Love wave dispersion obtained from the Helsinki observation.

Fig. 7 shows Porkka's¹⁶⁾ Love wave group velocity data for paths between (a) Japan and Helsinki and (b) Tibet and Helsinki, and the standard Love wave dispersion curve for Numbers 7, 8, 9 and 10. It is interesting to note that the Love waves recorded from the earthquakes around Japan show distinctly higher group velocities than those from the Tibet region; the former falls around the curve Number 8 and the latter between curve Numbers 9 and 10.

5. Conclusions

Love wave group velocity along various sections in Eurasia has been investigated, and it reveals that

1) It is possible to divide Eurasia into different regions having similar group velocity dispersion characteristics.

16) *loc. cit.*, 10).

2) This division supports Santô and Satô's division of Eurasia based on Rayleigh wave group velocity observations.

3) Extremely low group velocities, probably the lowest in the world, are observed in the Himalayan and the Tibet Plateau regions.

4) In general, a good agreement is observed between the division pattern and the regional topography.

Acknowledgments

The authors are thankful to Dr. T. Santô for useful discussions. Computations were carried out at the University of Tokyo Data Processing Centre.

3. ユーラシア大陸におけるラブ波群速度の地域特徴

National Geophysical Research Institute Harsh GUPTA
地震研究所 佐藤 泰夫

ユーラシア大陸におけるラブ波群速度の分散を調べ、その分散の特徴に従って同大陸を 13 の地域に分割した。ヒマラヤ及びチベット高原地域は非常に群速度が遅い。なおこの分割は三東及び佐藤の同大陸に対するレーリー波群速度による分割と良く一致する。又群速度の遅速は地形の高低によく対応するようである。